

SUPPORTING INFORMATION

Molecular Multifunctionalization via Electronically Coupled Lactones

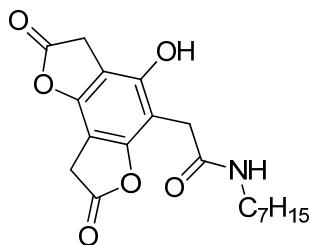
Matthew B. Baker, Ion Ghiviriga, and Ronald K. Castellano*

Department of Chemistry, P.O. Box 117200, University of Florida, Gainesville, FL 32611-7200, USA

<u>Table of Contents</u>	<u>Pages</u>
Synthesis of novel compounds.....	S2–S10
Statistical product distribution simulations	S11–S13
Temperature dependence of ring opening and reversibility	S14–S16
Infrared spectra of compounds 1 , 2a , and 3aa	S16–S17
HMQC data for compounds 2a and 3ad'	S18–S25
Quantum chemical structure calculations	S26–S31
Characterization of novel compounds.....	S32–S52
References	S53

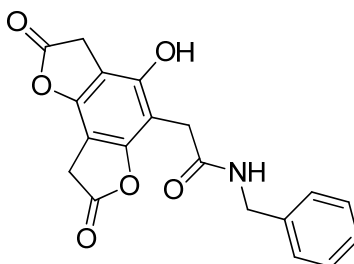
Supplementary Methods: General procedures

Reagents and solvents were purchased from Acros or Aldrich and used without further purification unless otherwise specified. DMF was degassed in 20 L drums and passed through two sequential purification columns (molecular sieves) under a positive argon atmosphere using a custom Glass Contour solvent system (Glass Contour, Inc.); DMF was also allowed to equilibrate to the atmosphere in order to show tolerance to atmospheric conditions. Thin layer chromatography (TLC) was performed on Dynamic Adsorbents, Inc. aluminum backed TLC plates with visualization via UV light and ninhydrin staining; interestingly, products stained different colors based on the number of lactone rings present. Flash column chromatography was performed using Purasil SiO₂-60 230-400 mesh silica gel from Whatman using mobile phases as indicated within procedures. Infrared spectra were obtained on a Perkin Elmer Spectrum One FT-IR spectrometer using a NaCl salt plate; samples were prepared by dropcasting compounds as a solution in chloroform. ¹H NMR, ¹³C NMR and ¹H-¹³C gHMQC spectra were recorded on a Varian Inova spectrometer operating at 500 MHz for ¹H and at 125 MHz for ¹³C, and on a Varian VNMRS system operating at 600 MHz for ¹H and 150 MHz for ¹³C. Chemical shifts (δ) are given in parts per million (ppm) relative to residual protonated solvent (DMSO: δ_H 2.50 ppm, δ_C 39.50 ppm). Abbreviations used are s (singlet), d (doublet), t (triplet), q (quartet), and m (multiplet). MS spectra (HRMS) were acquired on a Bruker APEX II 4.7 T Fourier Transform Ion Cyclone Resonance mass spectrometer (Bruker Daltonics, Billerica, MA).

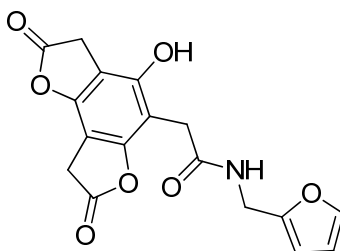


Representative ring opening procedure. *N*-heptyl-2-(4-hydroxy-2,7-dioxo-2,3,7,8-tetrahydrobenzo[1,2-*b*:3,4-*b'*]difuran-5-yl)acetamide (**2a**). To a reaction vessel equipped with stir bar was added **BTF** (**1**) (51.4 mg, 209 μmol) and DMF (3 mL). The solution was stirred at room temperature until complete dissolution of the **BTF**, then cooled in a dry ice/acetonitrile cold bath (−41°C). After temperature equilibration, one equivalent of a 0.500 M solution of heptylamine in DMF was slowly added dropwise (418 μL, 209 μmol). The reaction was then allowed to stir under a blanket of argon, in the cold bath, for 30 min; after this time, the reaction was allowed to warm to room temperature before being poured into EtOAc (about 100 mL). The organic layer was washed thrice with water (some brine may be needed to simplify extraction) and then once with brine. The

organics were dried over Na₂SO₄ and volatiles removed *in vacuo* yielding compound **2a** (75 mg, 99%) as an off-white solid. The product could be purified via column chromatography (5% acetone in DCM, R_f ≈ 0.3) to yield analytically pure material (57 mg, 75%). IR (film) ν 1808 cm⁻¹ (C=O stretch); ¹H NMR (*d*₆-DMSO) δ 10.64 (s, 1H), 8.21 (t, *J* = 5.3 Hz, 1H), 3.92 (s, 2H), 3.78 (s, 2H), 3.46 (s, 2H), 3.04 (q, *J* = 6.6 Hz, 2H), 1.34 (m, 10H), 0.85 (t, *J* = 6.0 Hz, 3H). ¹³C NMR (*d*₆-DMSO) δ 174.2, 173.9, 170.1, 153.2, 151.8, 147.8, 105.2, 102.7, 97.1, 38.9, 31.2, 30.9, 30.8, 30.6, 28.9, 28.4, 26.3, 22.1, 14.0. HRMS calcd for C₁₉H₂₃NO₆ [M+Na]⁺ 384.1418; found, 384.1419.

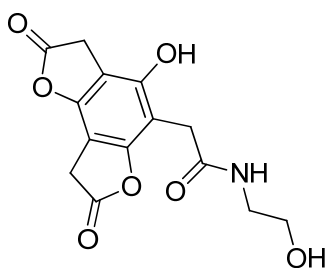


N-Benzyl-2-(4-hydroxy-2,7-dioxo-2,3,7,8-tetrahydrobenzo[1,2-*b*:3,4-*b'*]difuran-5-yl)acetamide (2b). To a stirred solution of **BTF** (62 mg, 250 μmol) in DMF (3 mL) at -41°C was dropwise added a benzylamine solution in DMF (500 μL of a 0.500 M solution, 250 μmol). After 2 h (reaction complete in 30 min via TLC), the reaction solution was worked up in the same manner as compound **2a**, yielding 88 mg of crude material (quant). Compound **2b** was further purified via column chromatography (5% acetone in DCM, R_f ≈ 0.4) to yield 65 mg (74%) of a white powder. ¹H NMR (*d*₆-DMSO) δ 10.38 (s, 1H), 8.61 (t, *J* = 5.8 Hz, 1H), 7.28 (m, 5H), 4.29 (d, *J* = 5.9 Hz, 2H), 3.94 (s, 2H), 3.81 (s, 2H), 3.54 (s, 2H). ¹³C NMR (*d*₆-DMSO) δ 174.2, 173.9, 169.9, 153.5, 151.5, 147.8, 139.2, 128.3, 127.2, 126.8, 105.0, 102.7, 97.1, 42.3, 31.0, 30.6, 30.6. HRMS calcd for C₁₉H₁₅NO₆ [M+CH₃OH+H]⁺ 386.1234; found, 386.1245.



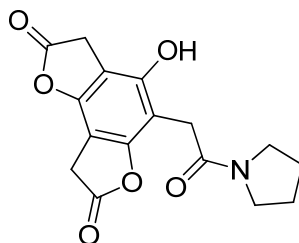
N-(Furan-2-ylmethyl)-2-(4-hydroxy-2,7-dioxo-2,3,7,8-tetrahydrobenzo[1,2-*b*:3,4-*b'*]difuran-5-yl)acetamide (2c). A solution of **BTF** (100 mg, 406 μmol) in DMF (6 mL) was cooled in an acetonitrile/dry ice bath under a blanket of argon. After temperature equilibration, a solution of furfurylamine in DMF (812 μL of a 0.500 M

solution, 406 μmol) was added dropwise over 5 minutes. The reaction was allowed to stir at low temperature for 3 h, before a work up similar to compound **2a**, yielding a dark yellow crude solid (138 mg, 99%). Product could be purified via column chromatography (5% acetone in DCM, $R_f \approx 0.3$) yielding **2c** as a yellow solid (83 mg, 60%). ^1H NMR (d_6 -DMSO) δ 10.32 (s, 1H), 8.57 (t, $J = 5.5$ Hz, 1H), 7.57 (s, 1H), 6.39 (dd, $J = 3.0, 1.9$ Hz, 1H), 6.25 (d, $J = 2.7$ Hz, 1H), 4.27 (d, $J = 5.6$ Hz, 2H), 3.92 (s, 2H), 3.79 (s, 2H), 3.49 (s, 2H). ^{13}C NMR (d_6 -DMSO) δ 174.2, 173.9, 169.8, 153.5, 152.0, 151.5, 147.8, 142.1, 110.4, 106.9, 105.0, 102.6, 97.1, 35.8, 31.0, 30.6, 30.4. HRMS not obtainable by various methods. Elemental analysis calcd for $\text{C}_{17}\text{H}_{13}\text{NO}_7$: C, 59.48; H, 3.82; N, 4.08. Found: C, 59.09; H, 3.74; N, 3.77.

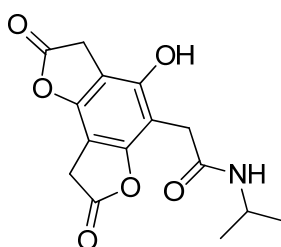


2-(4-Hydroxy-2,7-dioxo-2,3,7,8-tetrahydrobenzo[1,2-*b*:3,4-*b'*]difuran-5-yl)-*N*-(2-hydroxyethyl)acetamide (2d**).**

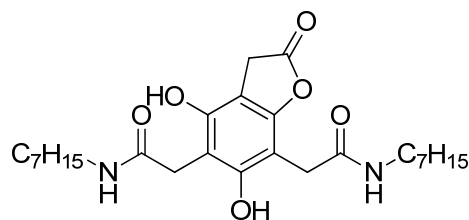
To a stirred solution of **BTF** (25.2 mg, 102 μmol) in DMF (1.5 mL) at -41°C was dropwise added ethanolamine solution in DMF (204 μL of a 0.500 M solution, 102 μmol). After 2 h (reaction complete in 30 min), the reaction solution was worked up in the same manner as compound **2a**, yielding 26 mg (78%) of crude material. The compound could be further purified via flash column chromatography (10% MeOH in DCM, $R_f = 0.4$) to yield **2d** (7 mg, 23 %) as an amorphous solid. ^1H NMR (d_6 -DMSO) δ 10.60 (s, 1H), 8.22 (t, $J = 5.4$ Hz, 1H), 4.68 (t, $J = 5.4$ Hz, 1H), 3.92 (s, 2H), 3.79 (s, 2H), 3.49 (s, 2H), 3.41 (q, $J = 5.8$ Hz, 2H), 3.13 (q, $J = 5.5$ Hz, 2H). ^{13}C NMR (d_6 -DMSO) δ 174.2, 173.9, 170.4, 153.3, 151.7, 147.8, 105.2, 102.7, 97.1, 59.6, 41.8, 30.9, 30.7, 30.6. HRMS calcd for $\text{C}_{14}\text{H}_{13}\text{NO}_7$ $[\text{M}+\text{H}]^+$ 308.0765; found, 308.0759.



4-Hydroxy-5-(2-oxo-2-(pyrrolidin-1-yl)ethyl)benzo[1,2-*b*:3,4-*b'*]difuran-2,7(3*H*,8*H*)-dione (2e). To a stirred solution of **BTF** (88 mg, 350 μmol) in DMF (5 mL) at -41°C was added pyrrolidine solution in DMF (690 μL of 0.503 M solution, 350 μmol). After 3 h (reaction complete by TLC in 15 min), the reaction solution was worked up in the same manner as compound **2a**, yielding 109 mg (quant) of crude white material. The compound could be further purified via column chromatography (5% acetone in DCM, $R_f \approx 0.4$) yielding **2e** (85 mg, 78%) as a fine white powder. ^1H NMR (d_6 -DMSO) δ 10.21 (s, 1H), 3.94 (s, 2H), 3.79 (s, 2H), 3.58 (m, 4H), 3.29 (m, 2H), 1.93 (q, $J = 6.8$, 2H), 1.80 (q, $J = 6.8$, 2H). ^{13}C NMR (d_6 -DMSO) δ 174.2, 173.9, 167.8, 153.4, 151.5, 147.7, 105.0, 102.8, 97.0, 46.4, 45.7, 31.0, 30.6, 29.6, 25.6, 24.0. HRMS calcd for $\text{C}_{16}\text{H}_{15}\text{NO}_6$ $[\text{M}+\text{H}]^+$ 318.0972; found, 318.0966.

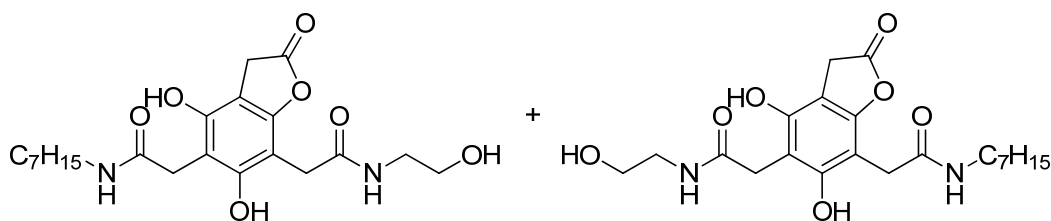


2-(4-Hydroxy-2,7-dioxo-2,3,7,8-tetrahydrobenzo[1,2-*b*:3,4-*b'*]difuran-5-yl)-*N*-isopropylacetamide (2f). To a cooled solution (-41°C) of **BTF** (51 mg, 210 μmol) in DMF (3 mL) was dropwise added a solution of isopropylamine in DMF (410 μL of a 0.500 M solution, 210 μmol). The reaction was completed in 3 h and worked up in the same manner as **2a**, yielding 62 mg (98%) of tan solids. Further purification via flash chromatography (5% acetone in DCM, $R_f \approx 0.4$) yielded **2f** as a semi-crystalline solid (50 mg, 79%). ^1H NMR (d_6 -DMSO) δ 10.78 (s, 1H), 8.24 (d, $J = 7.5$ Hz, 1H), 3.92 (s, 2H), 3.82 (m, 3H), 3.47 (s, 2H), 1.06 (d, $J = 6.6$ Hz, 6H). ^{13}C NMR (d_6 -DMSO) δ 174.2, 173.9, 169.5, 153.2, 151.9, 147.8, 105.3, 102.7, 97.1, 40.8, 30.9, 30.9, 30.6, 22.2. HRMS not obtainable by various methods. Elemental analysis calcd for $\text{C}_{15}\text{H}_{15}\text{NO}_6$: C, 59.01; H, 4.95; N, 4.59. Found: C, 58.01; H, 4.87; N, 4.26.

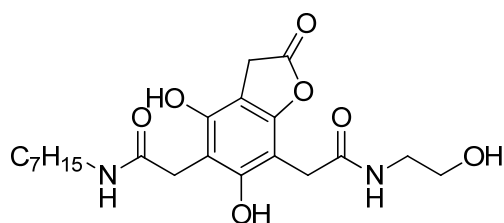


2,2'-(4,6-Dihydroxy-2-oxo-2,3-dihydrobenzofuran-5,7-diyl)bis(*N*-heptylacetamide) (3aa). To a cooled solution (-41°C) of **BTF** (51.2 mg, 208 μmol) in DMF (3 mL) was dropwise added a solution of heptylamine in

DMF (832 μL of a 0.500 M solution, 416 μmol). The reaction was complete within 3 h by TLC analysis, but was allowed to stir in the cold bath for 6 h before warming to room temperature. A work-up similar to compound **2a** was performed, yielding 95 mg (96%) of crude off-white material. Compound could be further purified via flash column chromatography (10% acetone in DCM, $R_f \approx 0.3$) to yield pure **3aa** (71 mg, 72%). IR (film) ν 1801 cm^{-1} (C=O stretch); ^1H NMR (d_6 -DMSO) δ 11.13 (s, 1H), 10.03 (s, 1H), 8.38 (br s, 1H), 8.15 (br s, 1H), 3.70 (s, 2H), 3.48 (s, 2H), 3.43 (s, 2H), 3.03 (m, 4H), 1.39 (m, 4H), 1.23 (br s, 16H), 0.85 (t, $J = 6.3$ Hz, 6H). ^{13}C NMR (d_6 -DMSO) δ 174.6, 172.3, 171.5, 155.5, 151.8, 150.7, 106.6, 100.7, 98.4, 38.9, 38.9, 31.6, 31.2, 31.2, 30.8, 28.8, 28.7, 28.4, 28.3, 26.3, 22.0, 13.9 (three carbon signals were not observed/resolved). HRMS calcd for $\text{C}_{26}\text{H}_{40}\text{N}_2\text{O}_6$ $[\text{M}+\text{Na}]^+$ 499.2779; found, 499.2791.

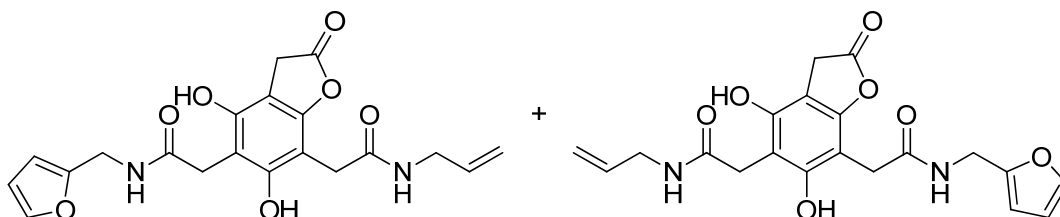


2-(4,6-Dihydroxy-7-(2-((2-hydroxyethyl)amino)-2-oxoethyl)-2-oxo-2,3-dihydrobenzofuran-5-yl)-N-heptylacetamide and 2-(4,6-dihydroxy-5-(2-((2-hydroxyethyl)amino)-2-oxoethyl)-2-oxo-2,3-dihydrobenzofuran-7-yl)-N-heptylacetamide (3ad' and 3ad''). To a stirred solution of **2a** (50.0 mg, 138 μmol) in DMF (3 mL) at -41°C was dropwise added ethanolamine solution in DMF (277 μL of 0.500 M solution, 138 μmol). After 6 h (the reaction was complete in about 3 h), the reaction solution was worked up in the same manner as compound **2a**, yielding 57 mg (98%) of crude material that was a 45:55 ratio of **3ad'** to **3ad''**. ^1H NMR in DMSO is shown below.

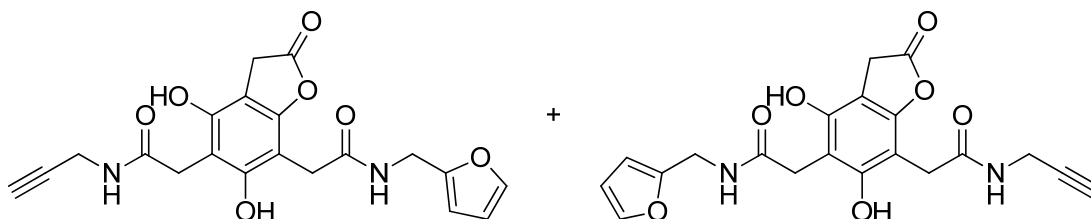


2-(4,6-Dihydroxy-7-(2-((2-hydroxyethyl)amino)-2-oxoethyl)-2-oxo-2,3-dihydrobenzofuran-5-yl)-N-heptylacetamide (3ad'). Compound **3ad'** could be partially separated by flash column chromatography ($R_f \approx 0.3$ in 80:20 EtOAc:hexanes), from the above reaction mixture. ^1H NMR (d_6 -DMSO) δ 11.10 (s, 1H), 10.03 (s, 1H),

8.43 (t, $J = 5.0$ Hz, 1H), 8.17 (t, $J = 5.0$, 1H), 4.69 (t, $J = 5.3$ Hz, 1H), 3.70 (s, 2H), 3.48, (s, 2H), 3.46 (s, 2H), 3.41 (q, $J = 5.5$ Hz, 2H), 3.13 (q, $J = 5.6$ Hz, 2H), 3.03 (q, $J = 6.4$ Hz, 2H), 1.39 (m, 2H), 1.23 (s, 8H), 0.85 (t, $J = 6.5$ Hz, 3H).
 ^{13}C NMR (d_6 -DMSO) δ 174.6, 172.3, 171.8, 155.5, 151.8, 150.7, 106.6, 100.7, 98.4, 59.5, 41.9, 38.9, 31.6, 31.2, 31.2, 30.8, 28.8, 28.4, 26.3, 22.0, 13.9. HRMS calcd for $\text{C}_{21}\text{H}_{30}\text{N}_2\text{O}_7$ $[\text{M}+\text{H}]^+$ 423.2126; found, 423.2136.

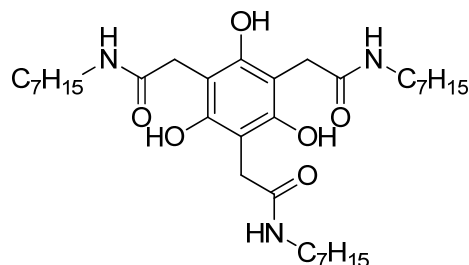


***N*-Allyl-2-(5-(2-((furan-2-ylmethyl)amino)-2-oxoethyl)-4,6-dihydroxy-2-oxo-2,3-dihydrobenzofuran-7-yl)acetamide and *N*-allyl-2-(7-(2-((furan-2-ylmethyl)amino)-2-oxoethyl)-4,6-dihydroxy-2-oxo-2,3-dihydrobenzofuran-5-yl)acetamide (3cg' and 3cg'')**. A solution of **2c** (90 mg, 260 μmol) in DMF (6 mL) was cooled to -41°C in a dry ice/acetonitrile bath before dropwise addition of allylamine (520 μL of a 0.500 M solution, 260 μmol). The reaction was allowed to stir at low temperature for 6 h, before warming to room temperature and working up similar to compound **2a**, yielding a yellowish crude solid (105 mg, quant). The compounds could be further purified via column chromatography (no separation of regioisomers was possible on silica) yielding a mixture of **3cg'** and **3cg''** as an amorphous solid (80 mg, 76% yield, 62:38 ratio of regioisomers). ^1H NMR in d_6 -DMSO and ^{13}C NMR in d_6 -DMSO provided below. HRMS calcd for $\text{C}_{20}\text{H}_{20}\text{N}_2\text{O}_7$ $[\text{M}+\text{Na}]^+$ 423.1163; found, 423.1183.

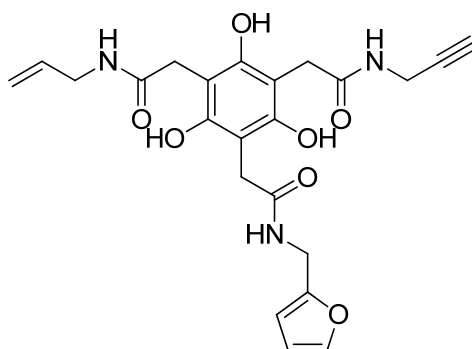


2-(4,6-Dihydroxy-2-oxo-5-(2-oxo-2-(prop-2-yn-1-ylamino)ethyl)-2,3-dihydrobenzofuran-7-yl)-*N*-(furan-2-ylmethyl)acetamide and 2-(4,6-dihydroxy-2-oxo-7-(2-oxo-2-(prop-2-yn-1-ylamino)ethyl)-2,3-dihydrobenzofuran-5-yl)-*N*-(furan-2-ylmethyl)acetamide (3ch' and 3ch''). A solution of **3c** (67 mg, 200 μmol) in DMF (3 mL) was cooled to -41°C in a dry ice/acetonitrile bath before dropwise addition of propargylamine (390 μL of a 0.5 M solution, 200 μmol). The reaction was allowed to stir at low temperature for 8 h, before warming to rt and pouring into EtOAc. The organic layer was washed with deionized H_2O (thrice) and brine, and then dried over Na_2SO_4 . The volatiles were removed *in vacuo* to yield an amorphous solid (79 mg, quant).

The compounds could be further purified via column chromatography (10% acetone in DCM, $R_f \approx 0.3$, no separation of regioisomers was possible on silica) yielding a mixture of **3ch'** and **3ch''** as an amorphous solid (54 mg, 70% yield). ^1H NMR in d_6 -DMSO and ^{13}C NMR in d_6 -DMSO provided below for comparison.



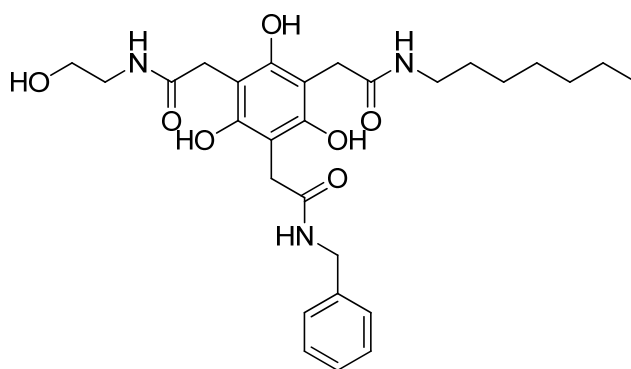
2,2',2''-(2,4,6-Trihydroxybenzene-1,3,5-triyl)tris(N-heptylacetamide) (4aaa). To a cooled solution ($-41\text{ }^\circ\text{C}$) of **BTF** (50 mg, 200 μmol) in DMF (3 mL) was dropwise added heptylamine (77 mg, 670 μmol) with stirring. The reaction was allowed to warm slowly to room temperature overnight. The next day, the reaction was worked up similar to compound **2a**, yielding 120 mg (quant) of crude material. The material could be further purified via column chromatography ($R_f \approx 0.3$ in 10% MeOH/DCM) yielding **4aaa** (110 mg, 92%) as a waxy solid. ^1H NMR (d_6 -DMSO) δ 10.72 (s, 3H), 8.46 (t, $J = 5.4$ Hz, 3H), 3.48 (s, 6H), 3.03 (q, $J = 6.6$ Hz, 6H), 1.40 (m, 6H), 1.23 (s, 24H), 0.84 (t, $J = 6.7$ Hz, 9H). ^{13}C NMR (d_6 -DMSO) δ 173.7, 153.8, 102.8, 39.0, 31.3, 31.2, 28.7, 28.3, 26.3, 22.0, 13.9. HRMS calcd for $\text{C}_{33}\text{H}_{57}\text{N}_3\text{O}_6$ $[\text{M}+\text{Na}]^+$ 614.4140; found, 614.4167.



N-Allyl-2-(3-(2-((furan-2-ylmethyl)amino)-2-oxoethyl)-2,4,6-trihydroxy-5-(2-oxo-2-(prop-2-yn-1-ylamino)ethyl)phenyl)acetamide (3cgh). *Stepwise procedure.* A solution of **3cg'** and **3cg''** (47 mg, 120 μmol) in DMF (3 mL) was cooled to $-41\text{ }^\circ\text{C}$ in a dry ice/acetonitrile bath before dropwise addition of allylamine (300 μL of a 0.500 M solution, 150 μmol). The reaction was allowed to stir at low temperature for 6 h before warming to room temperature. The reaction was worked up as described for compound **2a**, yielding a brown

amorphous solid (52 mg, 96%). The compound could be further purified via column chromatography ($R_f \approx 0.4$ in 5% MeOH/DCM) yielding **3cgh** as an amorphous solid (52 mg, 96% yield). $^1\text{H NMR}$ (d_6 -DMSO) δ 10.22 (s, 1H), 10.16 (s, 1H), 10.08 (s, 1H), 8.81 (t, $J = 4.9$ Hz, 1H), 8.73 (t, $J = 4.8$ Hz, 1H), 8.53 (t, $J = 5.0$ Hz, 1H), 7.57 (s, 1H), 6.38 (dd, $J = 2.9, 1.9$ Hz, 1H), 6.26 (d, $J = 2.9$ Hz, 1H), 5.78 (dddd, $J = 17.5, 10.2, 5.5, 5.1$ Hz, 1H), 5.14 (dd, $J = 17.2, 1.5$ Hz, 1H), 5.06 (dd, $J = 10.3, 1.4$ Hz, 1H), 4.27 (d, $J = 5.1$ Hz, 2H), 3.86 (dd, $J = 5.2, 2.3$ Hz, 2H), 3.70 (t, $J = 5.2$ Hz, 2H), 3.52 (s, 4H), 3.49 (s, 2H), 3.12 (t, $J = 2.4$ Hz, 1H). $^{13}\text{C NMR}$ (d_6 -DMSO) δ 173.4, 173.4, 173.1, 153.8, 153.8, 151.5, 142.2, 134.6, 115.6, 110.5, 107.2, 102.9, 102.9, 102.8, 80.6, 73.3, 41.3, 35.8, 31.2, 31.1, 30.9, 28.3 (one peak not observed/resolved). HRMS calcd for $\text{C}_{23}\text{H}_{25}\text{N}_3\text{O}_7$ $[\text{M}+\text{Na}]^+$ 478.1585; found, 478.1603.

One pot procedure. A solution of **1** (116 mg, 471 μmol) in DMF (6 mL) was cooled to -41°C in a dry ice/acetonitrile bath before dropwise addition of distilled furfurylamine (942 μL of a 0.500 M solution, 471 μmol). After allowing the reaction to proceed for 45 min, distilled allylamine (942 μL of a 0.500 M solution, 471 μmol) was added dropwise to the reaction mixture. After allowing the reaction to proceed for 6 h, distilled propargylamine (1.88 mL of a 0.500 M solution, 942 μL) was added dropwise; the reaction mixture was then allowed to stir overnight, slowly warming to room temperature. The next day, the reaction mixture was poured into EtOAc, and the organic layer was separated and washed with H_2O (thrice) and brine. After drying over Na_2SO_4 , the volatiles were removed *in vacuo* yielding a yellow powder (220 mg, quant). The reaction mixture could be further purified via column chromatography ($R_f \approx 0.4$ in 5% MeOH/DCM) yielding sufficiently pure **3cgh** as a yellow solid (182 mg, 85% yield). Mass spectrum, $^1\text{H NMR}$, and $^{13}\text{C NMR}$ shown below. Elemental analysis calcd for $\text{C}_{23}\text{H}_{25}\text{N}_3\text{O}_7$: C, 60.65; H, 5.53; N, 9.23. Found: C, 60.50; H, 5.55; N, 9.17.



N-Benzyl-2-(3-(2-(heptylamino)-2-oxoethyl)-2,4,6-trihydroxy-5-(2-((2-hydroxyethyl)amino)-2-oxoethyl)phenyl)acetamide (4abd). **One pot procedure.** A solution of **1** (35 mg, 142 μmol) in DMF (3 mL) was cooled to -41°C in a dry ice/acetonitrile bath before dropwise addition of heptylamine (284 μL of a 0.500 M solution, 142 μmol). After allowing the reaction to proceed for 45 min, benzylamine (284 μL of a 0.500 M solution, 142 μmol) was added dropwise to the reaction mixture. After allowing the reaction to proceed for 6

h, aminoethanol (284 μmol of a 0.500 M solution, 142 μmol) was added dropwise; the reaction mixture was then allowed to stir overnight, slowly warming to room temperature. The next day, the reaction mixture was poured into EtOAc, and the organic layer was separated and washed with H_2O (thrice) and brine. After drying over Na_2SO_4 , the volatiles were removed *in vacuo* yielding a tan powder (75 mg, quant). The reaction mixture could be further purified via column chromatography ($R_f \approx 0.4$ in 10% MeOH/DCM) yielding sufficiently pure **4abd** as a white solid (60 mg, 80% yield). ^1H NMR and ^{13}C NMR shown below. HRMS calcd for $\text{C}_{28}\text{H}_{39}\text{N}_3\text{O}_7$ $[\text{M}+\text{Na}]^+$ 552.2680; found, 552.2694.

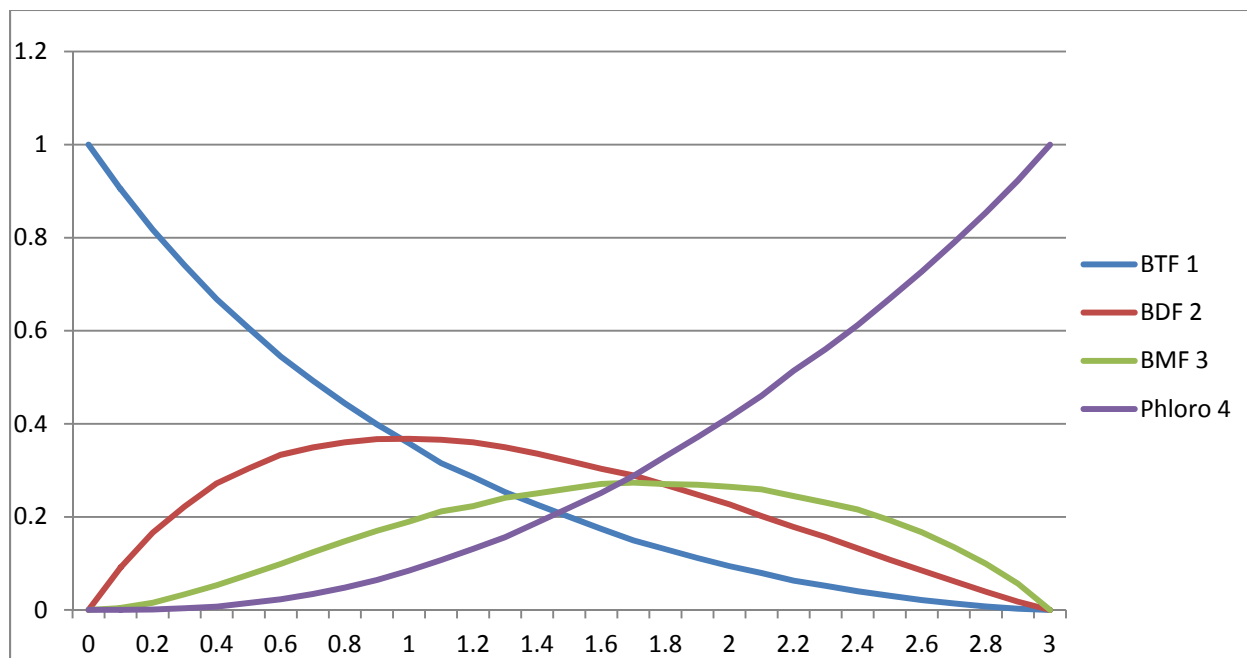
Supplementary Data: Expected statistical distribution of products

In the absence of rigorous kinetic modeling, statistical simulations can accurately determine expected product ratios depending on the stoichiometry of the reactants. The reaction outcome can be modeled as balls being placed into barrels. Consequently, the simulation was initially set up to randomly place 100 balls into 100 barrels; given the maximum number of nucleophiles able to react with BTF (**1**) is three, the number of balls that can go into a barrel was limited to three as well. This simulation was repeated 1000 times, and the average number of barrels with 0 (unreacted BTF (**1**)), 1 (BDF (**2**)), 2 (BMF (**3**)), or 3 (phloroglucinol (**4**)) balls was calculated along with each value's variance. These simulations were repeated with the number of balls ranging from 10 (0.1 equiv) to 300 (3.0 equiv) to obtain product distributions as a function of stoichiometry. The simulations were performed using R (<http://cran.r-project.org/>). Averaged data for the simulations is provided below (**Table S1** and **Figure S1**).

From these simulations, the expected product distribution when adding 1.0 equiv of an amine to BTF (**1**) is 35.8% of **1**, 36.8% of **2**, 19.0% of **3**, and 8.4% of **4**; under purely statistical control, addition of 1.0 equiv of amine to BTF would provide the highest yield of **2**, 36.8%. Looking a bit further, adding 2.0 equiv of amine to BTF would provide 9.4% of **1**, 22.7% of **2**, 26.5% of **3**, and 41.5% of **4**. Under purely statistical control, addition of 1.7 equiv of amine to BTF would provide the highest maximum theoretical yield of **3**, a mere 27.4%.

Supplementary Table S1. Calculated product distributions (averages and variances from simulations) as a function of stoichiometry.

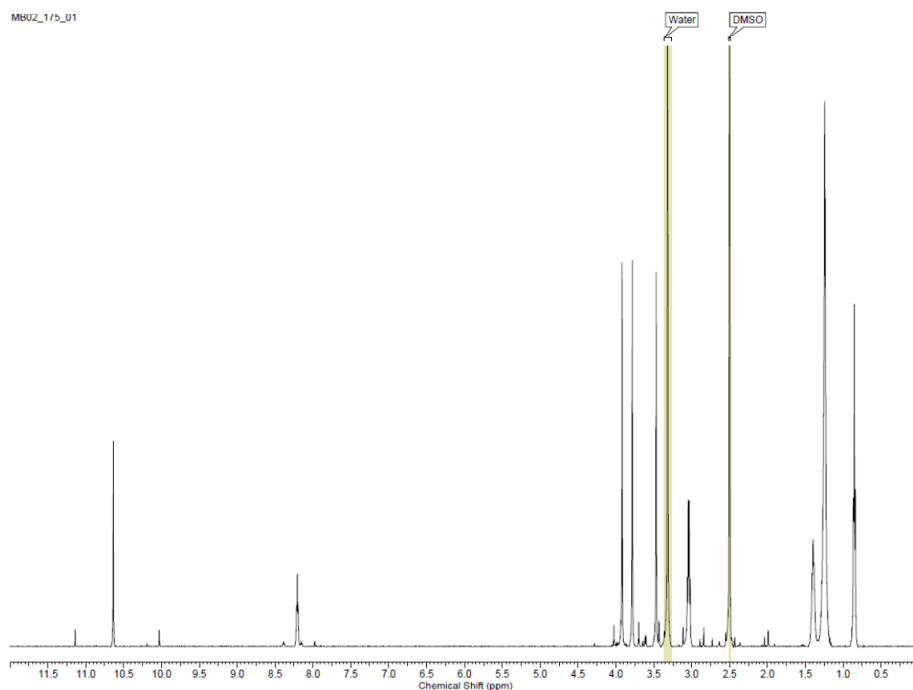
Equiv of amine to BTF	BTF (1)	BDF (2)	BMF (3)	Phloro (4)	Var of BTF	Var of BDF	Var of BMF	Var of Phloro
0	1	0	0	0	0	0	0	0
0.1	0.90445	0.09123	0.00419	0.00013	0.0000379	0.00144	0.0000338	0.00000128
0.2	0.81749	0.16603	0.01547	0.00101	0.00014	0.000501	0.000112	0.0000103
0.3	0.74068	0.22227	0.03342	0.00363	0.000267	0.000926	0.000225	0.0000328
0.4	0.6675	0.27214	0.05322	0.00714	0.000366	0.001222	0.000311	0.0000613
0.5	0.6054	0.30404	0.07572	0.01484	0.000455	0.00146	0.000431	0.000112
0.6	0.54465	0.33355	0.09895	0.02285	0.00059	0.0018	0.000557	0.000175
0.7	0.49253	0.3492	0.12401	0.03426	0.000745	0.00221	0.00065	0.000225
0.8	0.44381	0.36041	0.14775	0.04803	0.000795	0.00236	0.000927	0.000318
0.9	0.39868	0.36695	0.17006	0.06431	0.000882	0.00252	0.000993	0.000373
1	0.35818	0.36796	0.18954	0.08432	0.000802	0.0022	0.00113	0.000447
1.1	0.31565	0.36575	0.21155	0.10705	0.000805	0.00219	0.00132	0.000516
1.2	0.28549	0.36019	0.22315	0.13117	0.000833	0.00215	0.00144	0.000599
1.3	0.25325	0.34972	0.24081	0.15622	0.000815	0.00199	0.00157	0.000677
1.4	0.2261	0.33566	0.25038	0.18786	0.000812	0.00204	0.0017	0.000697
1.5	0.19998	0.31953	0.261	0.21949	0.000752	0.00185	0.00185	0.000752
1.6	0.17422	0.30322	0.2709	0.25166	0.000797	0.00191	0.00189	0.000792
1.7	0.14948	0.28894	0.27368	0.2879	0.000725	0.00175	0.0022	0.000874
1.8	0.13071	0.26862	0.27063	0.33004	0.000647	0.00152	0.00197	0.000798
1.9	0.11166	0.24794	0.26914	0.37126	0.000605	0.00141	0.00202	0.000806
2	0.09397	0.22668	0.26473	0.41462	0.00051	0.0012	0.00202	0.000784
2.1	0.0793	0.20156	0.25898	0.46016	0.000406	0.00103	0.00194	0.00071
2.2	0.06286	0.17832	0.24478	0.51404	0.000368	0.000996	0.00194	0.000683
2.3	0.05194	0.15671	0.23076	0.56059	0.000329	0.000854	0.00174	0.000624
2.4	0.04	0.13215	0.2157	0.61215	0.000257	0.00069	0.00155	0.000543
2.5	0.03052	0.10791	0.19262	0.66895	0.000218	0.000614	0.00148	0.000506
2.6	0.0212	0.08473	0.16694	0.72713	0.000149	0.000457	0.0012	0.000398
2.7	0.01384	0.06167	0.13514	0.78935	0.0000985	0.0031	0.000961	0.000316
2.8	0.0074	0.03924	0.09932	0.85404	0.0000585	0.000201	0.000665	0.000213
2.9	0.00268	0.01763	0.0567	0.92299	0.0000232	0.0000954	0.000365	0.000113
3	0	0	0	1	0	0	0	0



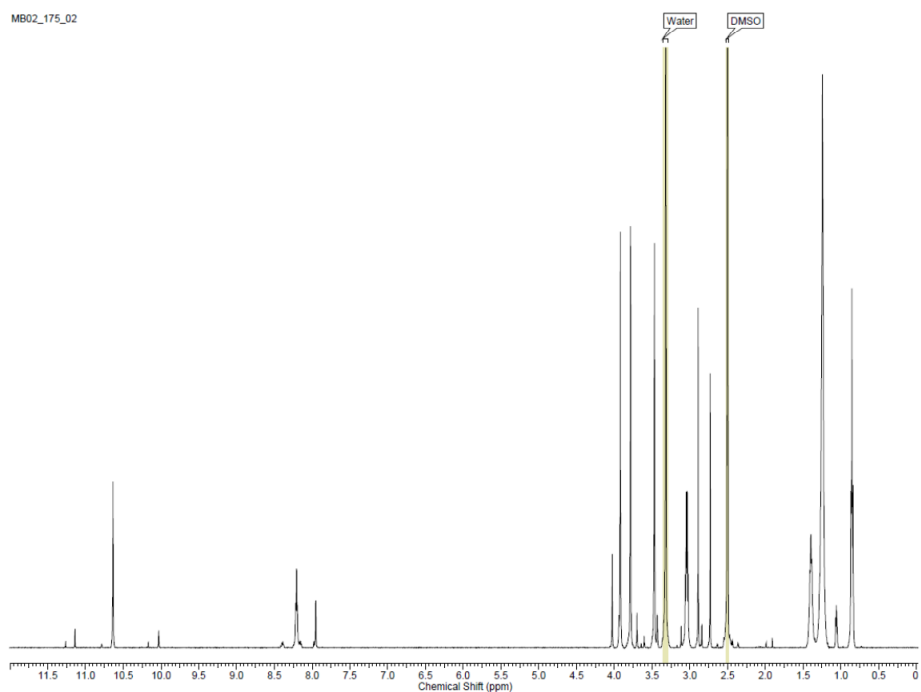
Supplementary Figure S1. Plot of simulated average product distributions as a function of reactant stoichiometry.

Supplementary Data: Temperature dependence of first ring opening of BTF

Runs were performed identically to the formation of compound **2a** shown above with respect to scale, stoichiometry, reaction time, and workup. Only the temperature of the reaction was varied. The ^1H NMR spectrum of the crude reaction mixture for the $-41\text{ }^\circ\text{C}$ run can be found as Figure S26.



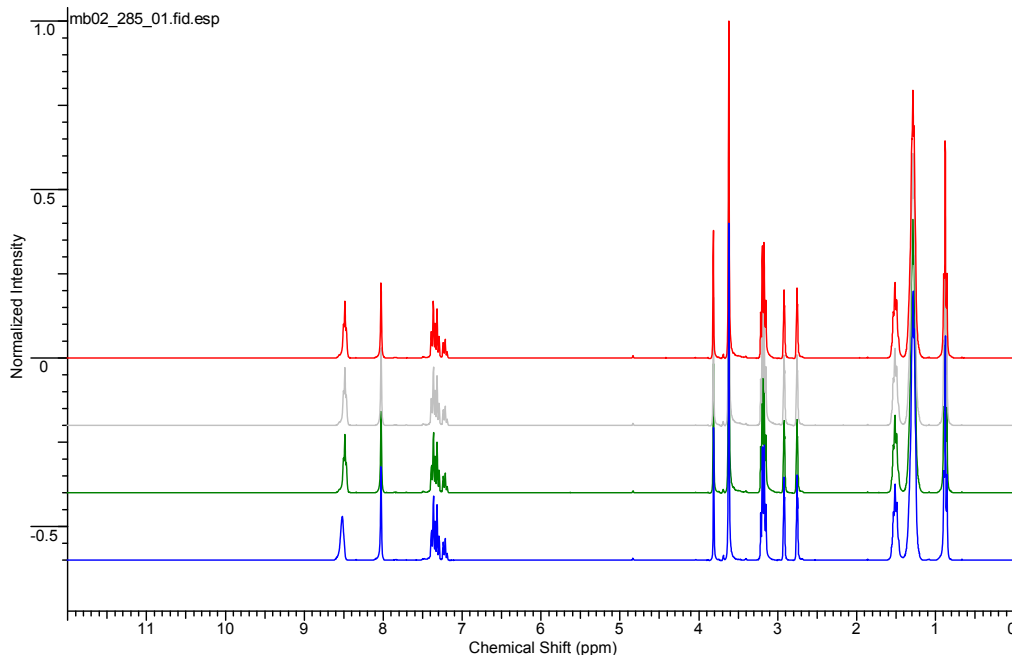
Supplementary Figure S2. ^1H NMR (d₆-DMSO) of crude reaction mixture to form **2a** from **BTF** at $0\text{ }^\circ\text{C}$.



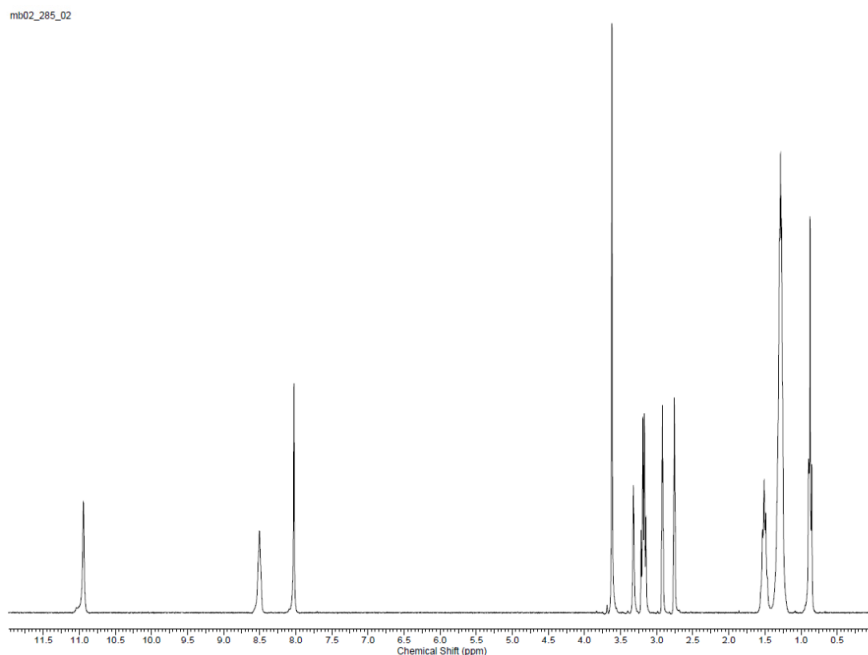
Supplementary Figure S3. ^1H NMR (d₆-DMSO) of crude reaction mixture to form **2a** from **BTF** at $40\text{ }^\circ\text{C}$.

Supplementary Data: Reversibility of reaction under elevated temperature conditions

To an NMR tube was added 13.7 mg (23 μmol) of compound **4aaa**, 0.7 mL of d_7 -DMF, and 2.3 mg (21 μmol) of benzylamine (**b**). The tube was then put into a VT controlled Mercury 300 spectrometer and held at a constant temperature of 50.0 ± 0.1 °C while ^1H NMR spectra were recorded at $t = 0, 1 \text{ h}, 2 \text{ h},$ and 3 h .

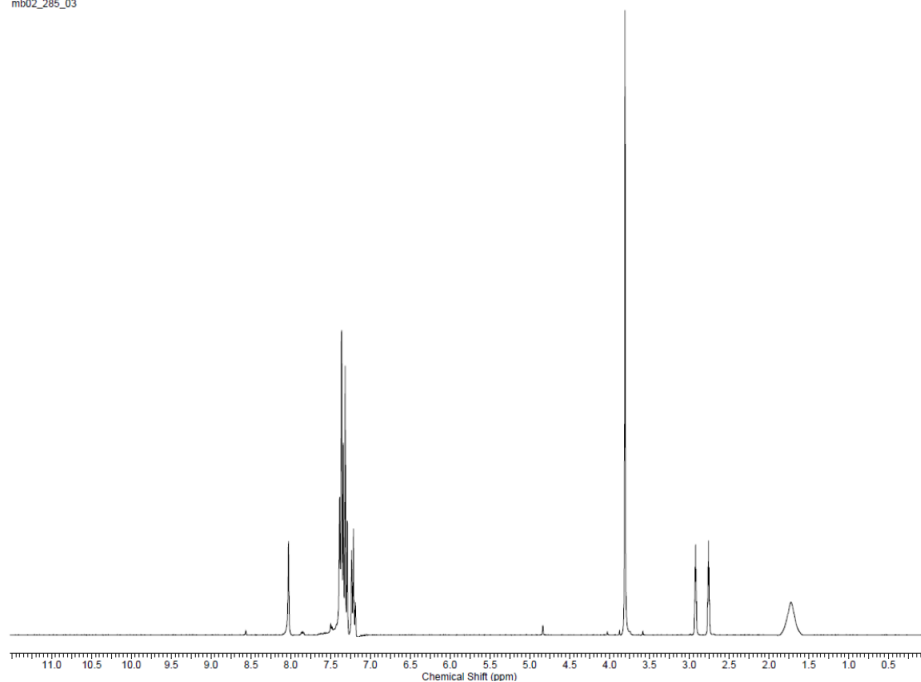


Supplementary Figure S4. Time arrayed ^1H NMR (d_7 -DMF) of reaction mixture at 50 °C; $t = 0$ is the bottommost spectrum, while $t = 3 \text{ h}$ is the topmost spectrum.



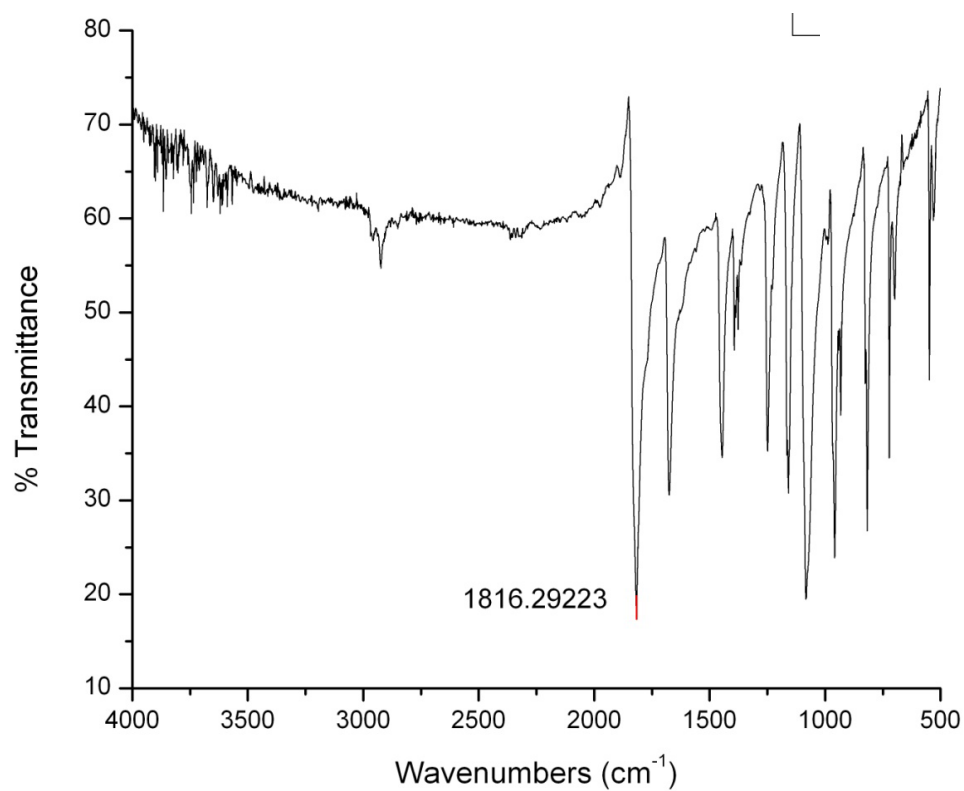
Supplementary Figure S5. ^1H NMR (d_7 -DMF) of compound **4aaa** at 50 °C.

mb02_285_03

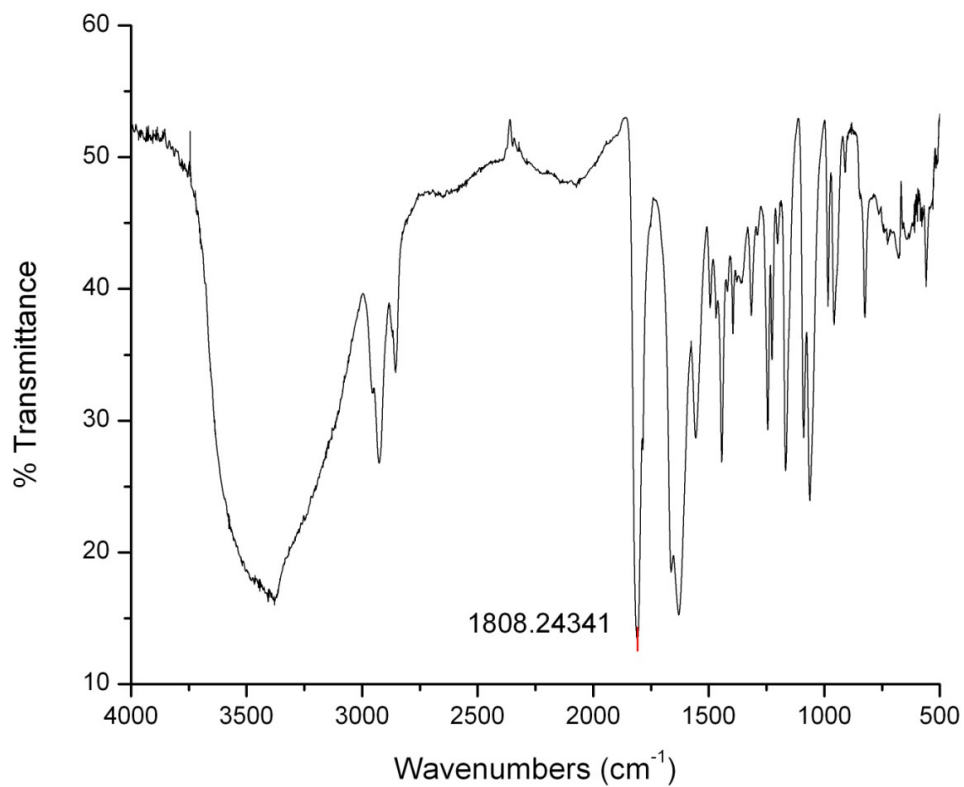


Supplementary Figure S6. ^1H NMR (d_7 -DMF) of benzylamine (**b**) at 50 °C.

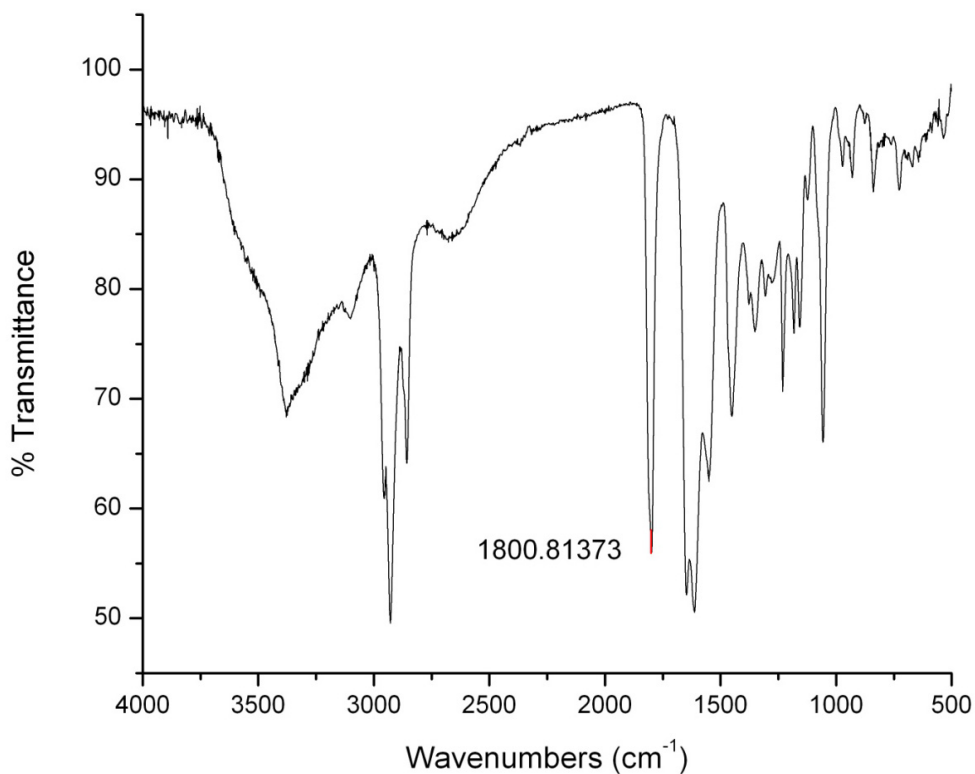
Supplementary Data: Infrared spectra of compounds **1**, **2a**, and **3aa**



Supplementary Figure S7. IR of compound **1** (BTF). The peak attributed to the lactone carbonyl is labeled.

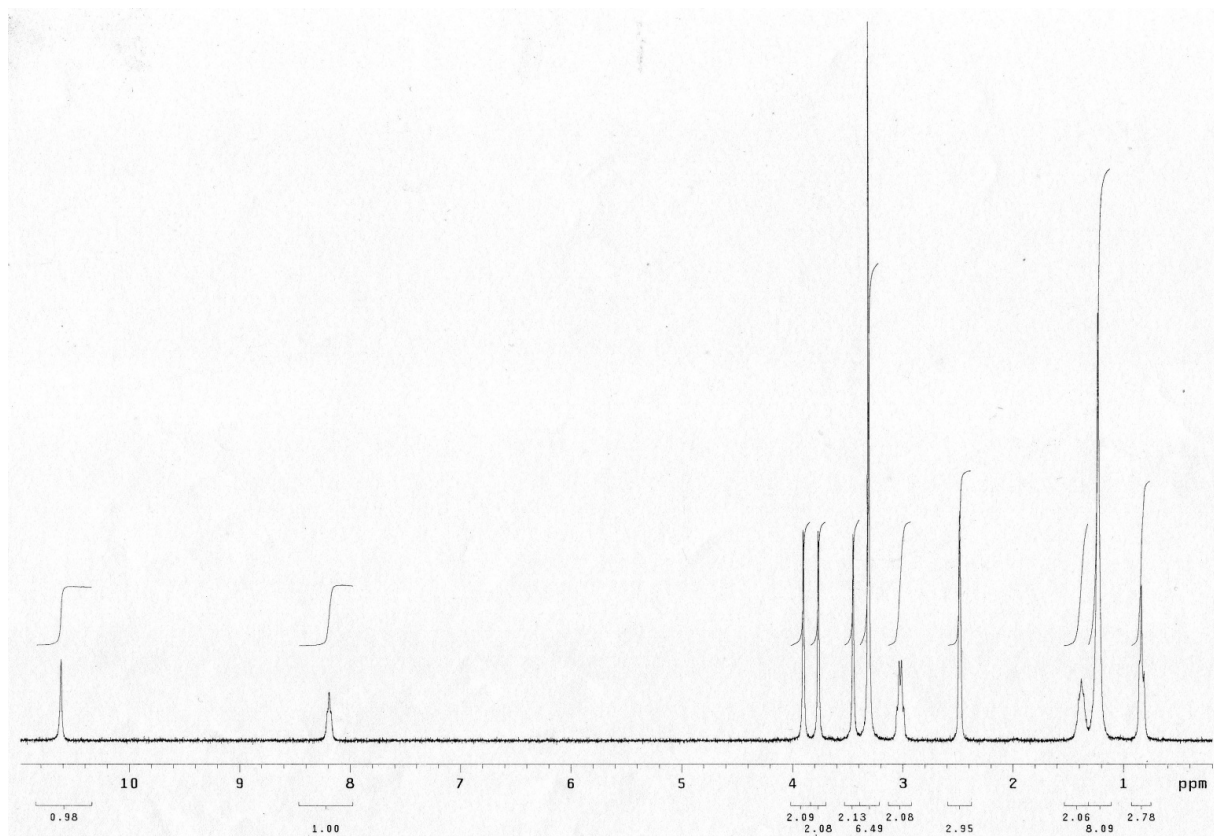


Supplementary Figure S8. IR of compound **2a**. The peak attributed to the lactone carbonyls (overlapped) is labeled.

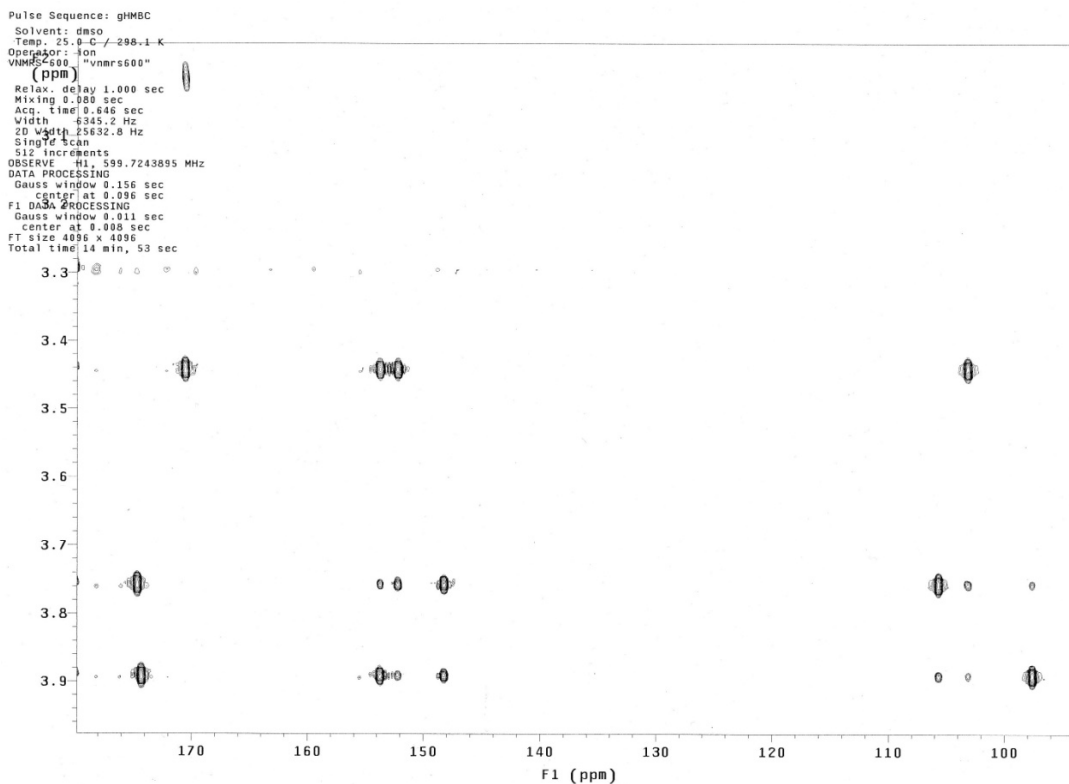


Supplementary Figure S9. IR of compound **3aa**. The peak attributed to the lactone carbonyl is labeled.

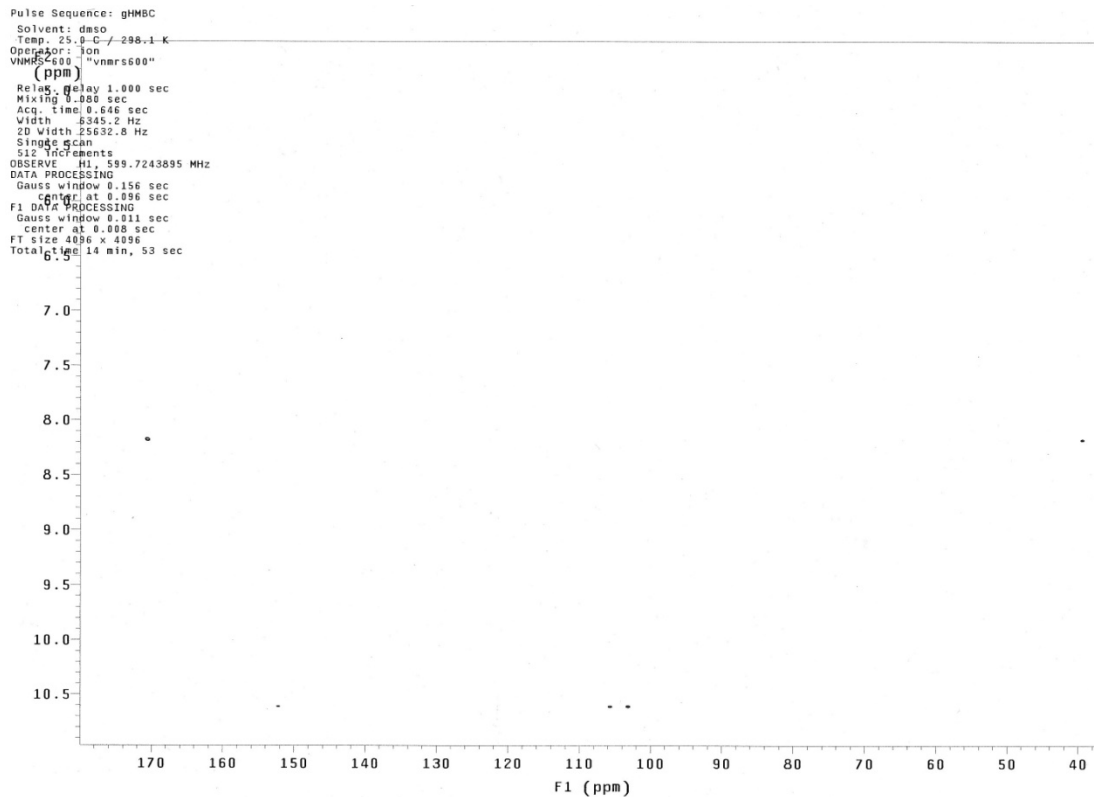
Supplementary Data : Assignment of compound 2a ^1H and ^{13}C NMR chemical shifts



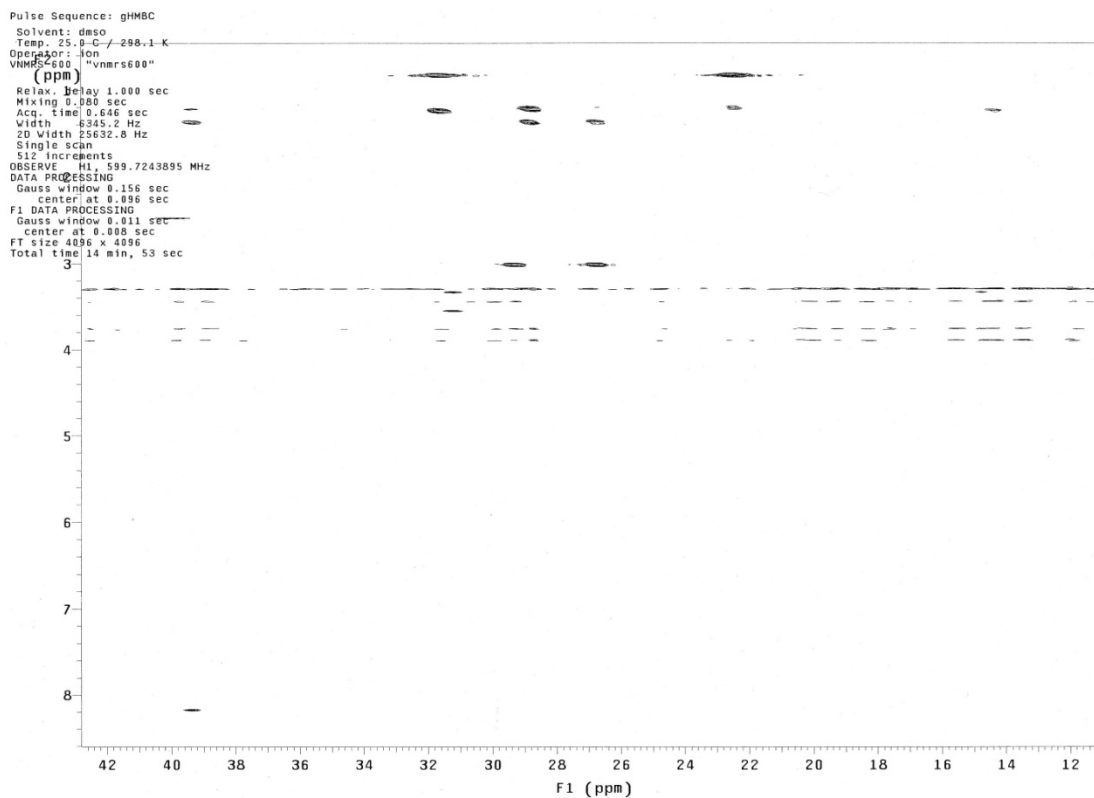
Supplementary Figure S10. ^1H NMR spectrum of compound 2a in DMSO- d_6 .



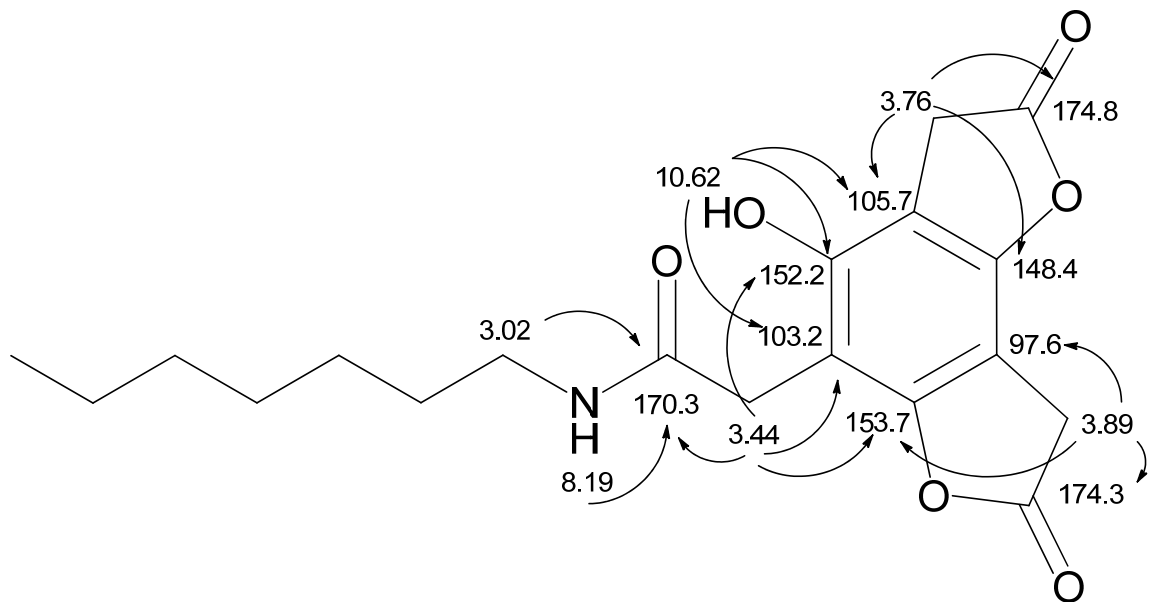
Supplementary Figure S11. Expansion of the gHMBC spectrum of compound 2a in DMSO- d_6 .



Supplementary Figure S12. Expansion of the gHMBC spectrum of compound **2a** in DMSO-*d*₆.



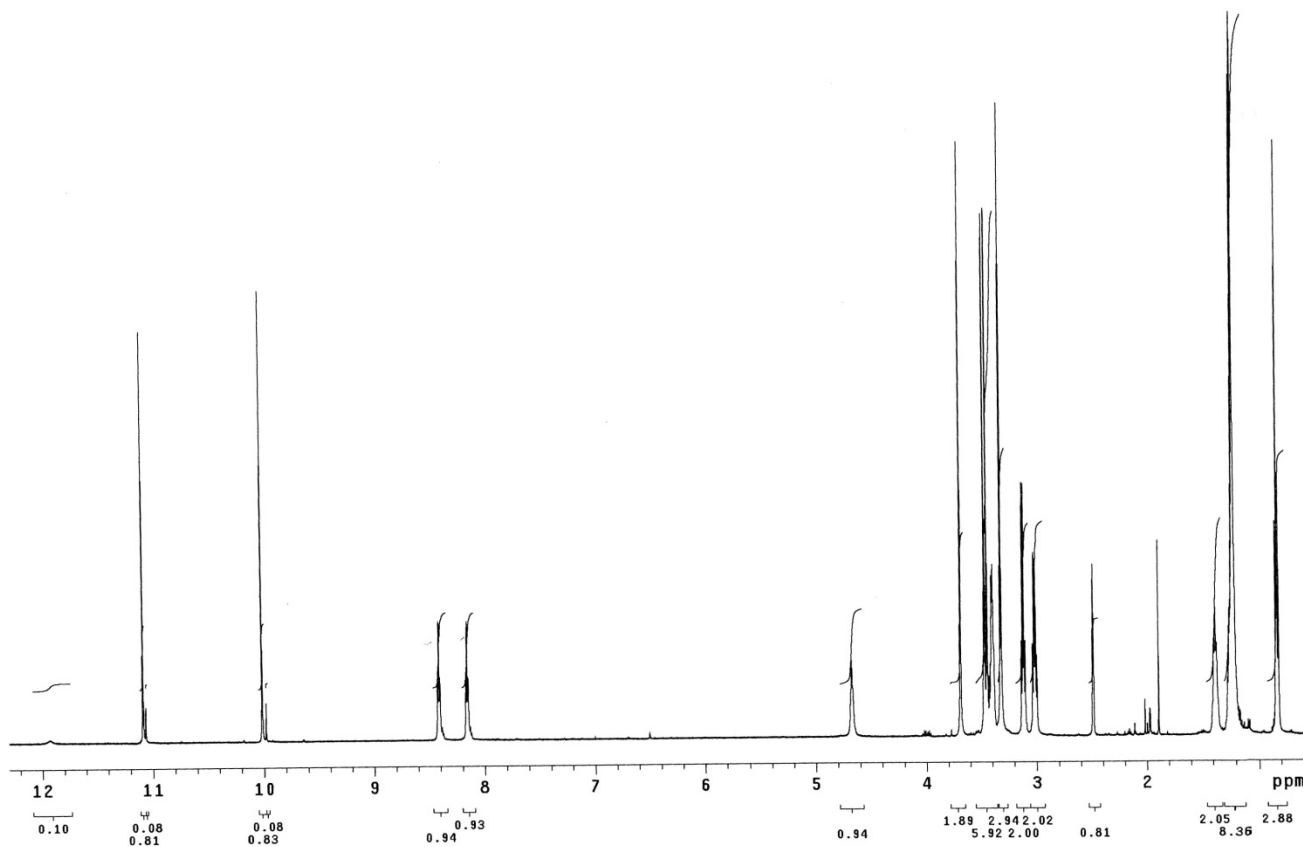
Supplementary Figure S13. Expansion of the gHMBC spectrum of compound **2a** in DMSO-*d*₆.



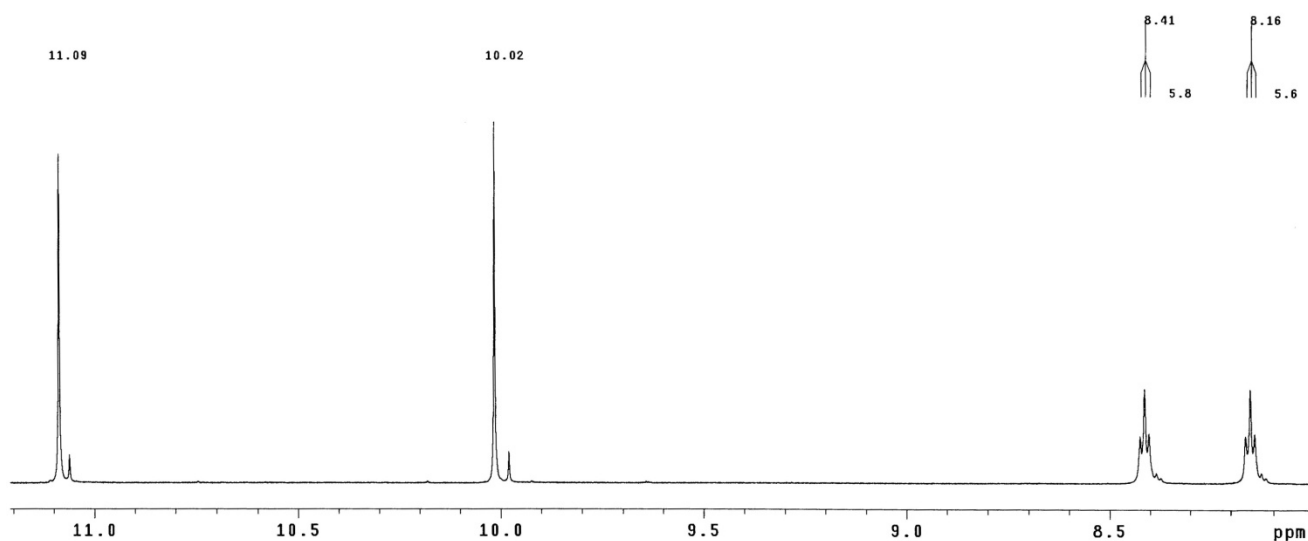
Supplementary Figure S14. Structure 2a with ¹H NMR chemical shifts (in ppm), ¹³C NMR chemical shifts (in ppm), and diagnostic heteronuclear couplings labeled.

The chemical shift assignments for compound 2 are based on the ¹H-¹³C one-bond and long-range couplings observed in the gHMBC spectrum. The triplet at 8.19 ppm is assigned as the NH, based on its chemical shift and multiplicity. It correlates with the carbonyl carbon at 170.3 ppm, which also couples with the methylene protons at 3.44 ppm. The 3.44 ppm protons couple with the carbon at 103.2 ppm, assigned as the carbon two bonds away based on its chemical shift, and with the carbons at 152.2 and 153.7 ppm. The former couples with the OH proton at 10.62 ppm, and is assigned as the carbon two bonds away from this proton. The latter couples with the methylene protons at 3.89 ppm, which in turn couple with the carbons at 97.6 and 174.3 ppm, assigned on the basis of the chemical shifts.

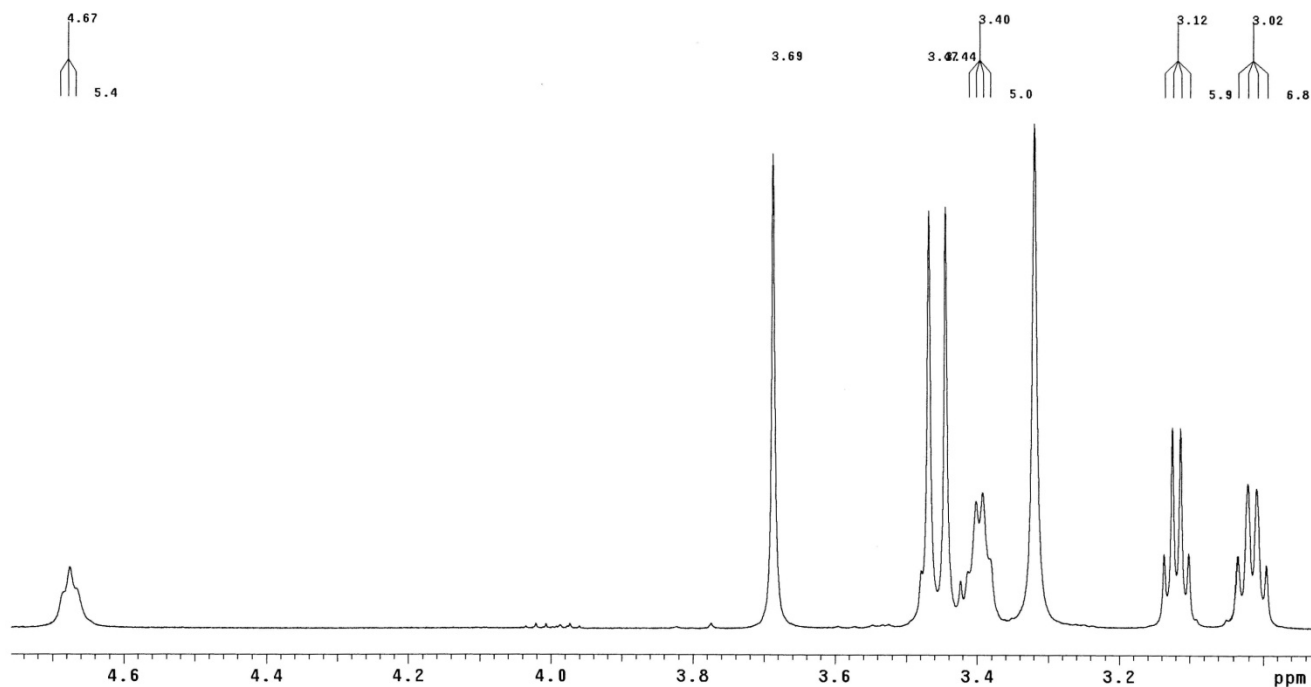
Supplementary Data: Assignment of regioisomerism for compound 3ad'



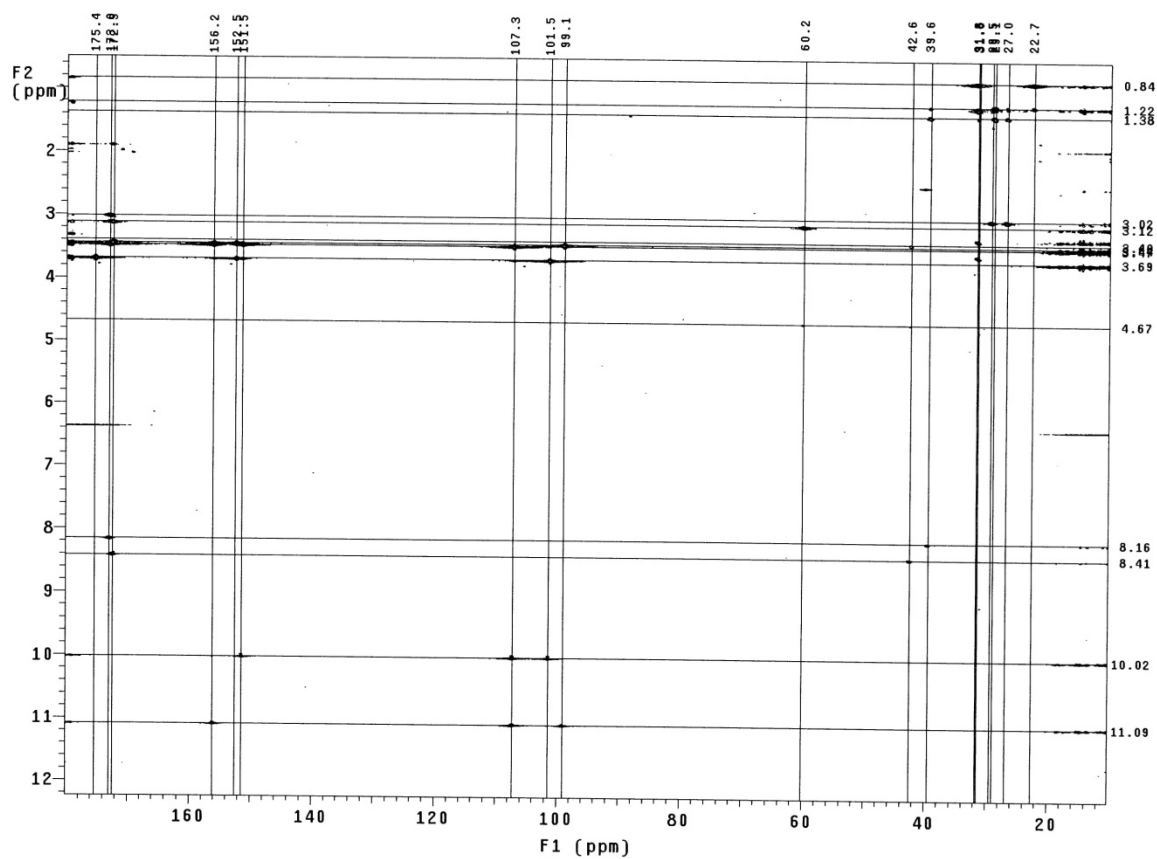
Supplementary Figure S15. ^1H NMR spectrum of compound 3ad' in DMSO- d_6 .



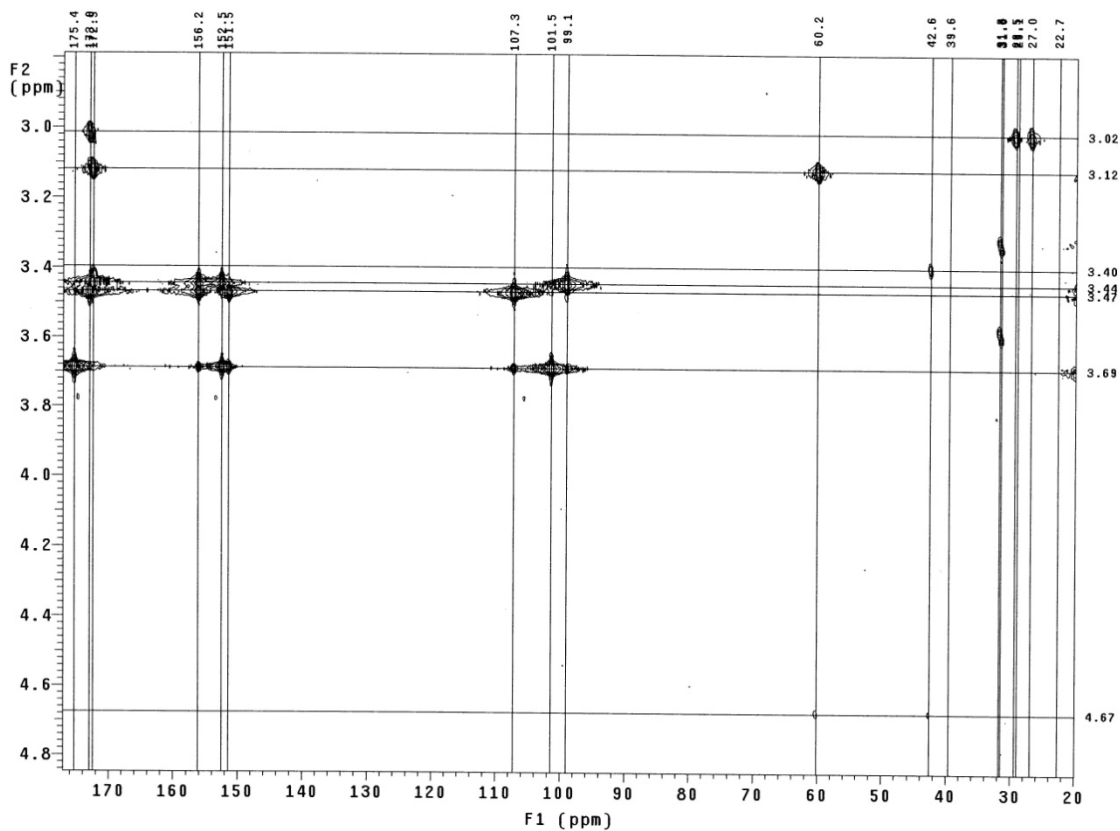
Supplementary Figure S16. Expansion (downfield region) of ^1H NMR spectrum of compound 3ad' in DMSO- d_6 .



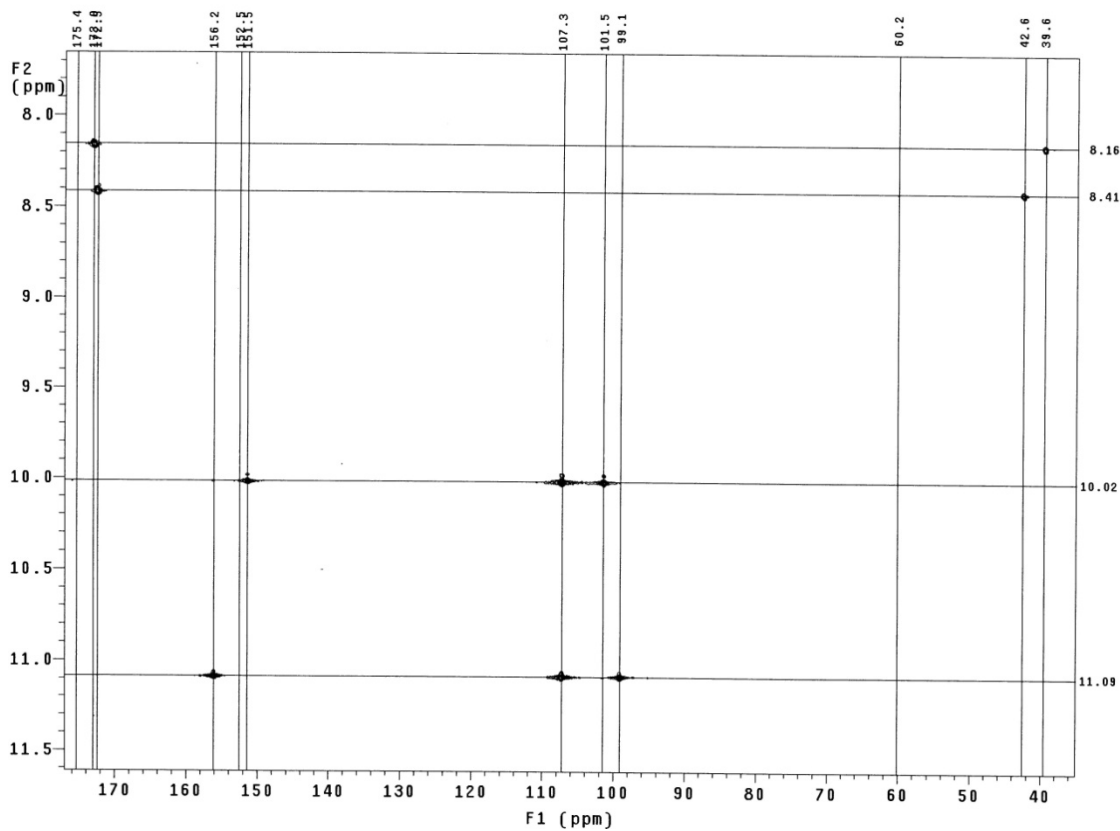
Supplementary Figure S17. Expansion (upfield region) of ^1H NMR spectrum of compound **3ad'** in $\text{DMSO-}d_6$.



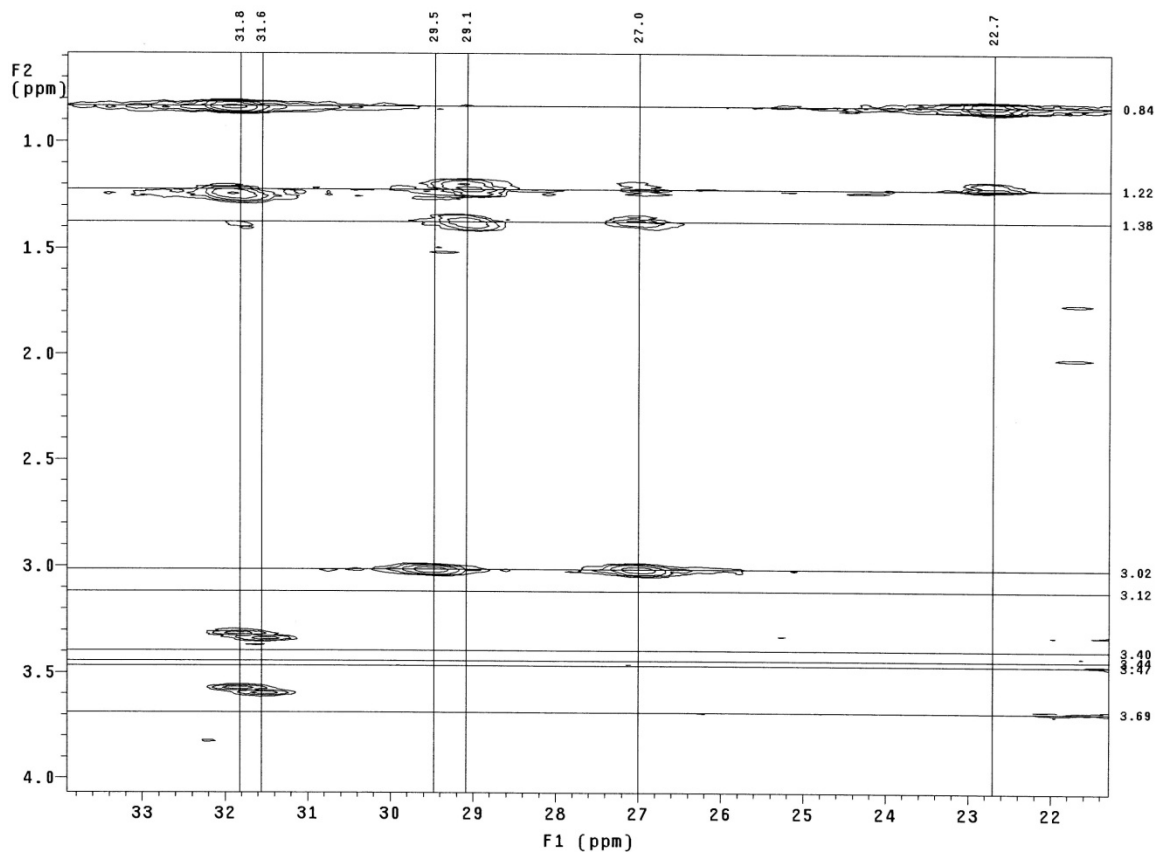
Supplementary Figure S18. gHMBC spectrum of compound **3ad'** in $\text{DMSO-}d_6$.



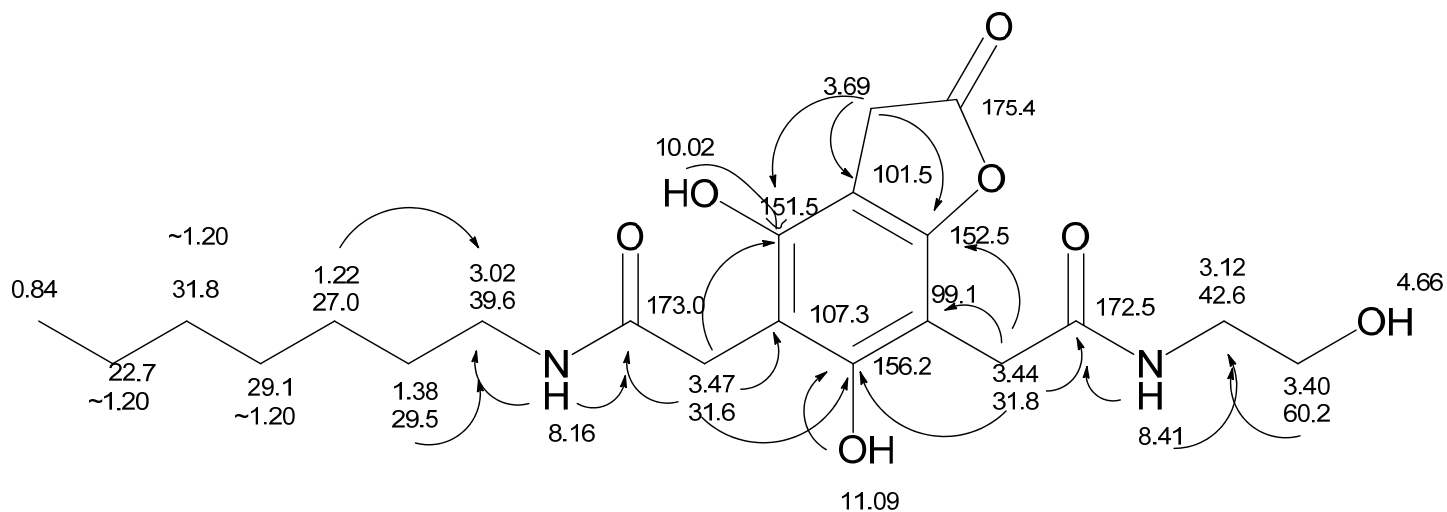
Supplementary Figure S19. Expansion of the gHMBC spectrum of compound 3ad' in DMSO-d₆.



Supplementary Figure S20. Expansion of the gHMBC spectrum of compound 3ad' in DMSO-d₆.



Supplementary Figure S21. Expansion of the gHMBC spectrum of compound **3ad'** in DMSO-*d*₆.



Supplementary Figure S22. Structure **3ad'** with ¹H NMR chemical shifts (in ppm), ¹³C NMR chemical shifts (in ppm), and diagnostic heteronuclear couplings labeled.

The assignment of the regiomerism and of the chemical shifts in compound **3ad'** was made based on the ^1H - ^{13}C one-bond and long-range couplings observed in the gHMBC spectrum. The triplets at 8.16 and 8.41 ppm have to be the NH protons, based on their chemical shifts and multiplicity. The latter couples with the carbon at 42.6 ppm, which also couples with the methylene protons at 3.40 ppm (which are on the carbon at 60.2 ppm and therefore adjacent to the hydroxyl group). The NH at 8.16 ppm couples with the carbon at 39.6 ppm, which in turn couples with the alkyl chain protons at 1.38 and 1.22 ppm. Couplings with the NH protons identify the adjacent CO carbons, which displayed couplings with the methylene protons two bonds away. Each of these methylene protons coupled with a carbon in the region 99–110 ppm (assigned as two-bonds away), and with two carbons in the region 151–157 ppm, which are assigned based on these couplings. The regiochemistry of compound **3ad'** is revealed by the OH protons at 10.02 and 11.09 ppm, which each couple with the carbon two bonds away.

Supplementary Data: Quantum chemical structure calculations

Input files, molecular geometries and orbital density plots were generated using Gabedit.¹ Low energy structures were optimized in G03² employing the B3LYP functional³⁻⁵ up to the 6-311++G(d,p) basis set;^{6,7} in all cases no negative frequencies were found in the optimized geometries.

Atomic charges were calculated via two different partitioning methods: Mulliken charges⁸ and NBO charges.⁹ NBO partitioning also allows for the calculation of orbital occupancies.

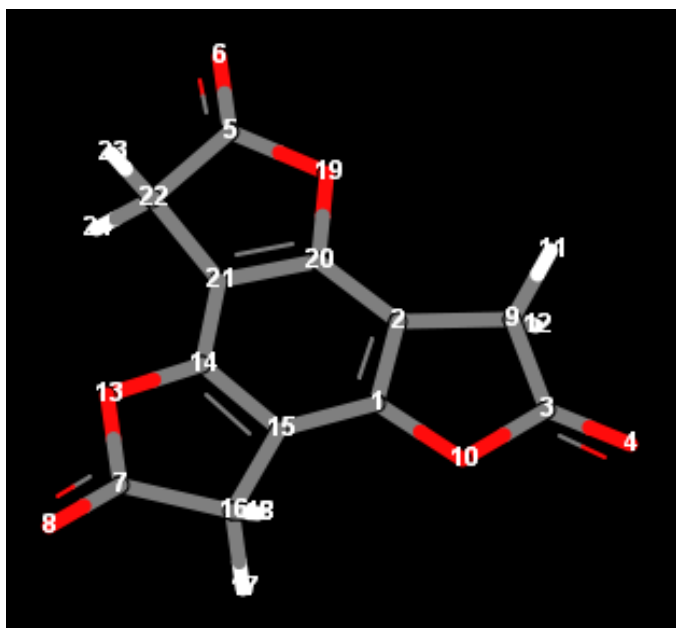
Electrophilicity values (ω) were calculated according to the relationship $\omega = \mu^2/\eta$, where μ is the electronic chemical potential and η is the global hardness.¹⁰ The values of μ and η can be approximated, applying Koopman's theorem,¹¹ by $\mu = \frac{\epsilon_{HOMO} + \epsilon_{LUMO}}{2}$ and $\eta = \epsilon_{LUMO} - \epsilon_{HOMO}$.

Further discussion: Atomic charges

The atomic charge (q_C) of the electrophilic carbonyl carbon of an ester has been shown to predict the aminolysis rate for simple *para* substituted phenyl acetates; this relationship has been thoroughly examined by Galabov, et al.¹² The authors find that increasing positive atomic charge at the carbonyl carbon correlates linearly to an increased rate in aminolysis (*n*-butylaminolysis in acetonitrile). We find no trend for **1–3** when using Mulliken partitioning (Table S5) and a negative qualitative relationship between atomic charge and reaction rate when employing NBO partitioning (for a general treatment of the accuracy of both partitioning methods, see the work of Bultinck, et al.¹³). The NBO carbonyl atomic charges do, however, parallel the experimentally determined ¹³C NMR chemical shifts discussed in the manuscript. The origin of the discrepancy is not clear at this stage, but may relate to intrinsic differences between the structures of the two systems (our multifunctionalized and effectively *meta* substituted aromatics versus Galabov's *para* substituted and resonance stabilized/destabilized derivatives) and/or to disparate aminolysis mechanisms. A dedicated quantum chemical investigation of *meta* substituted phenyl acetates may be required to probe strictly inductive effects in simple aminolysis processes.

Also reported below (Table S6) are the atomic charges of the phenolic oxygens (q_O) for **1–3**. The qualitative trend gleaned from the NBO values, that higher negative charge on the phenolic oxygen corresponds to slower aminolysis, may be mechanistically interpretable in the context of a putative phenoxide leaving group. Further discussion would be premature at this stage since a) atomic charges at these positions have not been evaluated systematically in the context of aminolysis rates in any systems and b) the mutual electronic

delocalization of the phenolic oxygen lone pairs into the aromatic ring and into the lactone ester carbonyls complicates a straightforward analysis in the absence of established empirical trends.

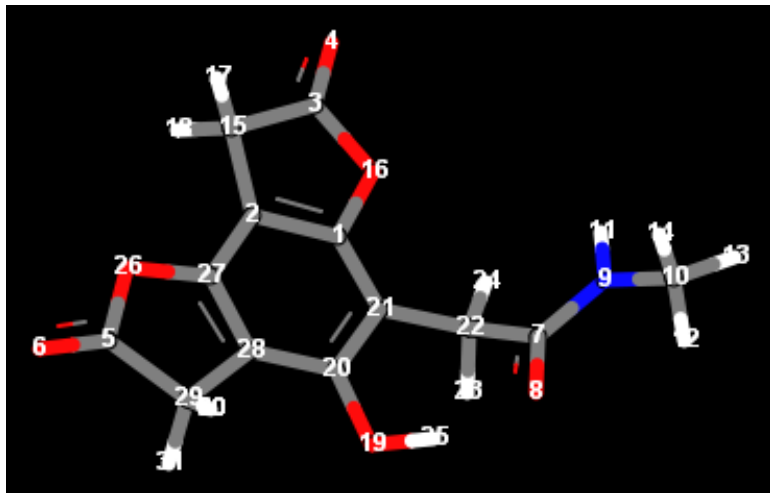


Supplementary Figure S23. Atomic numbering for optimized structure of **1** (BTF).

Supplementary Table S2. Atomic coordinates for the optimized structure of **1** (no imaginary frequencies; HF = -912.5115279).

C	0.958502	-0.978557	0.000422
C	1.361888	0.364726	0.000271
C	3.215233	-1.093385	-0.000212
O	4.279758	-1.620812	-0.001255
C	-0.660516	3.330871	0.000210
O	-0.736292	4.516507	-0.001315
C	-2.555058	-2.237230	-0.000537
O	-3.544571	-2.894698	-0.000899
C	2.857892	0.393287	0.000558
O	2.030855	-1.841579	0.000431
H	3.300904	0.866186	0.881392
H	3.301296	0.866863	-0.879785
O	-2.609593	-0.837278	0.000220
C	-1.325880	-0.341029	0.000198
C	-0.364967	-1.362308	0.000159
C	-1.088914	-2.671980	0.000486
H	-0.900421	-3.292670	-0.879839
H	-0.900597	-3.291822	0.881465
O	0.579683	2.679192	0.000161
C	0.368111	1.319190	0.000402
C	-0.996508	0.996957	0.000277

C	-1.769452	2.278080	0.000545
H	-2.400621	2.424730	0.881338
H	-2.401270	2.424331	-0.880001

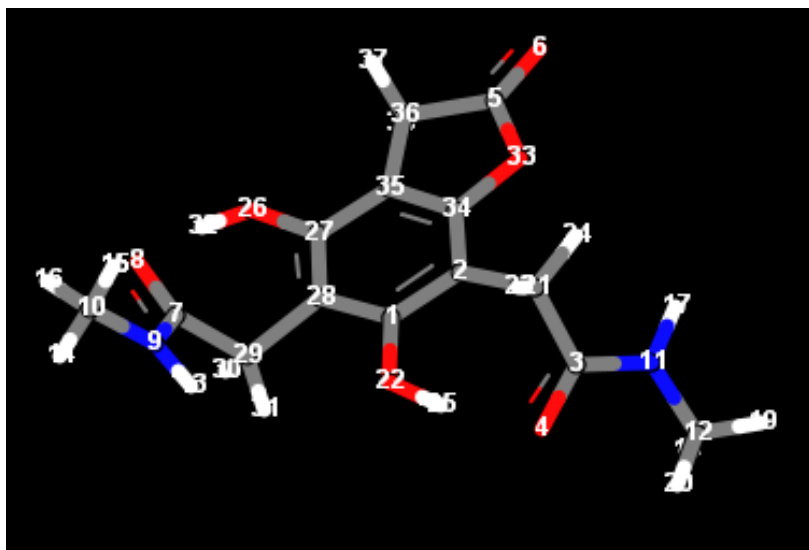


Supplementary Figure S24. Atomic numbering for optimized structure of **2** (BDF).

Supplementary Table S3. Atomic coordinates for the optimized structure of **2** (no imaginary frequencies; HF = -1008.4404542)

C	0.060447	1.075995	-0.310104
C	-1.281147	1.240914	0.036668
C	-0.167238	3.313500	-0.019145
O	0.179737	4.452066	0.021226
C	-3.759295	-1.332234	0.377183
O	-4.878573	-1.652305	0.623439
C	3.046954	-0.930399	-0.157171
O	2.876896	-2.135785	0.053587
N	4.057096	-0.233783	0.401738
C	5.005268	-0.827054	1.337452
H	4.098890	0.759576	0.235262
H	5.090309	-1.890018	1.119275
H	5.979102	-0.351582	1.216019
H	4.673223	-0.708722	2.372979
C	-1.539130	2.698186	0.254105
O	0.725048	2.295090	-0.350118
H	-1.852832	2.959750	1.269039
H	-2.271012	3.136790	-0.430550
O	0.356152	-2.531799	-0.743627
C	-0.124448	-1.293260	-0.505666
C	0.683015	-0.128712	-0.603924
C	2.117114	-0.167834	-1.092900
H	2.158919	-0.690634	-2.055533
H	2.467604	0.850789	-1.259775
H	1.324732	-2.560612	-0.544307

O	-3.365697	0.011465	0.408044
C	-2.028338	0.084712	0.082405
C	-1.472704	-1.164677	-0.180377
C	-2.552526	-2.186907	-0.004520
H	-2.357340	-2.914648	0.788737
H	-2.787591	-2.757441	-0.907750



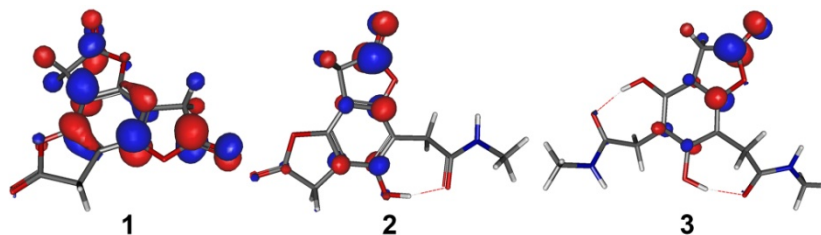
Supplementary Figure S25. Atomic numbering for the optimized structure of **3** (BMF).

Supplementary Table S4. Atomic coordinates for the optimized structure of **3** (no imaginary frequencies; HF = -1104.3665103)

C	-0.173054	-0.841579	0.008325
C	1.015561	-0.214472	0.445965
C	2.840686	-1.953826	0.241628
O	2.235538	-2.929813	-0.215507
C	1.851475	3.275796	0.359639
O	2.642385	4.139899	0.582871
C	-3.708973	-0.586933	-0.288808
O	-4.240654	0.529126	-0.291590
N	-4.203471	-1.625623	0.417778
C	-5.360069	-1.509264	1.295725
N	4.143699	-1.723528	-0.021353
C	4.932935	-2.566721	-0.910737
H	-3.663189	-2.476859	0.436483
H	-5.928913	-2.440055	1.276693
H	-5.062206	-1.291455	2.326027
H	-5.986562	-0.694733	0.936554
H	4.553080	-0.870368	0.326211
H	4.889896	-2.210239	-1.944200
H	5.971109	-2.573311	-0.576693
H	4.534253	-3.579149	-0.876337
C	2.132706	-0.956506	1.149182

O	-0.323307	-2.191246	0.115424
H	1.721953	-1.538862	1.981994
H	2.834011	-0.234617	1.568945
H	0.558004	-2.631443	0.040309
O	-2.169047	2.060507	-1.098873
C	-1.159189	1.295291	-0.625279
C	-1.244831	-0.111536	-0.534454
C	-2.446481	-0.845650	-1.096964
H	-2.652547	-0.486354	-2.111234
H	-2.218462	-1.908600	-1.154633
H	-3.035235	1.616591	-0.930990
O	2.147798	1.940260	0.627170
C	1.059307	1.157240	0.259813
C	0.024301	1.922205	-0.253220
C	0.443680	3.358601	-0.223968
H	-0.176327	3.996368	0.413650
H	0.489502	3.841385	-1.204776

Supplementary Table S5. Summary of calculated molecular reactivity descriptors for optimized structures



LUMO plots

Molecule	HOMO (eV)	LUMO (eV)	ω (eV)
1 (BTF)	-7.35149	-1.58943	1.73
2 (BDF)	-6.62602	-1.14207	1.38
3 (BMF)	-6.11717	-0.74451	1.09

Supplementary Table S6. Summary of calculated reactivity descriptors (localized to each carbonyl) for optimized structures

Molecule	Lactone (C=O)	q_C Mulliken	q_C NBO	$\pi^*_{C=O_{occ}}$
1 (BTF)	C ₃ =O ₄	0.331329	0.81445	0.18042
	C ₅ =O ₆	0.330912	0.81571	0.18036
	C ₇ =O ₈	0.330068	0.81586	0.18036
2 (BDF)	C ₃ =O ₄	0.236066	0.81697	0.18718
	C ₅ =O ₆	0.461656	0.81703	0.18328
3 (BMF)	C ₃ =O ₄	0.203391	0.81885	0.18951

Supplementary Table S7. Summary of calculated charges for phenolic oxygens for optimized structures

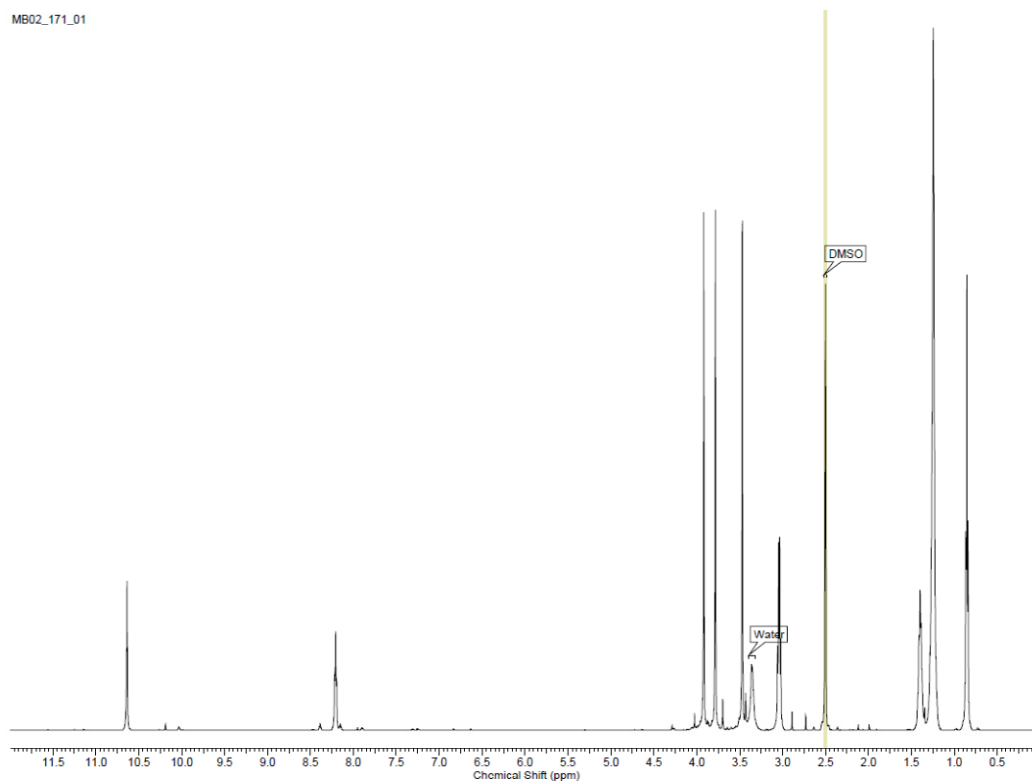
Molecule	Oxygen atom	q_{O} Mulliken	q_{O} NBO
1 (BTF)	O ₁₀ (C ₃ =O ₄)	-0.121061	-0.52149
	O ₁₉ (C ₅ =O ₆)	-0.120898	-0.52135
	O ₁₃ (C ₇ =O ₈)	-0.120635	-0.52086
2 (BDF)	O ₁₆ (C ₃ =O ₄)	-0.117032	-0.54245
	O ₂₆ (C ₅ =O ₆)	-0.097476	-0.52412
3 (BMF)	O ₃₃ (C ₃ =O ₄)	-0.120278	-0.54458

Supplementary Table S8. Summary of measured bond lengths for optimized structures

Molecule	Bond	Length (Å)
1 (BTF)	C ₃ =O ₄	1.18802
	C ₅ =O ₆	1.18806
	C ₇ =O ₈	1.18802
Average	C=O	1.18803
Average	C ₃ -O ₁₀	1.40091
	C ₅ -O ₁₉	1.40099
	C ₇ -O ₁₃	1.40101
Average	O-C(=O)	1.40091
2 (BDF)	C ₃ =O ₄	1.19095
	C ₅ =O ₆	1.18990
Average	C=O	1.19043
Average	C ₃ -O ₁₆	1.39387
	C ₅ -O ₂₆	1.40050
	O-C(=O)	1.39719
3 (BMF)	C ₃ =O ₄	1.19250
	C ₅ -O ₃₃	1.39393

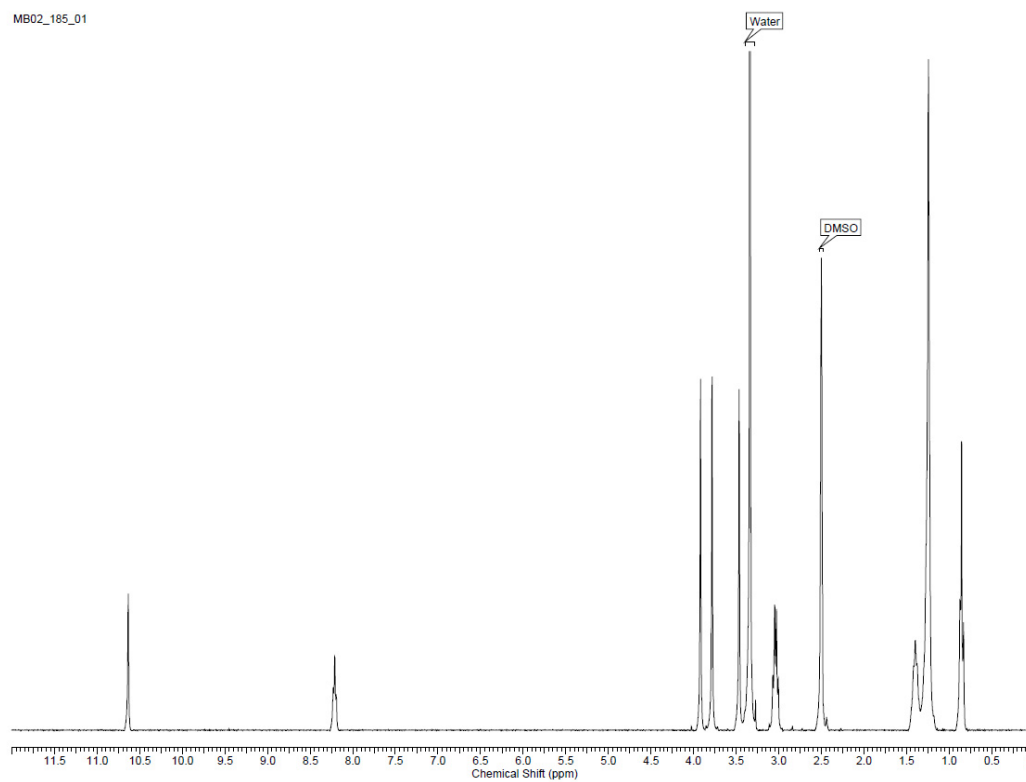
Supplementary Data: Characterization of novel compounds

MB02_171_01



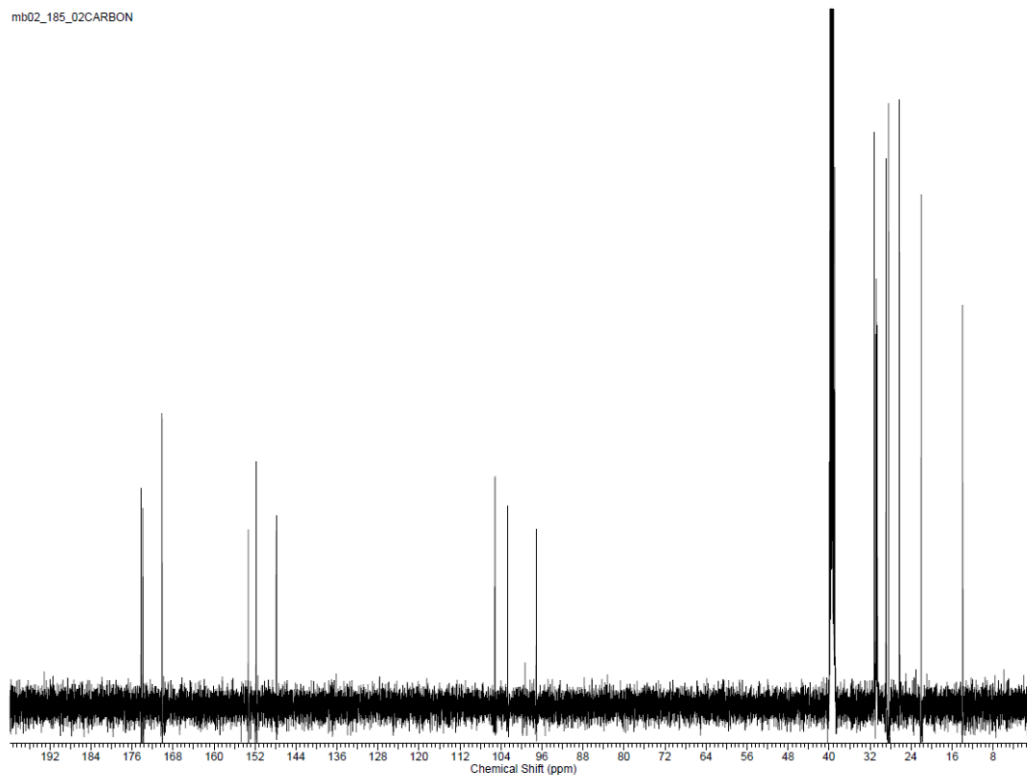
Supplementary Figure S26. ¹H NMR of 2a in *d*₆-DMSO (crude).

MB02_185_01



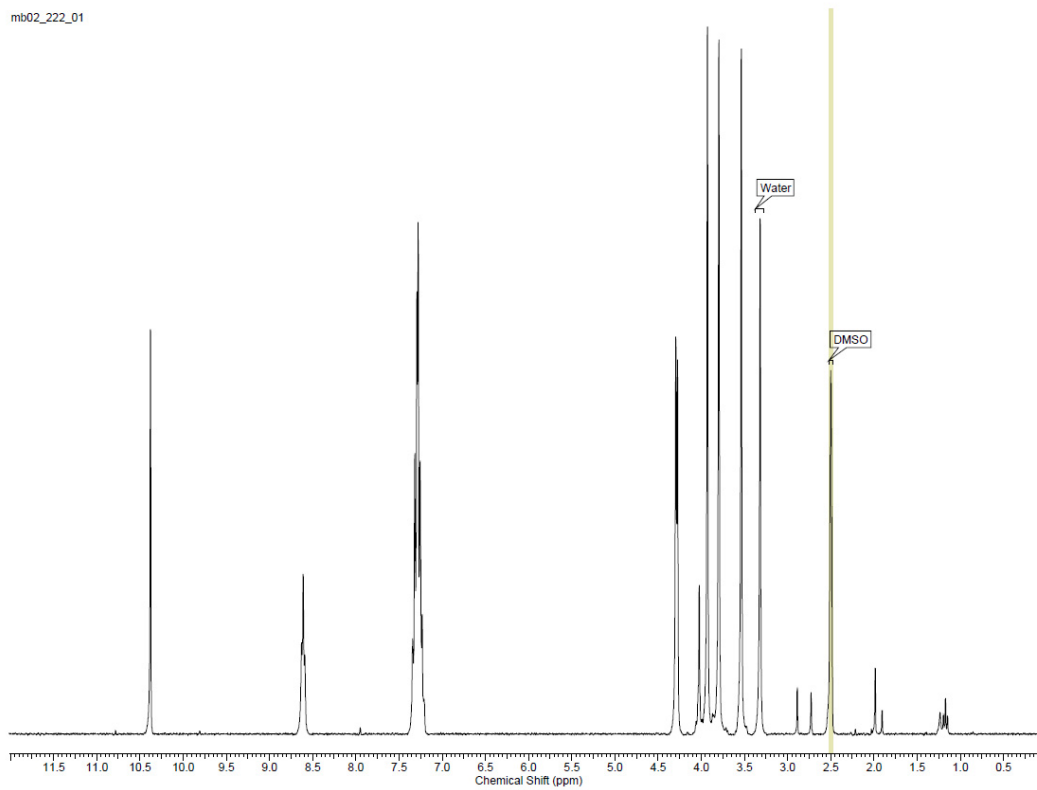
Supplementary Figure S27. ¹H NMR of 2a in *d*₆-DMSO (purified).

mb02_185_02CARBON

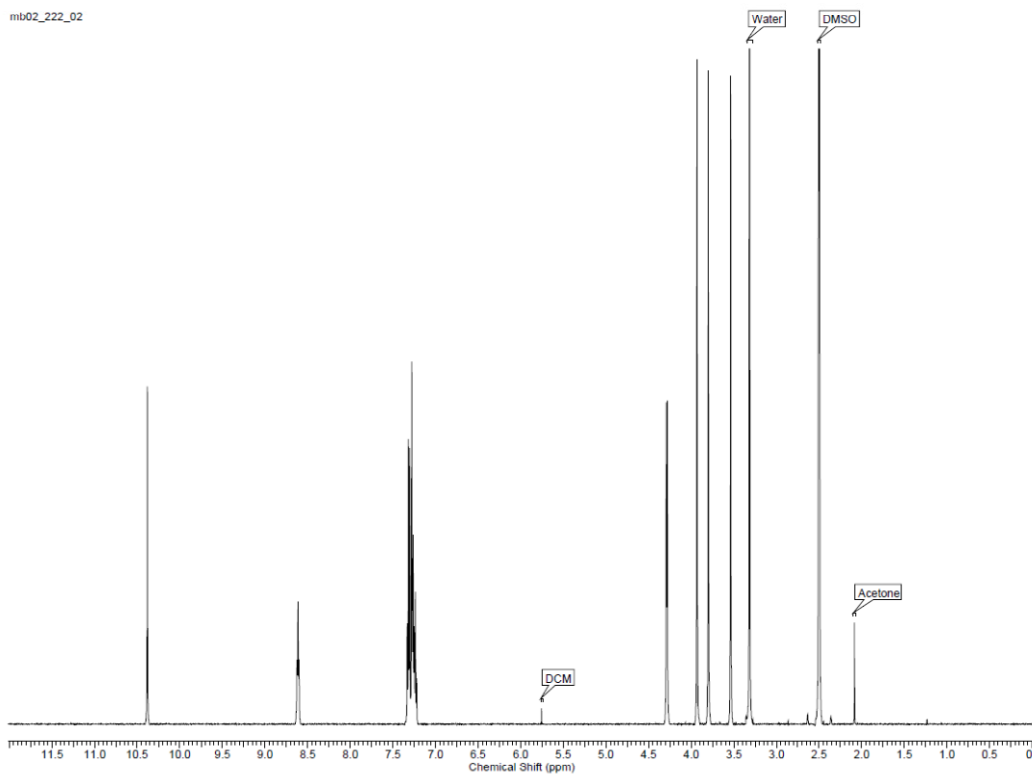


Supplementary Figure S28. ^{13}C NMR of **2a** in d_6 -DMSO (purified).

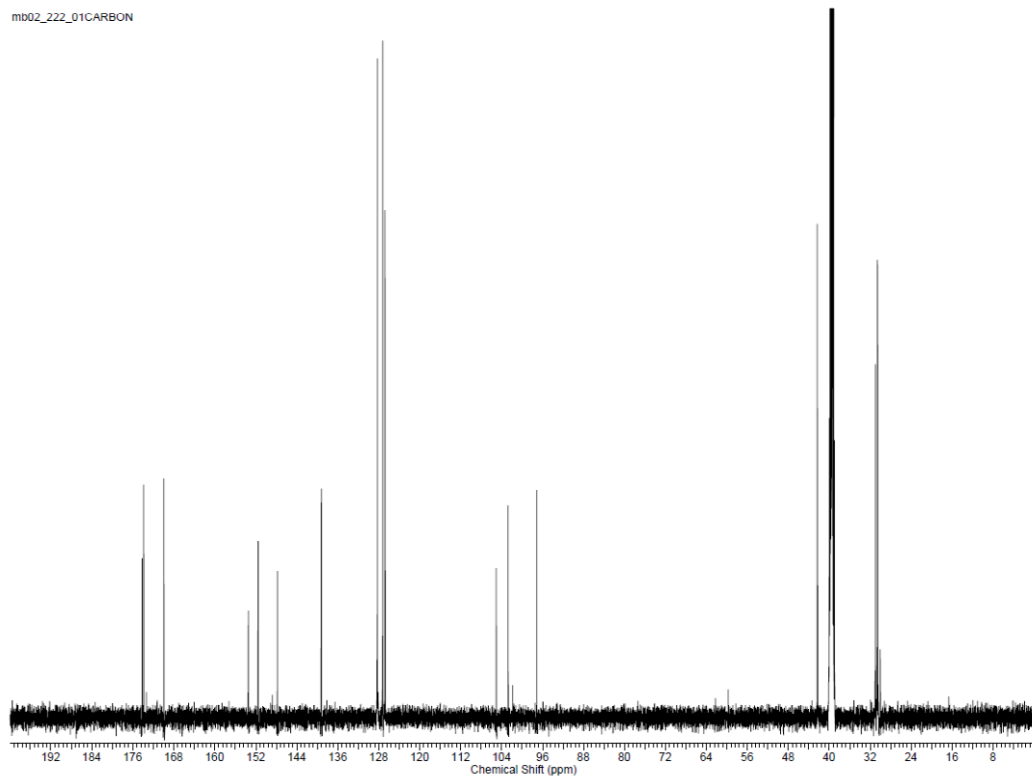
mb02_222_01



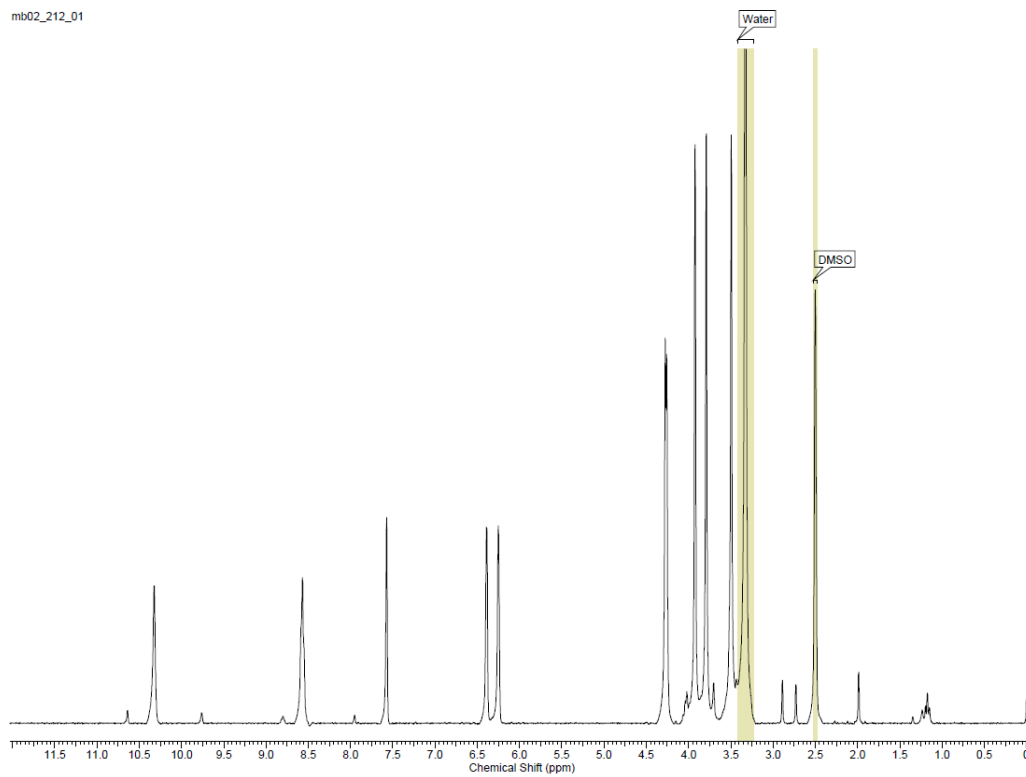
Supplementary Figure S29. ^1H NMR of **2b** in d_6 -DMSO (crude).



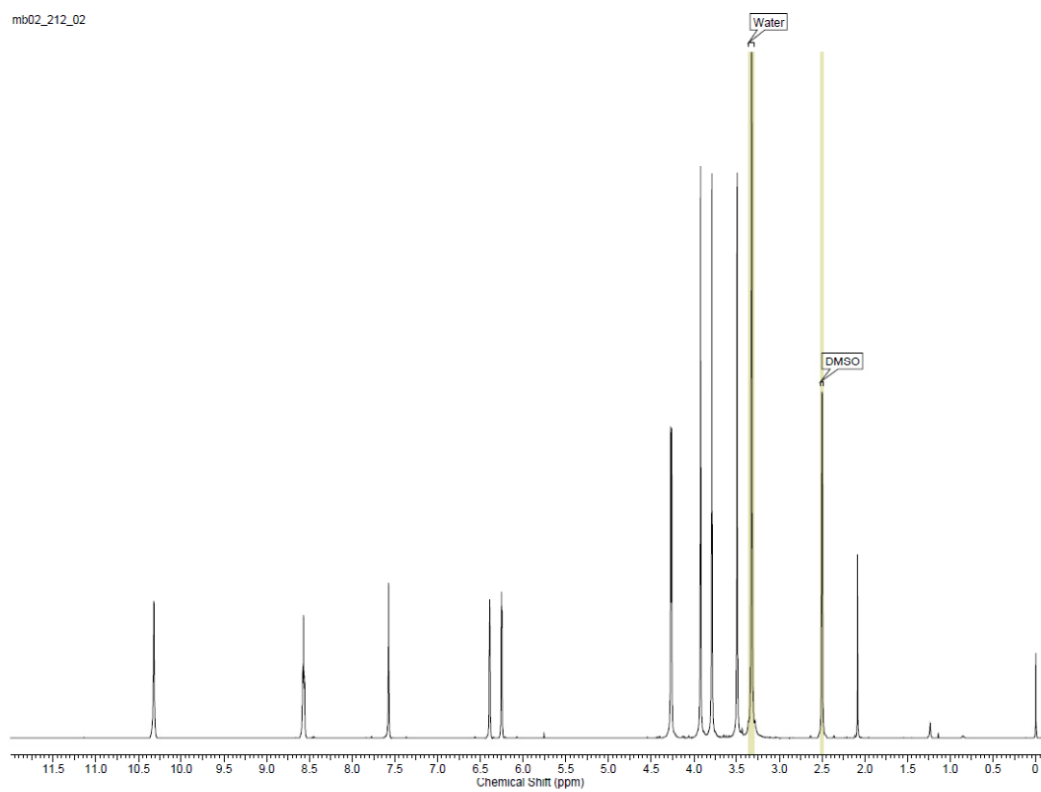
Supplementary Figure S30. ^1H NMR of **2b** in d_6 -DMSO (purified).



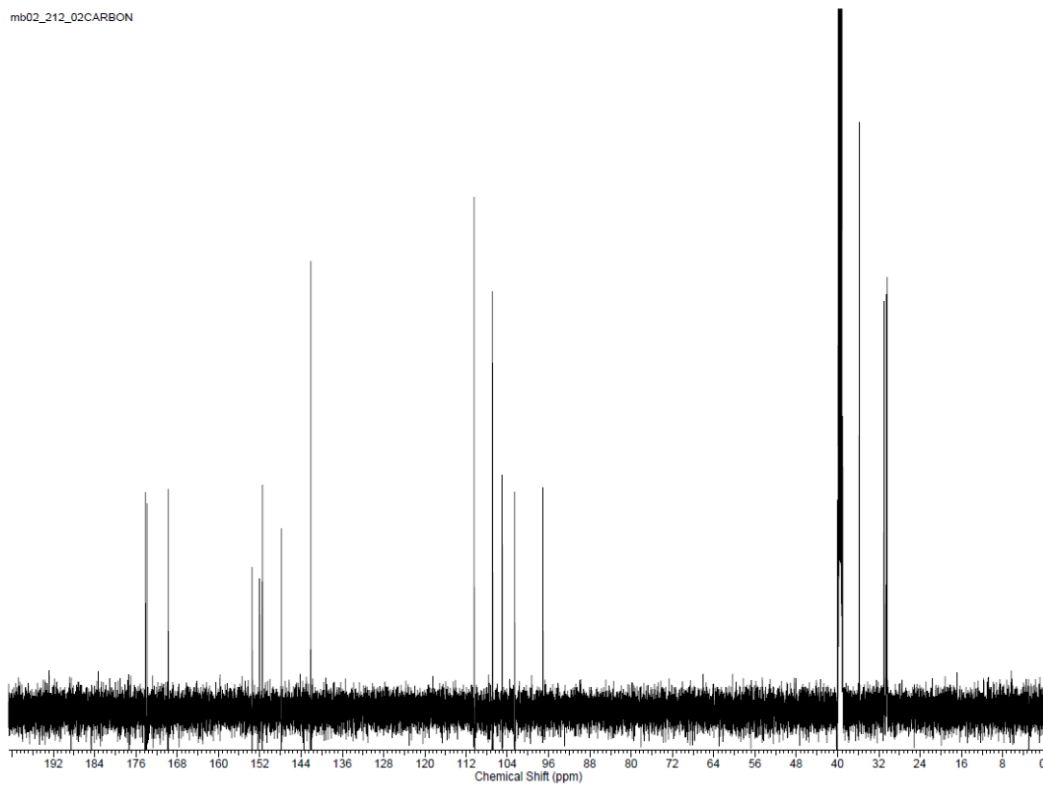
Supplementary Figure S31. ^{13}C NMR of **2b** in d_6 -DMSO (purified).



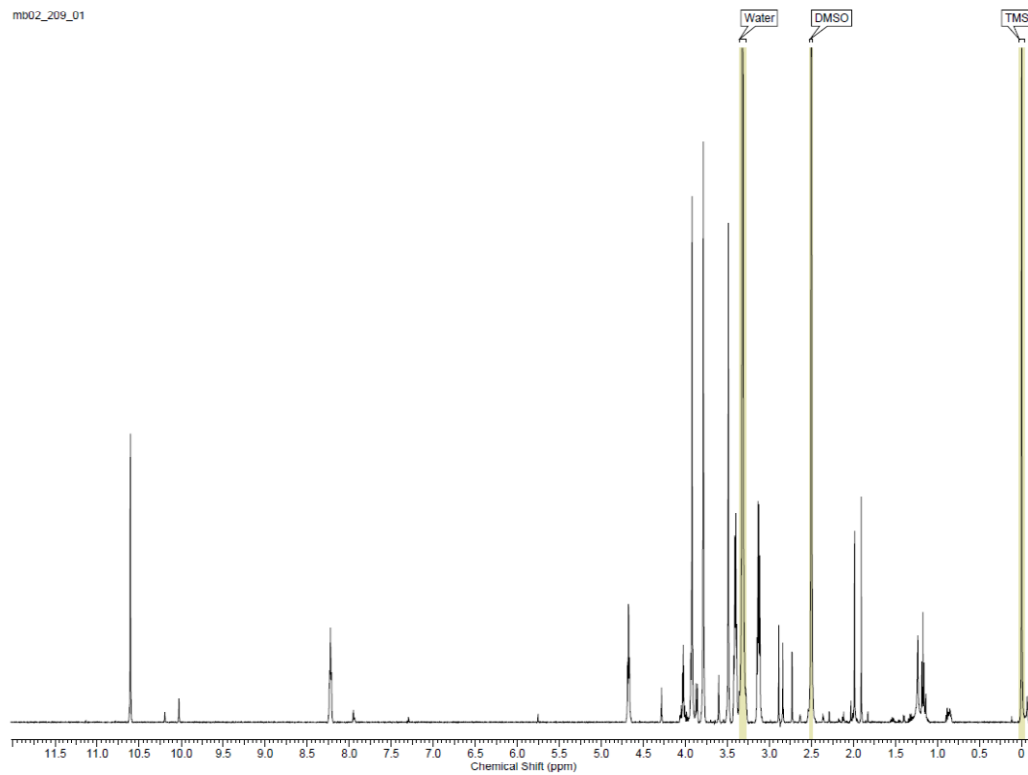
Supplementary Figure S32. ^1H NMR of **2c** in d_6 -DMSO (crude).



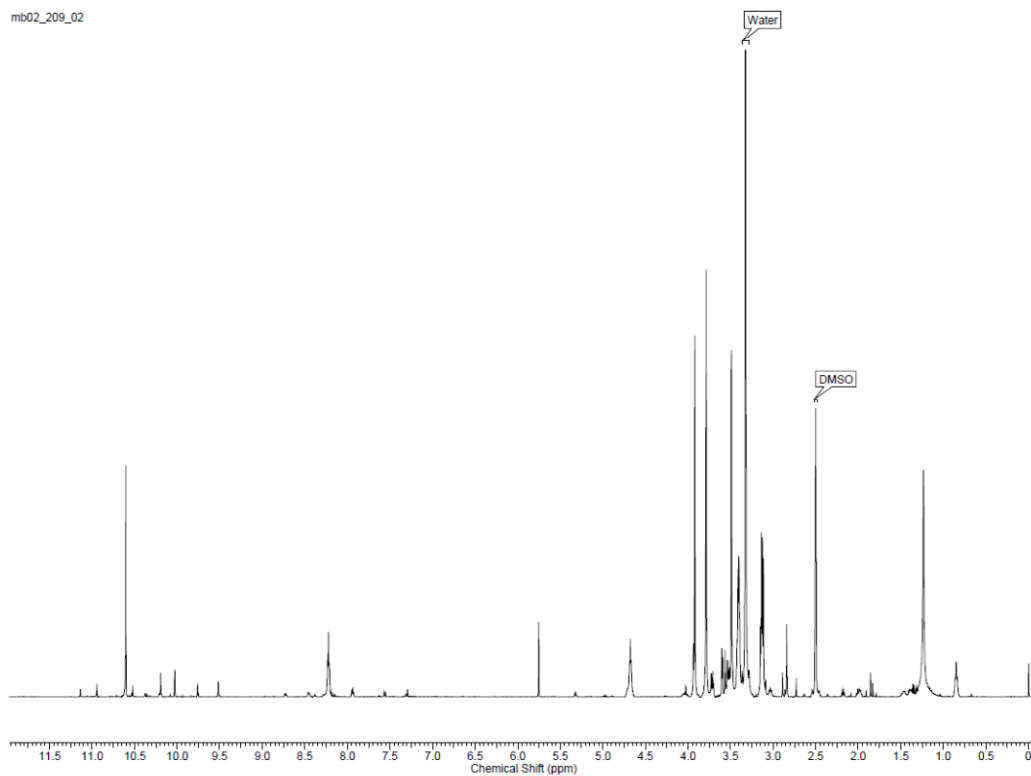
Supplementary Figure S33. ^1H NMR of **2c** in d_6 -DMSO (purified).



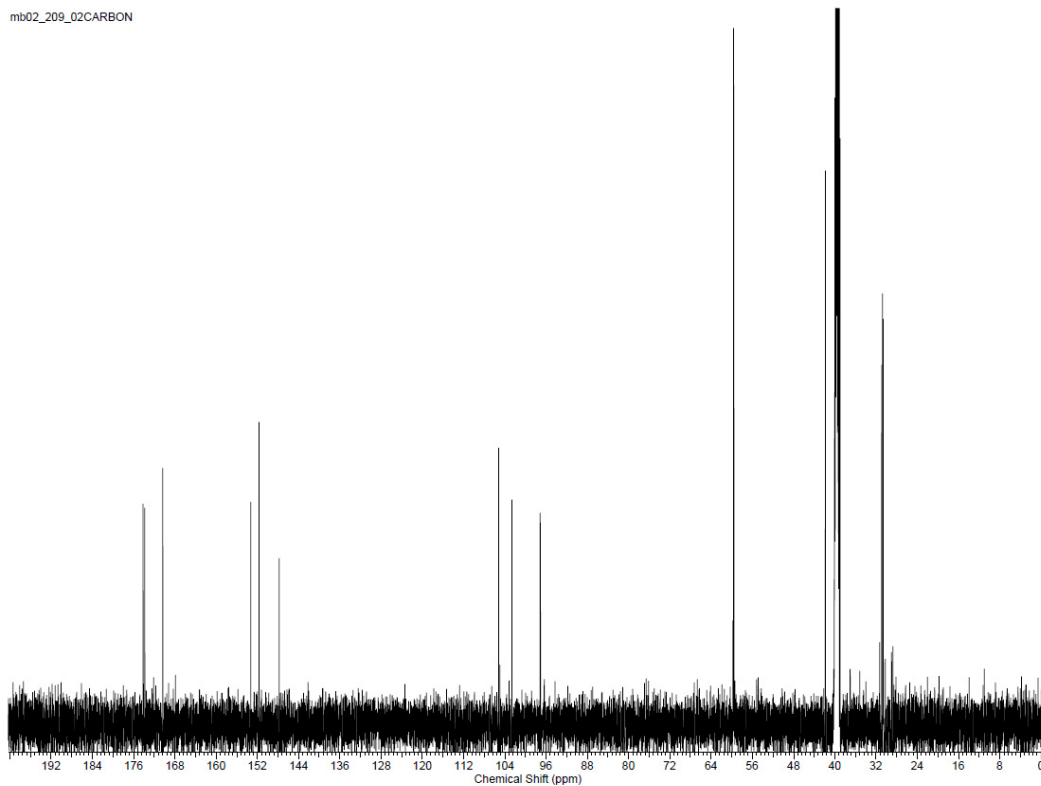
Supplementary Figure S34. ^{13}C NMR of **2c** in d_6 -DMSO (purified).



Supplementary Figure S35. ^1H NMR of **2d** in d_6 -DMSO (crude).

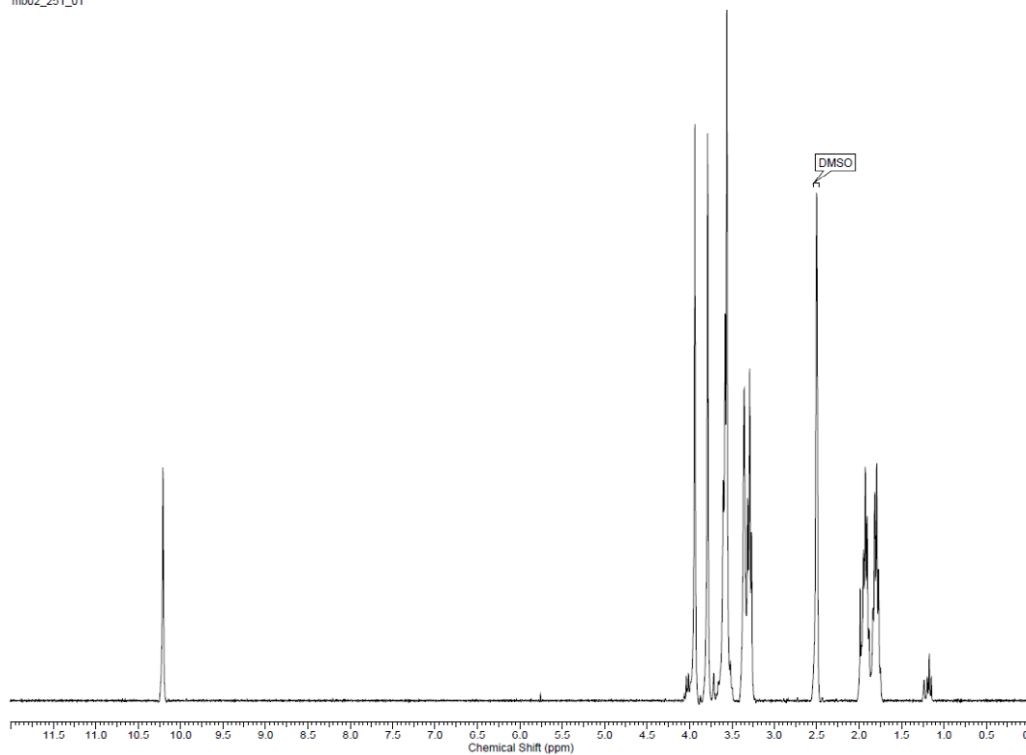


Supplementary Figure S36. ^1H NMR of **2d** in d_6 -DMSO (purified).



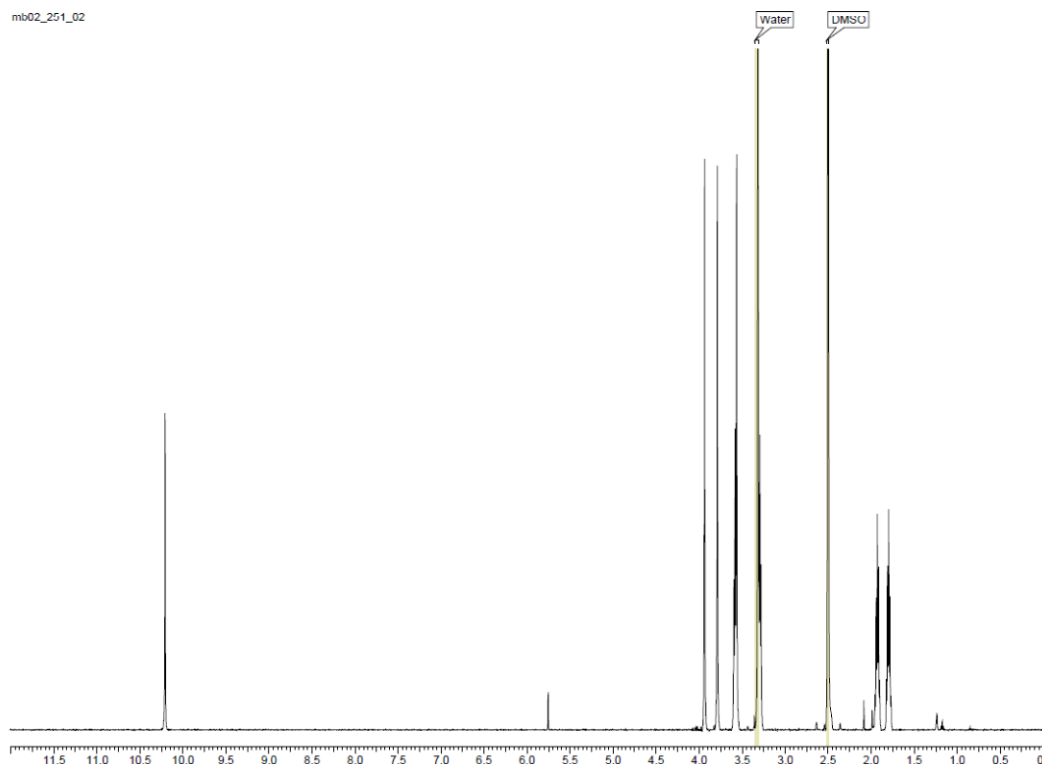
Supplementary Figure S37. ^{13}C NMR of **2d** in d_6 -DMSO (purified).

mb02_251_01



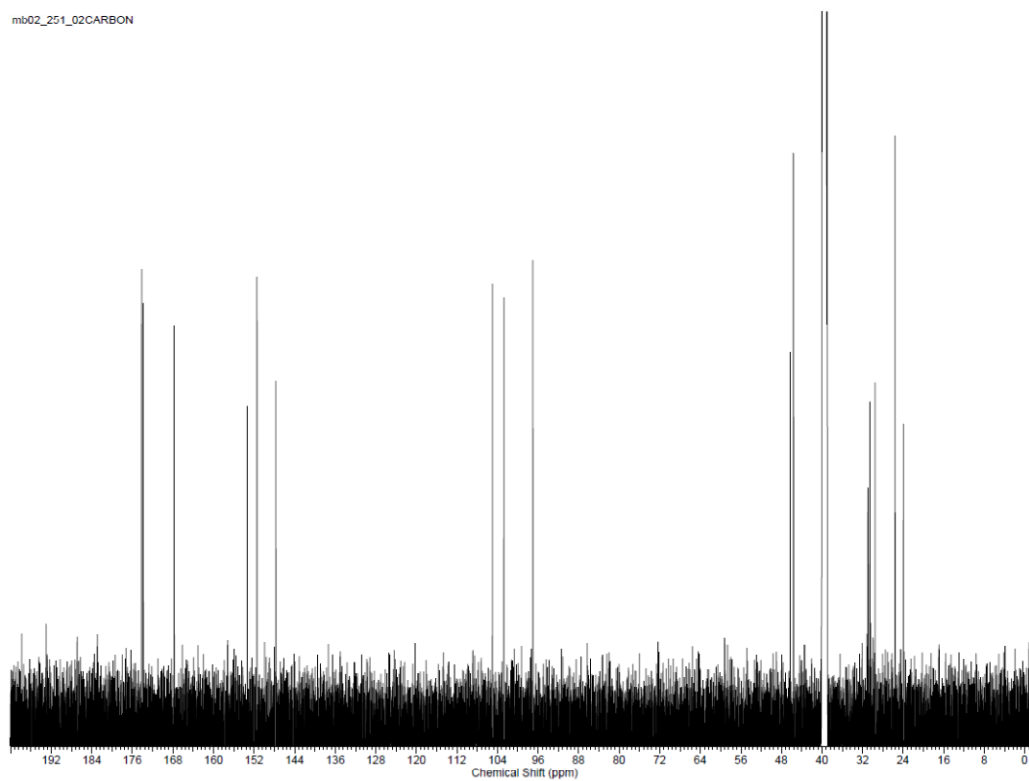
Supplementary Figure S38. ¹H NMR of 2e in d₆-DMSO (crude).

mb02_251_02



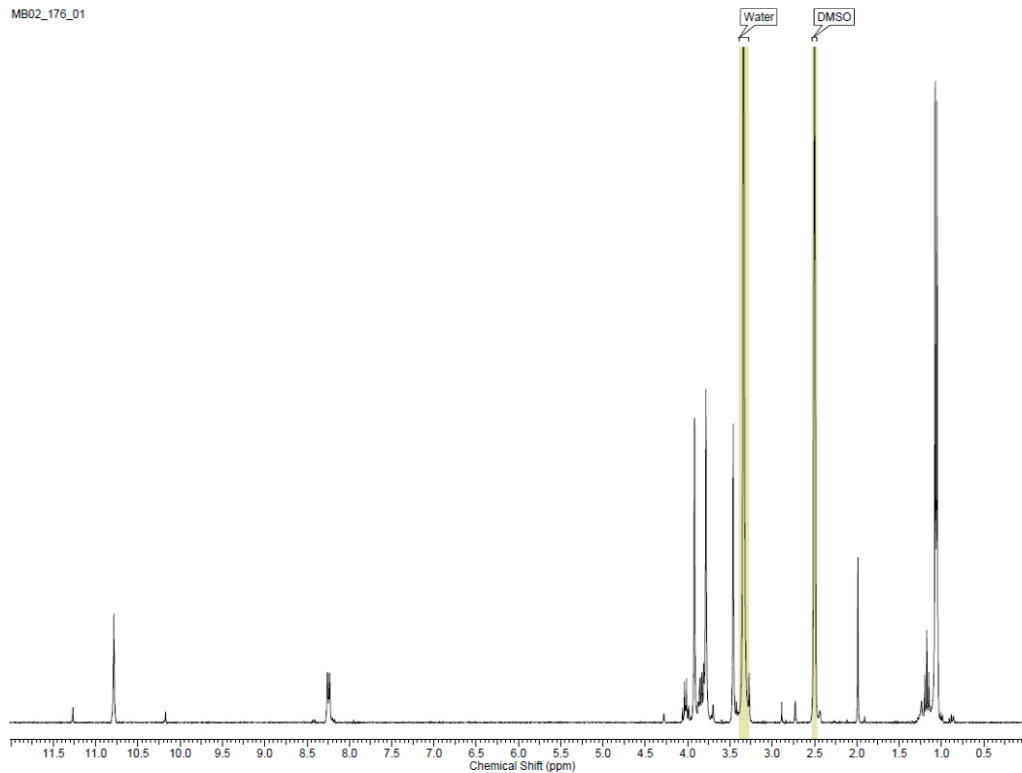
Supplementary Figure S39. ¹H NMR of 2e in d₆-DMSO (purified).

mb02_251_02CARBON

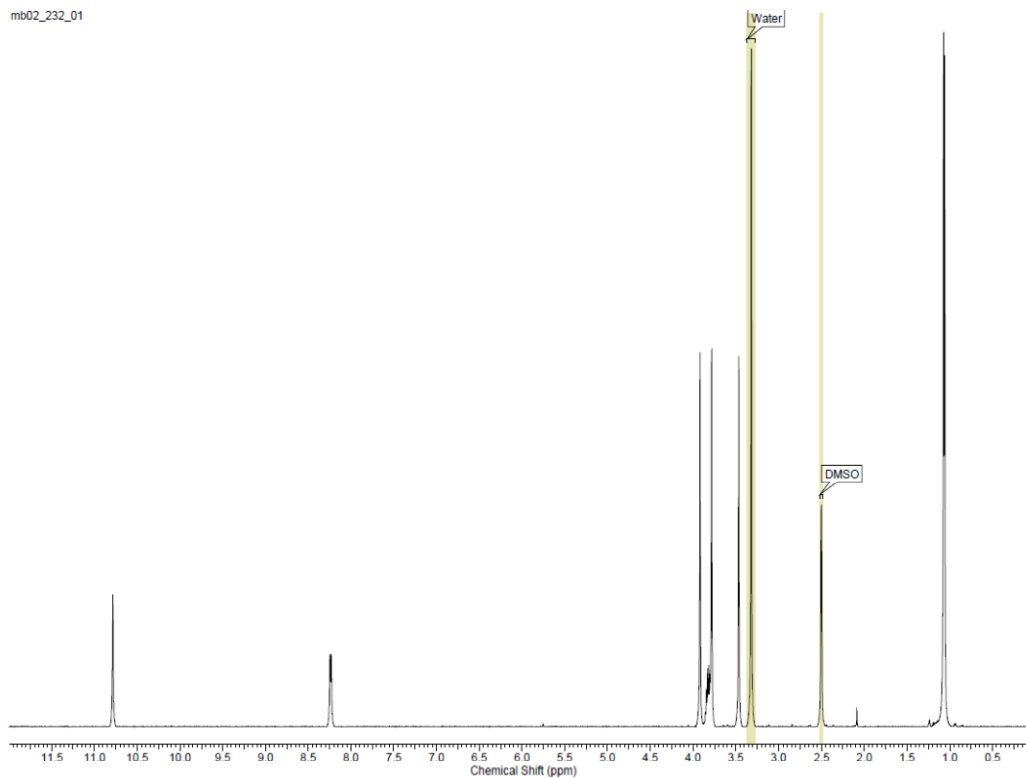


Supplementary Figure S40. ^{13}C NMR of 2e in d_6 -DMSO (purified).

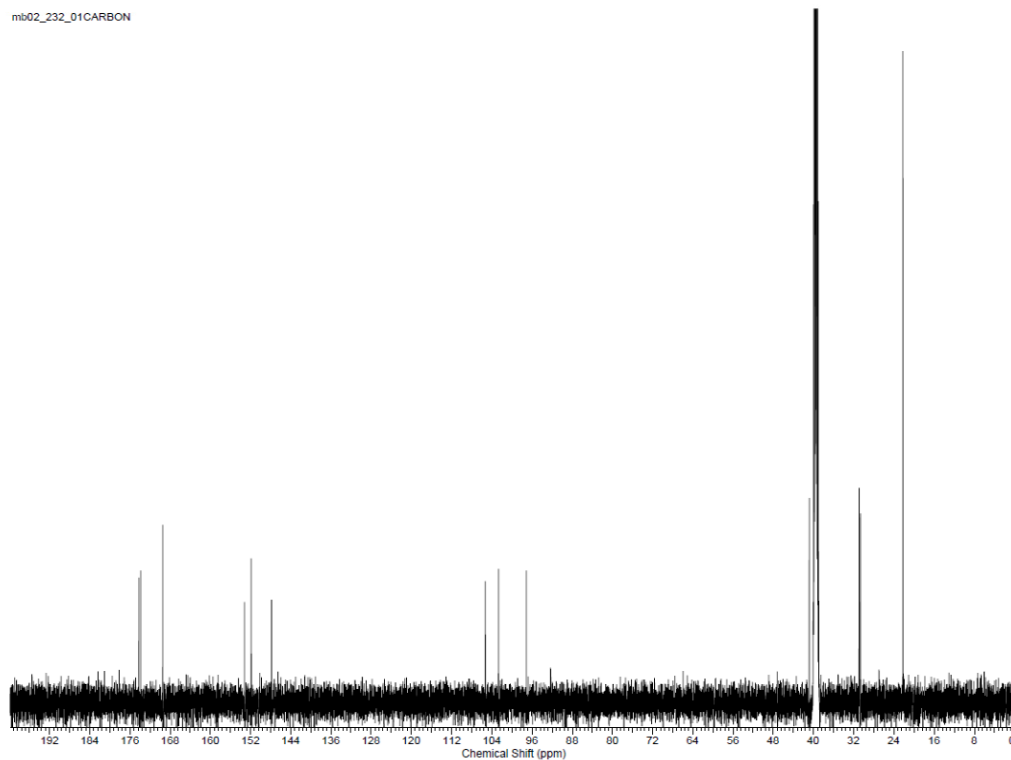
MB02_176_01



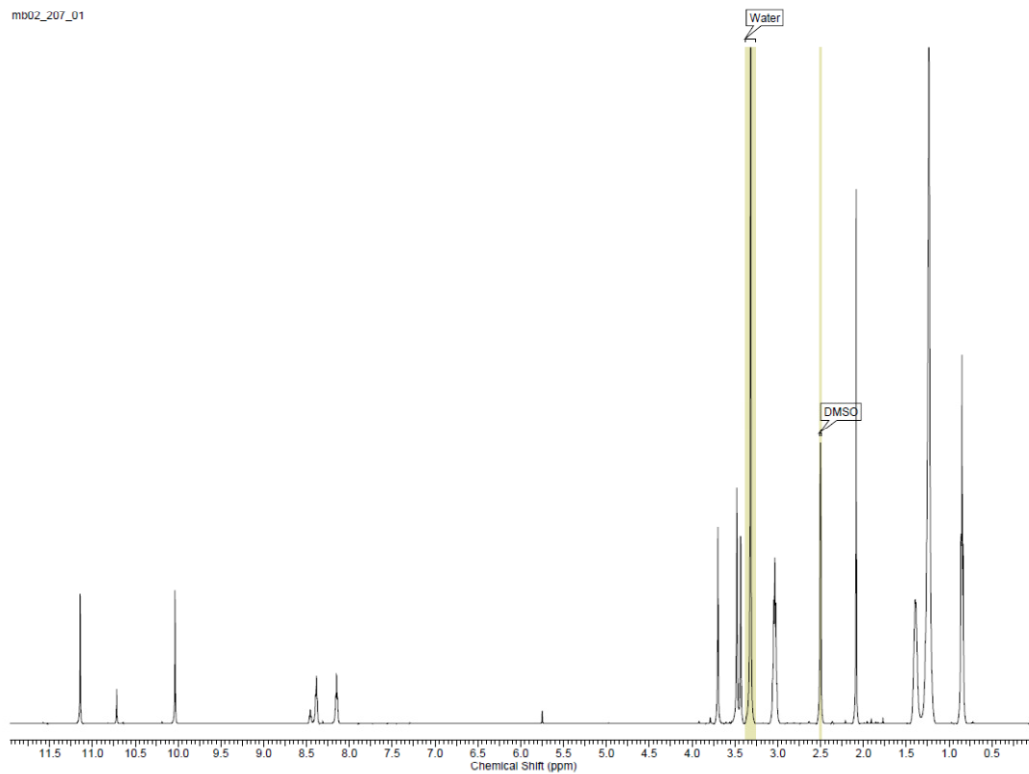
Supplementary Figure S41. ^1H NMR of 2 in d_6 -DMSO (crude).



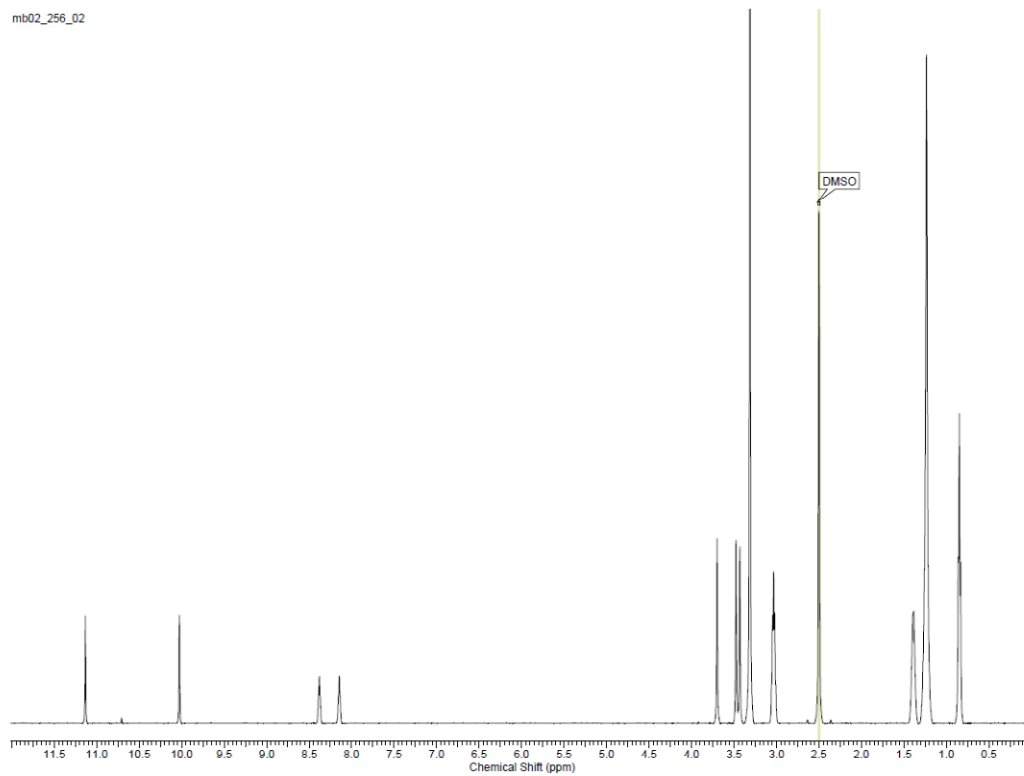
Supplementary Figure S42. ^1H NMR of **2f** in d_6 -DMSO (purified).



Supplementary Figure S43. ^{13}C NMR of **2f** in d_6 -DMSO (purified).

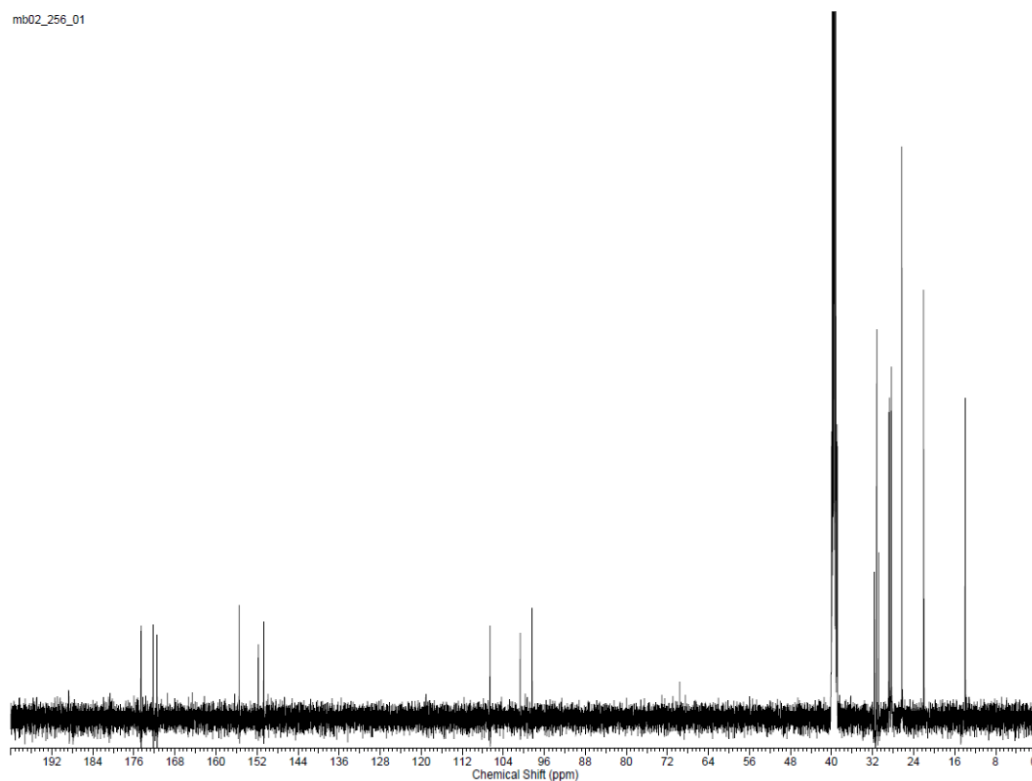


Supplementary Figure S44. ^1H NMR of **3aa** in d_6 -DMSO (crude).



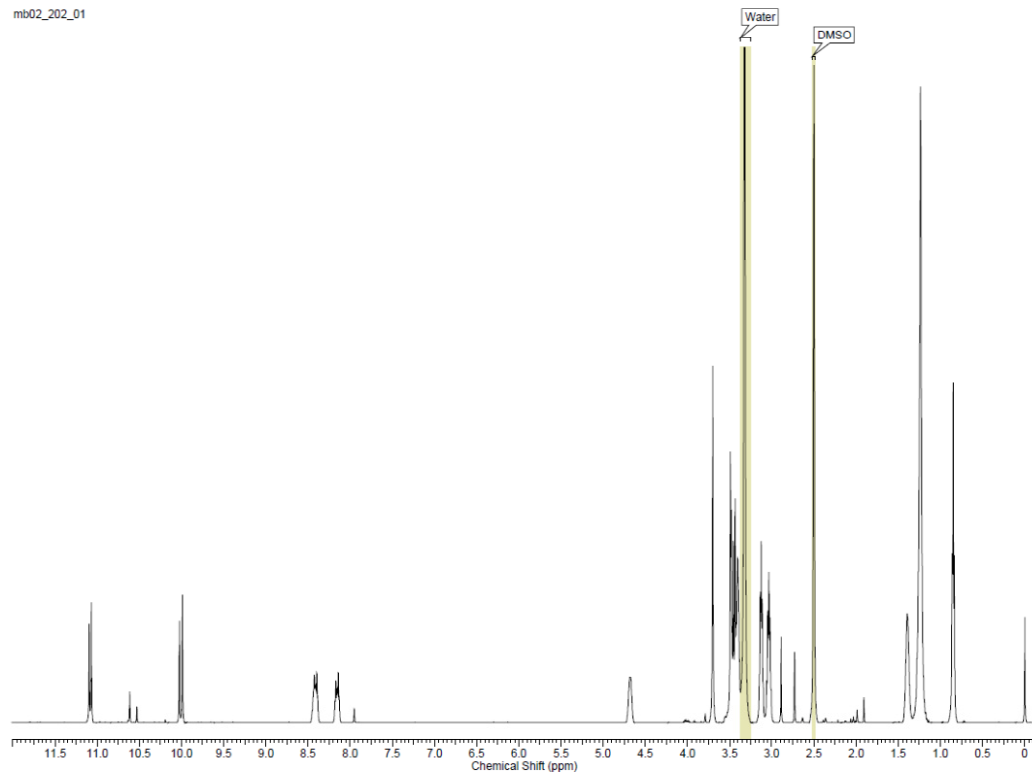
Supplementary Figure S45. ^1H NMR of **3aa** in d_6 -DMSO (purified).

mb02_256_01

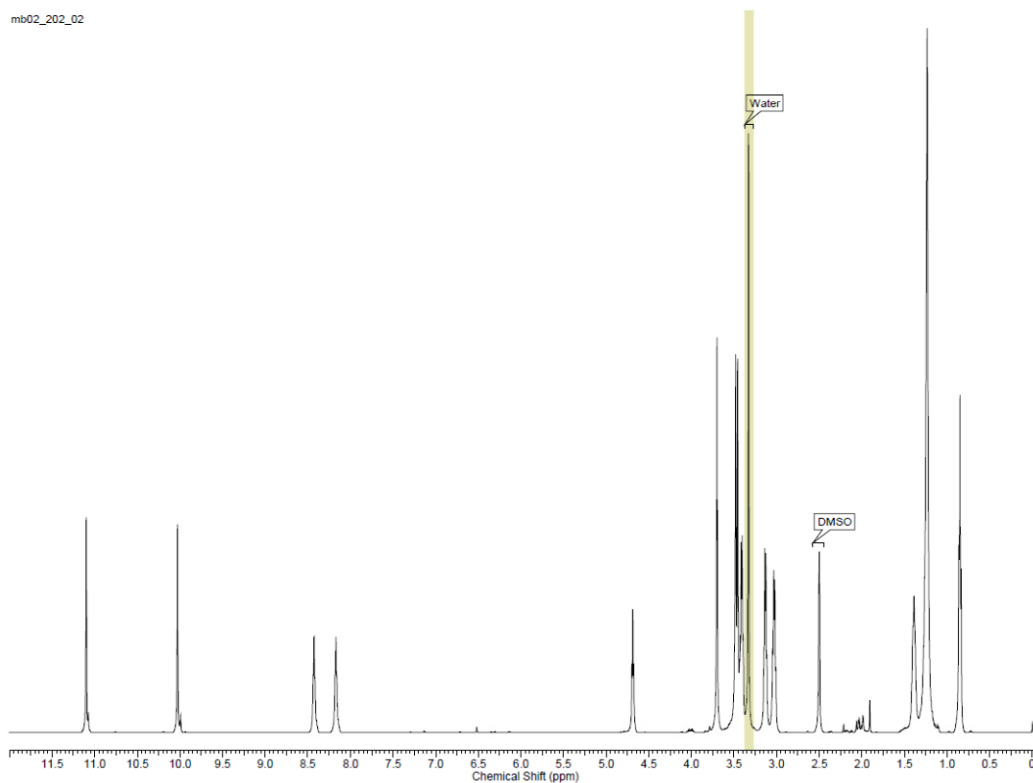


Supplementary Figure S46. ^{13}C NMR of **3aa** in d_6 -DMSO (purified).

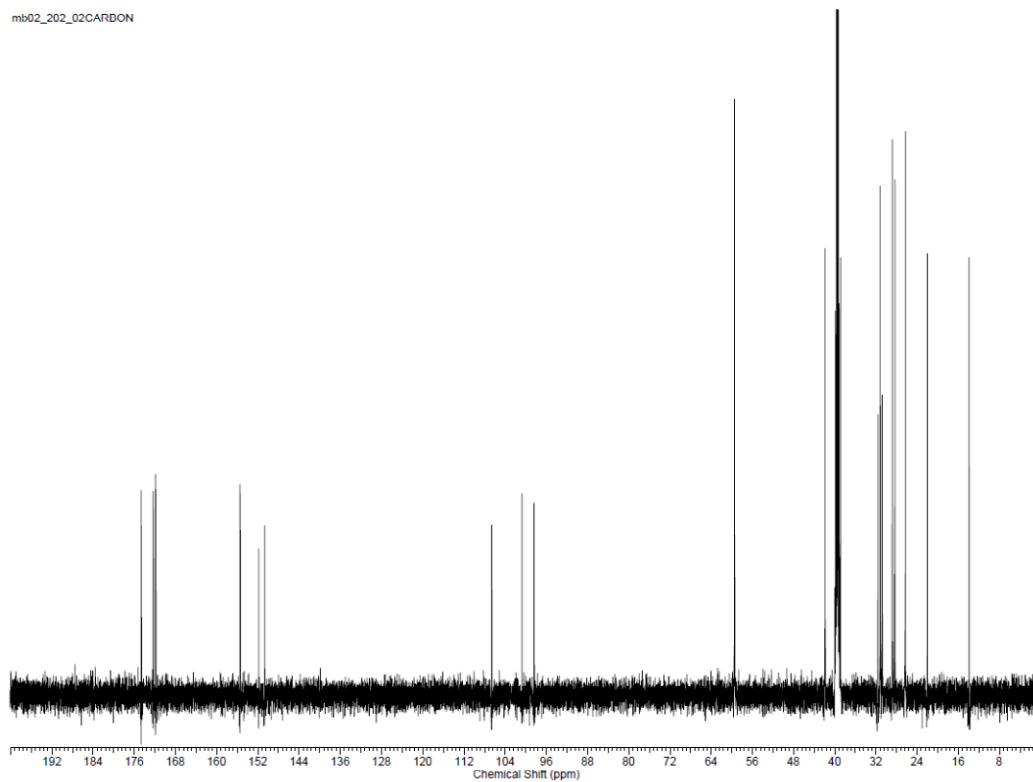
mb02_202_01



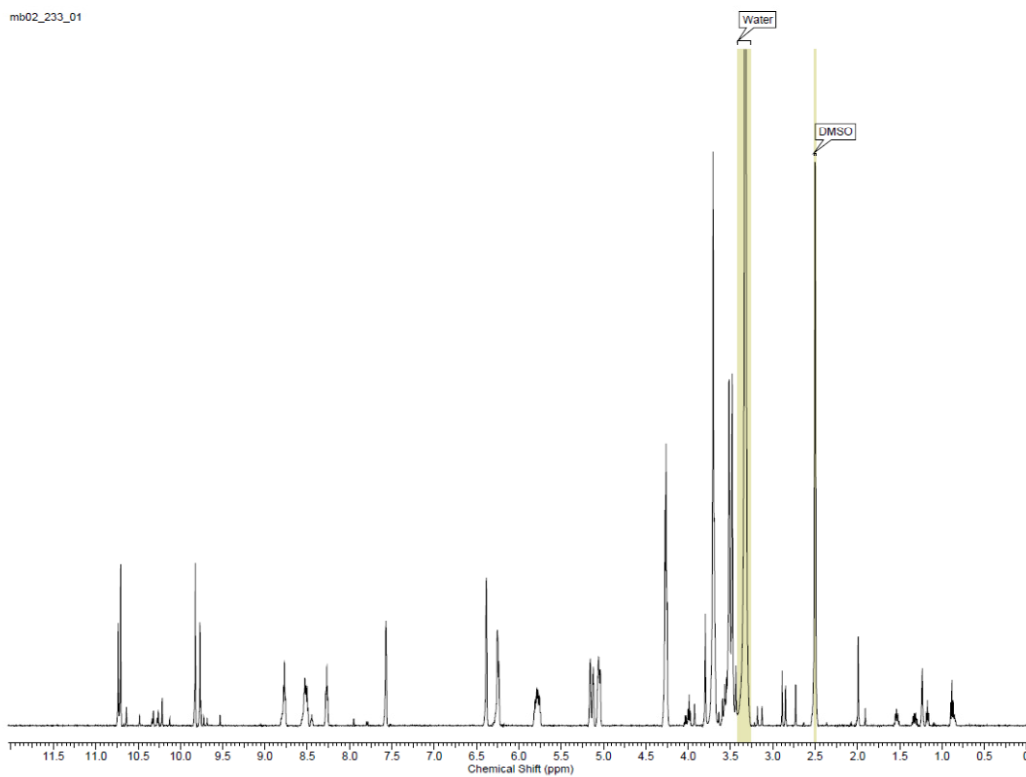
Supplementary Figure S47. ^1H NMR of **3ad'** and **3ad''** in d_6 -DMSO (crude).



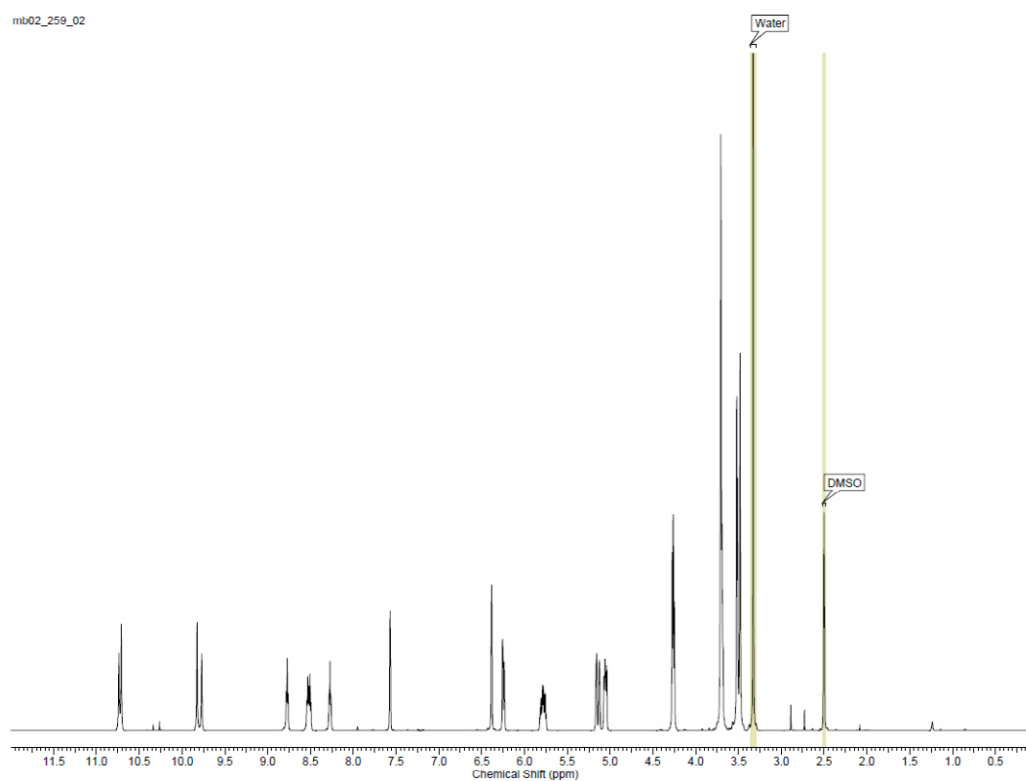
Supplementary Figure S48. ^1H NMR of **3ad'** in d_6 -DMSO (purified).



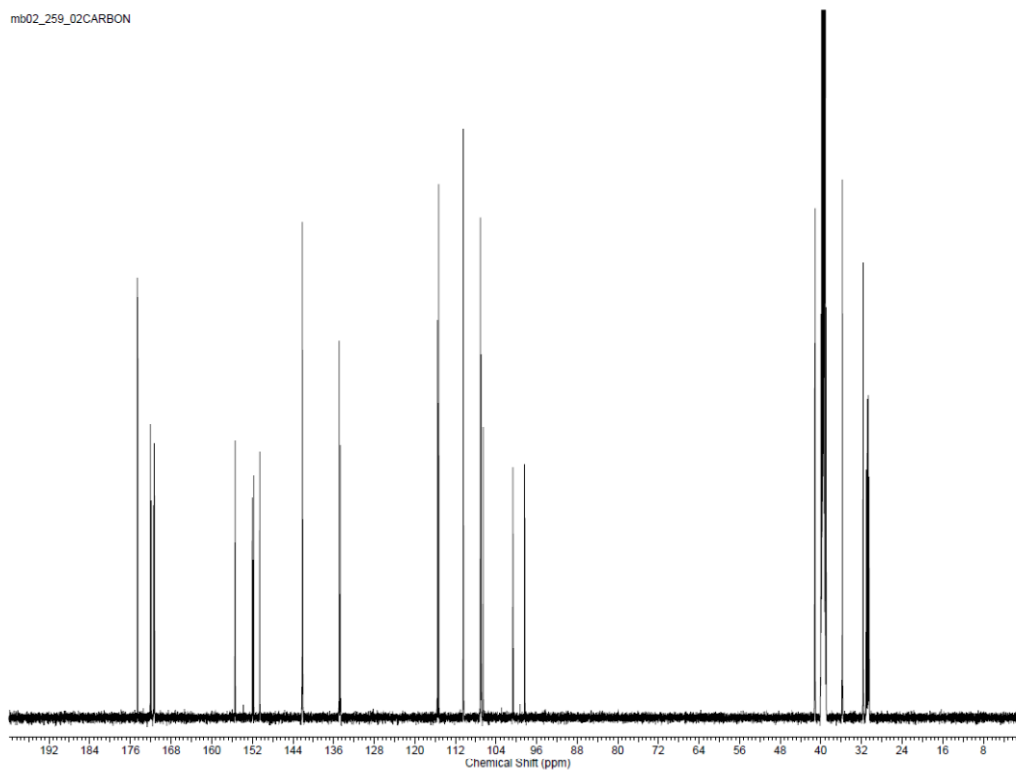
Supplementary Figure S49. ^{13}C NMR of **3ad'** in d_6 -DMSO (purified).



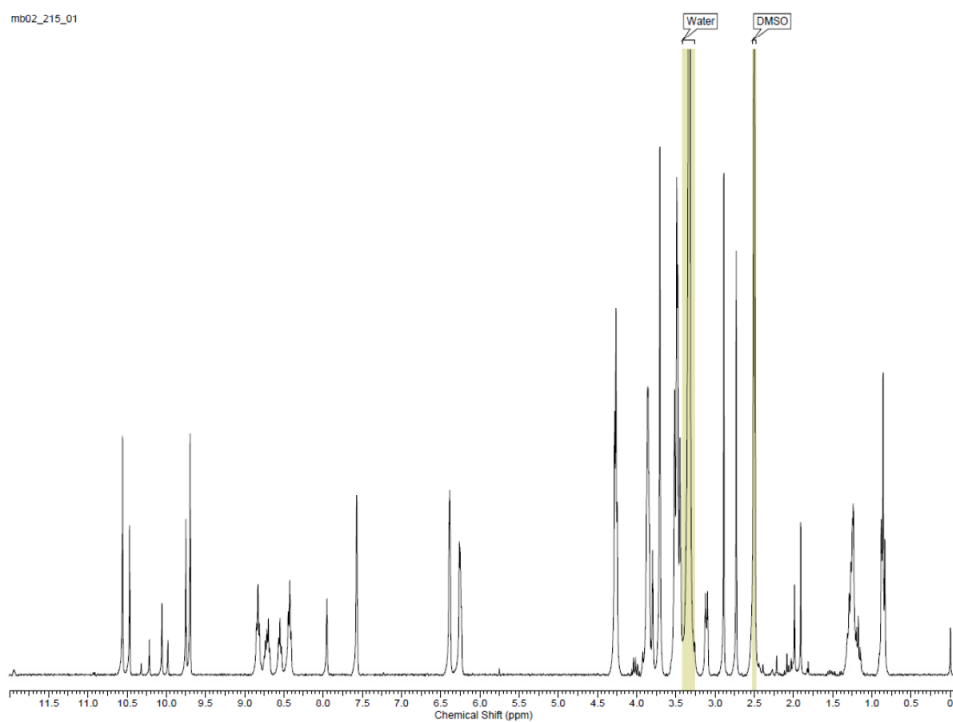
Supplementary Figure S50. ^1H NMR of $3\text{cg}'$ and $3\text{cg}''$ in d_6 -DMSO (crude).



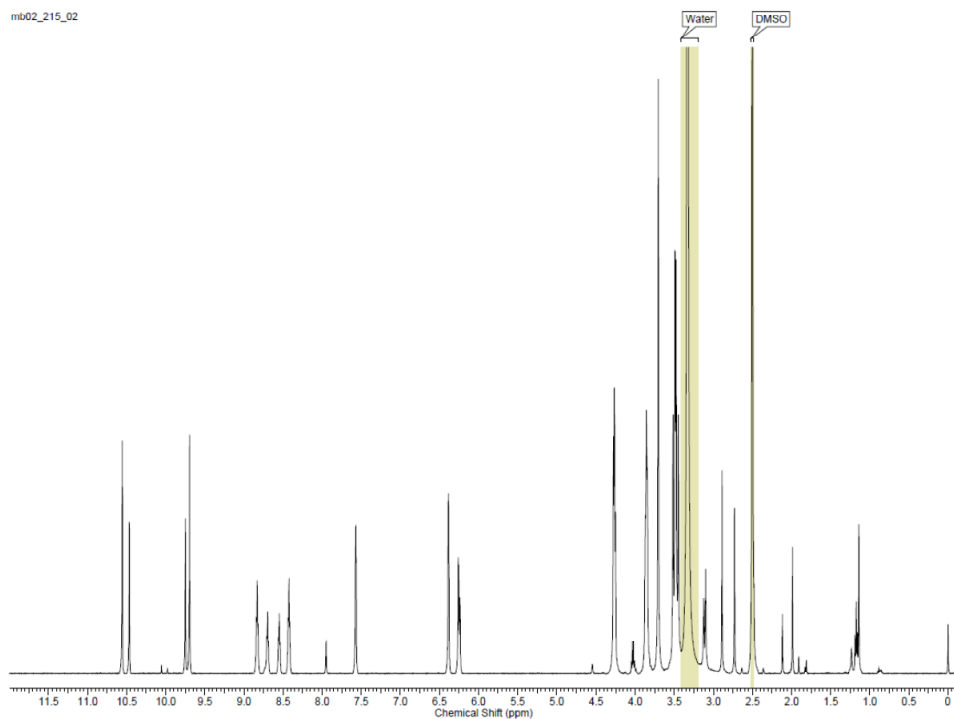
Supplementary Figure S51. ^1H NMR of $3\text{cg}'$ and $3\text{cg}''$ in d_6 -DMSO (purified).



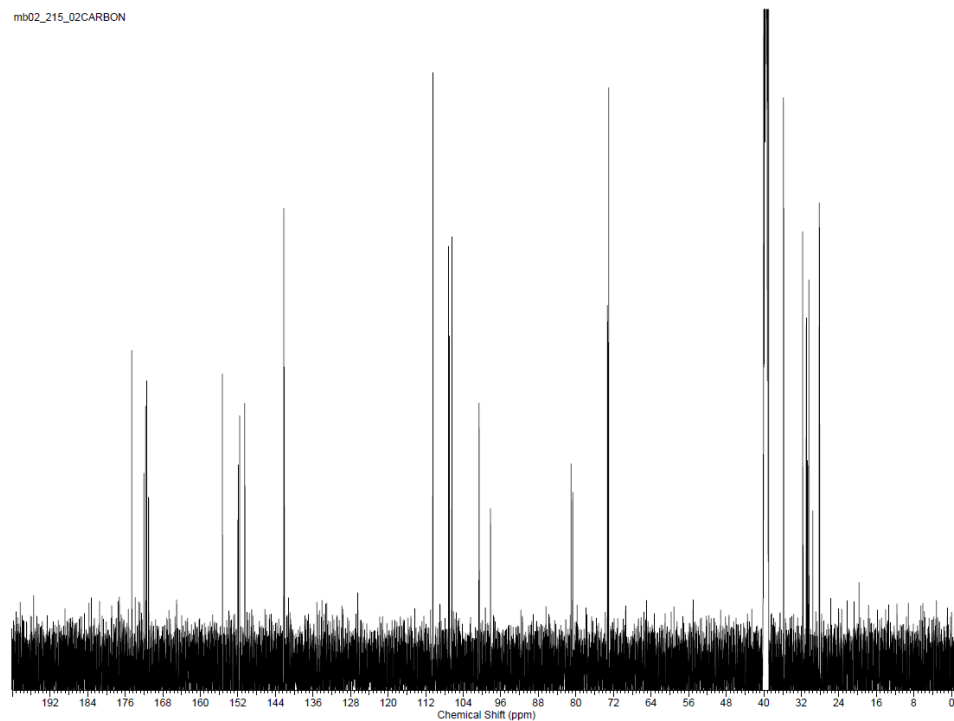
Supplementary Figure S52. ^{13}C NMR of $3\text{cg}'$ and $3\text{cg}''$ in d_6 -DMSO (purified).



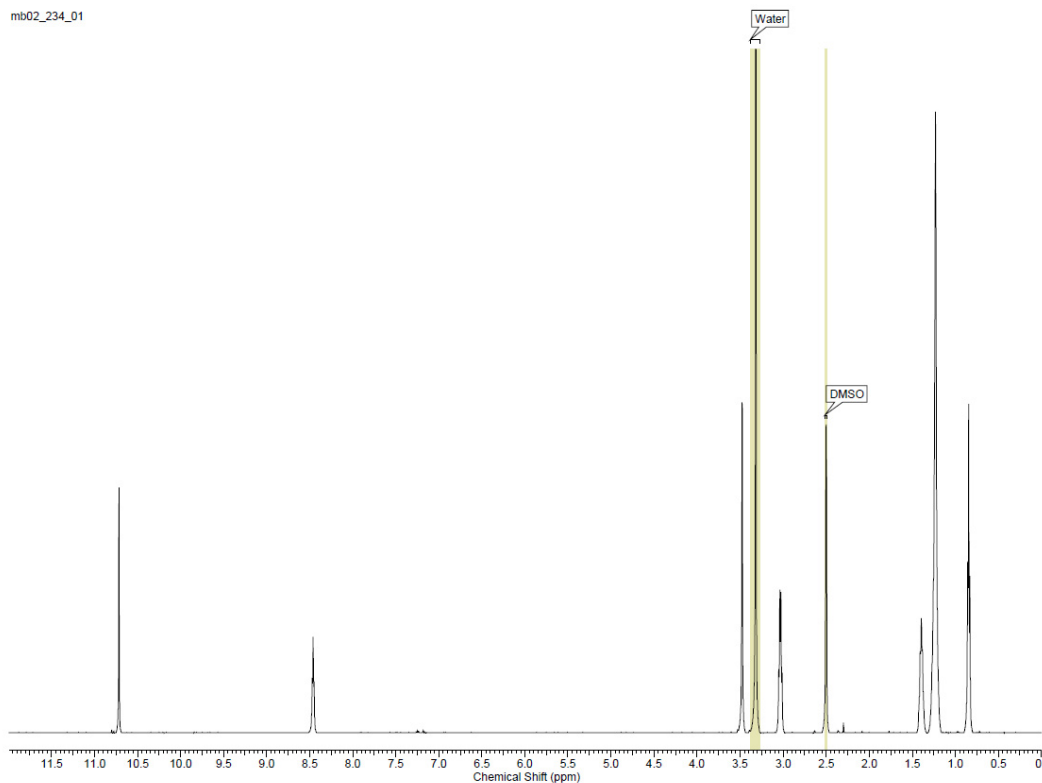
Supplementary Figure S53. ^1H NMR of $3\text{ch}'$ and $3\text{ch}''$ d_6 -DMSO (crude)



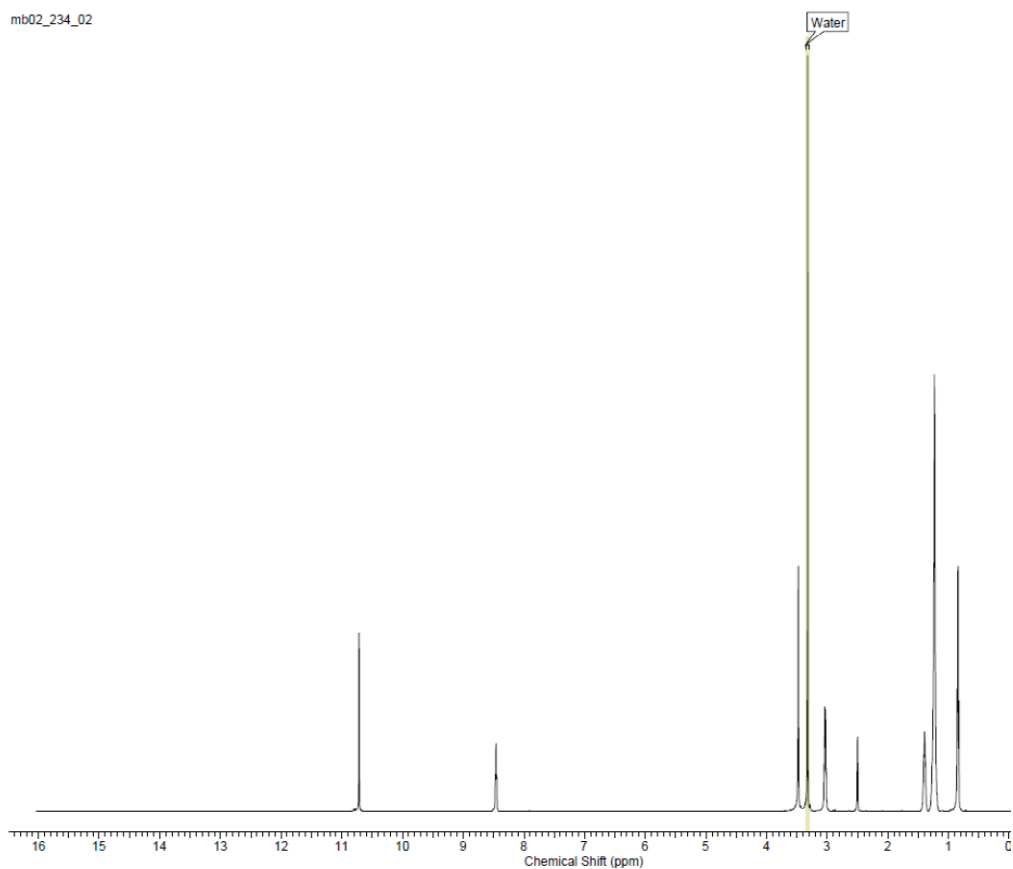
Supplementary Figure S54. ^1H NMR of **3ch'** and **3ch''** d_6 -DMSO (pure)



Supplementary Figure S55. ^{13}C NMR of **3ch'** and **3ch''** d_6 -DMSO (pure)

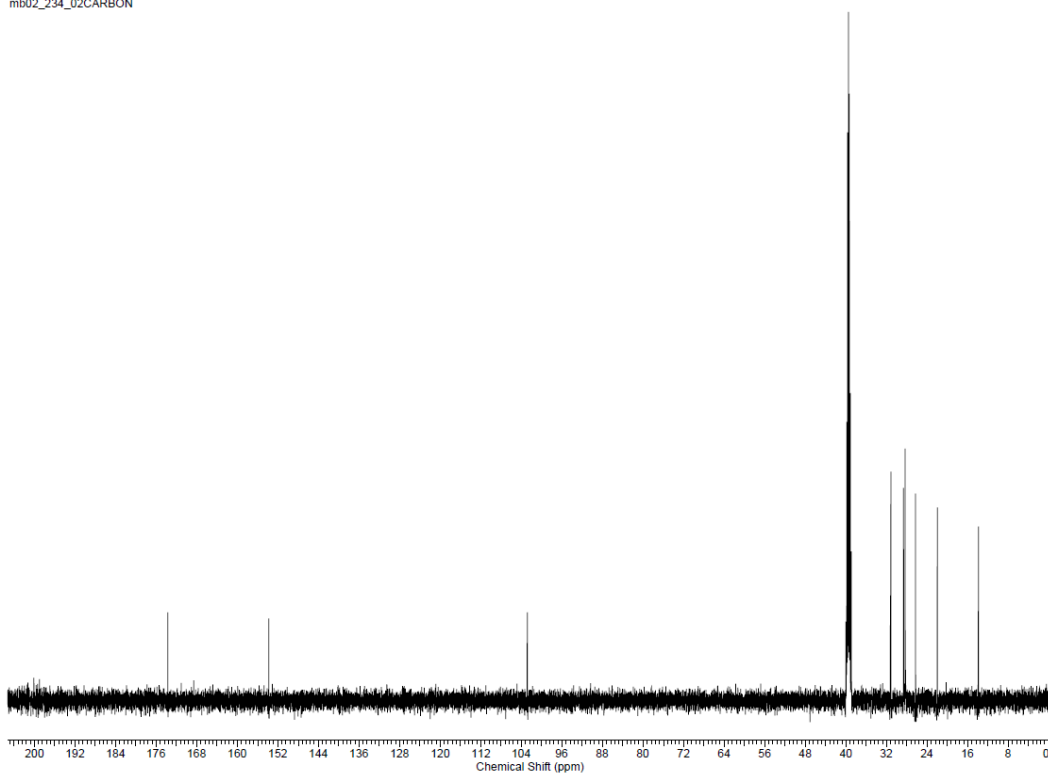


Supplementary Figure S56. ^1H NMR of **4aaa** in d_6 -DMSO (crude).



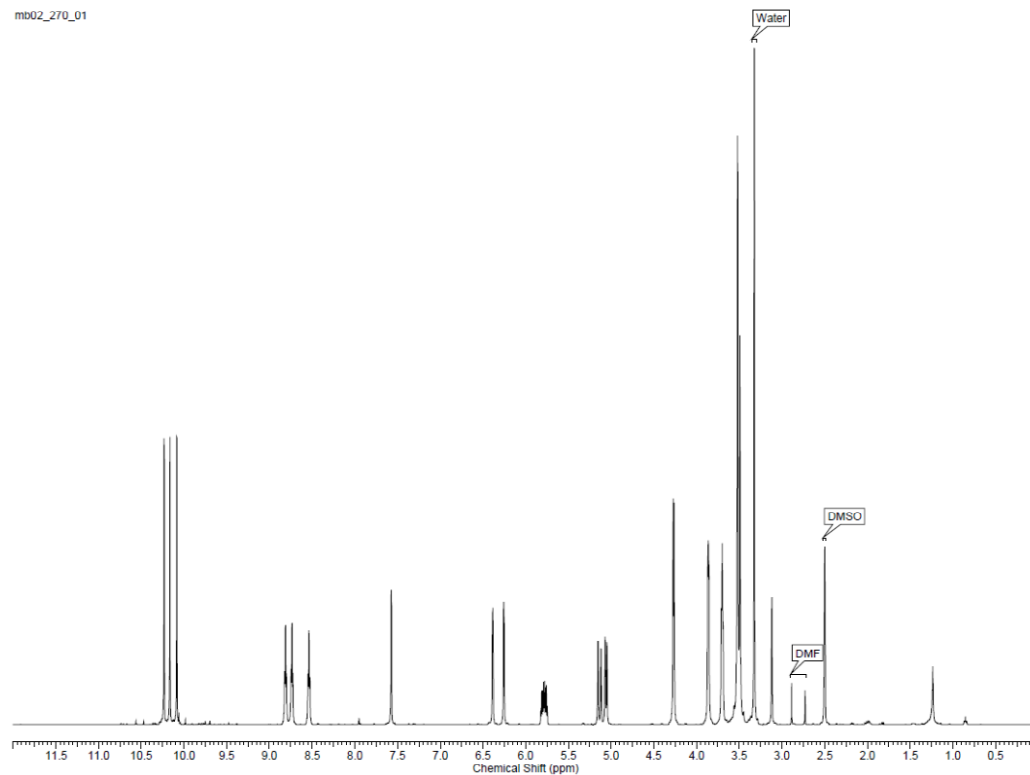
Supplementary Figure S57. ^1H NMR of **4aaa** in d_6 -DMSO (purified).

mb02_234_02CARBON



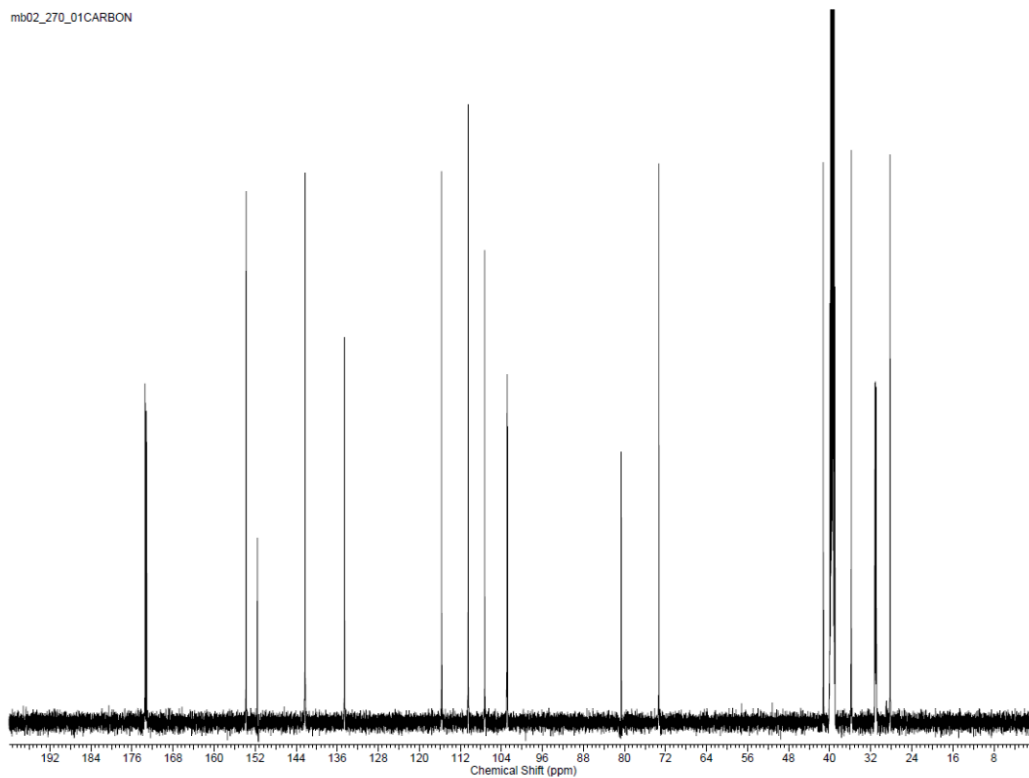
Supplementary Figure S58. ^{13}C NMR of **4aaa** in d_6 -DMSO (purified).

mb02_270_01



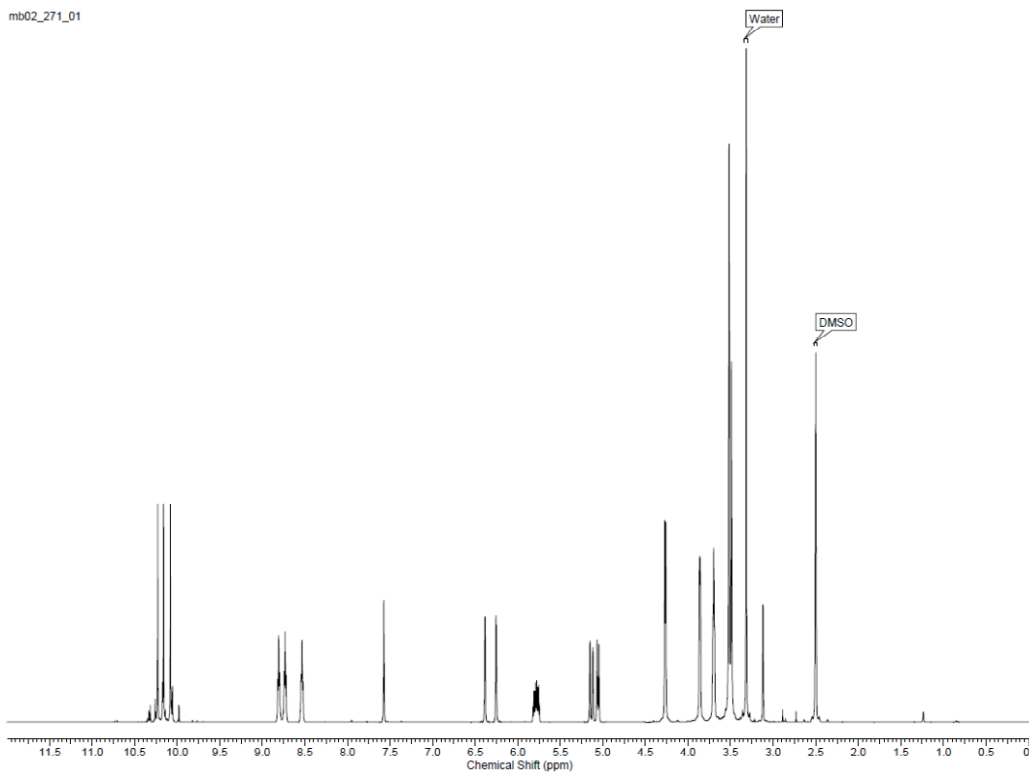
Supplementary Figure S59. ^1H NMR of **4cgh** in d_6 -DMSO (purified).

mb02_270_01CARBON

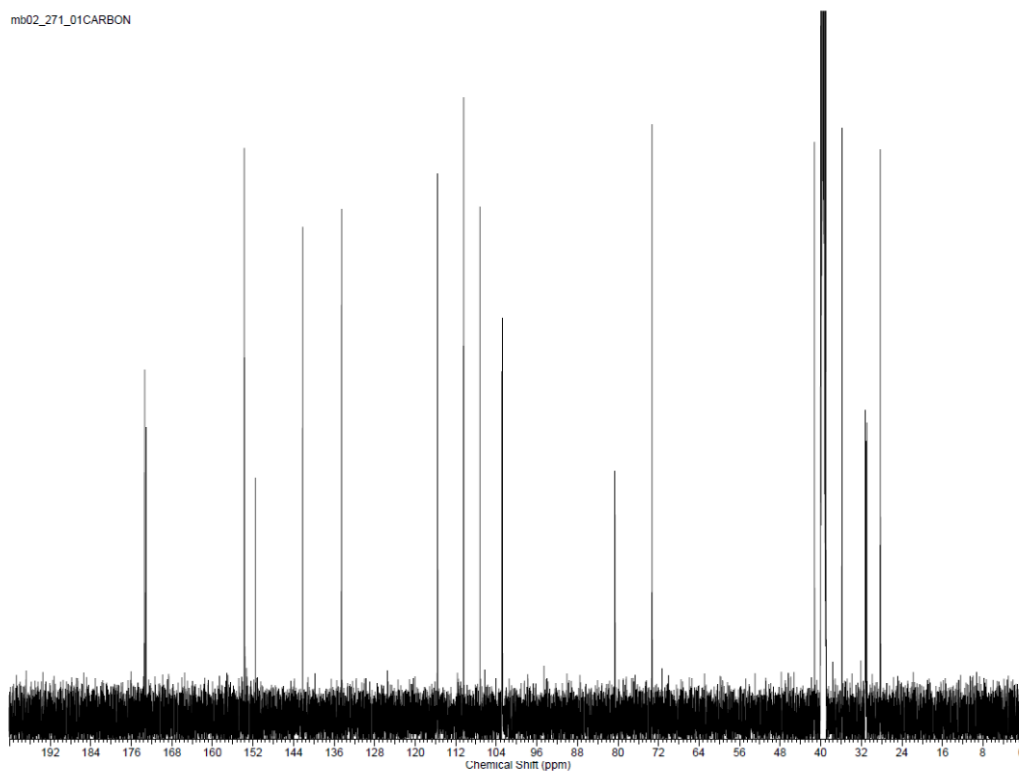


Supplementary Figure S60. ^{13}C NMR of 4cgh in d_6 -DMSO (purified).

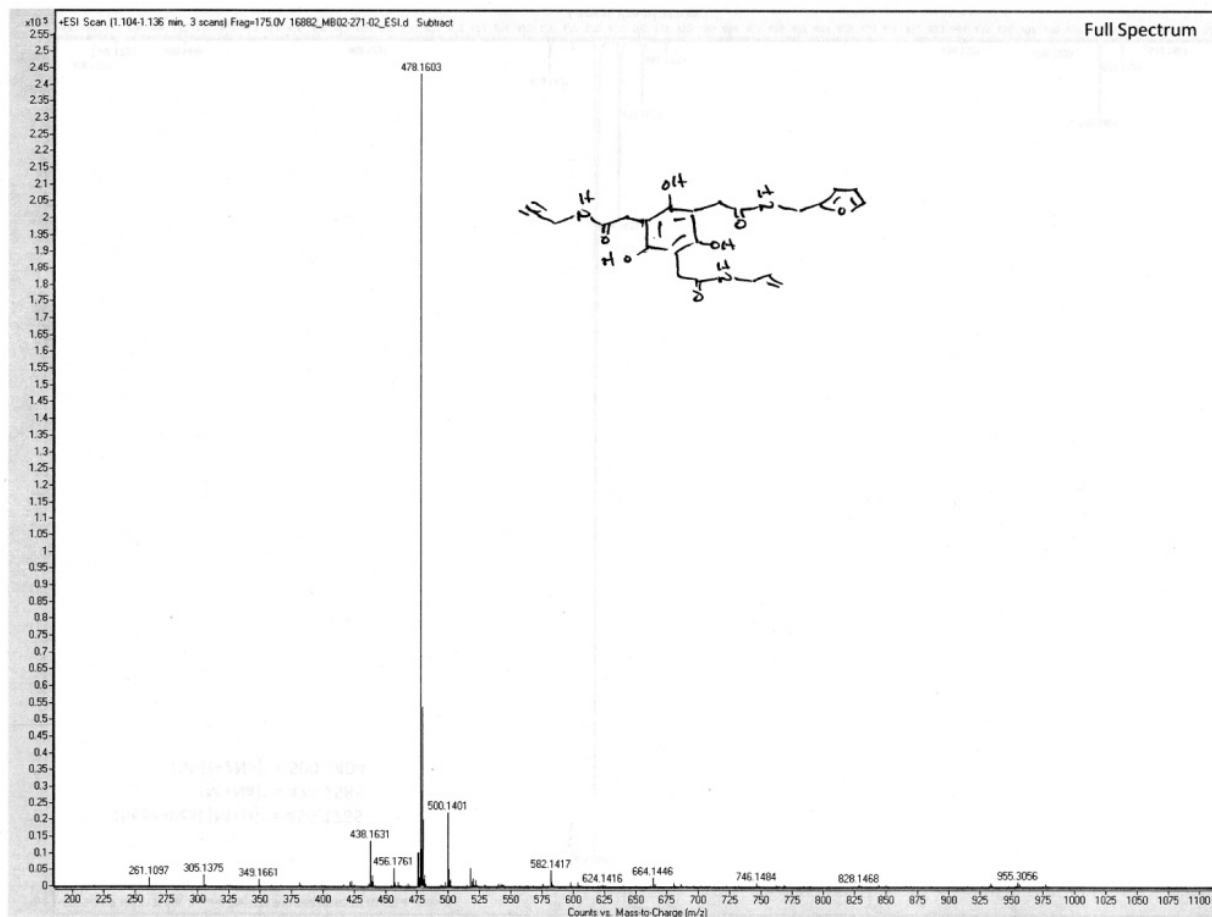
mb02_271_01



Supplementary Figure S61. ^1H NMR of 4cgh in d_6 -DMSO (one pot procedure, column purified).

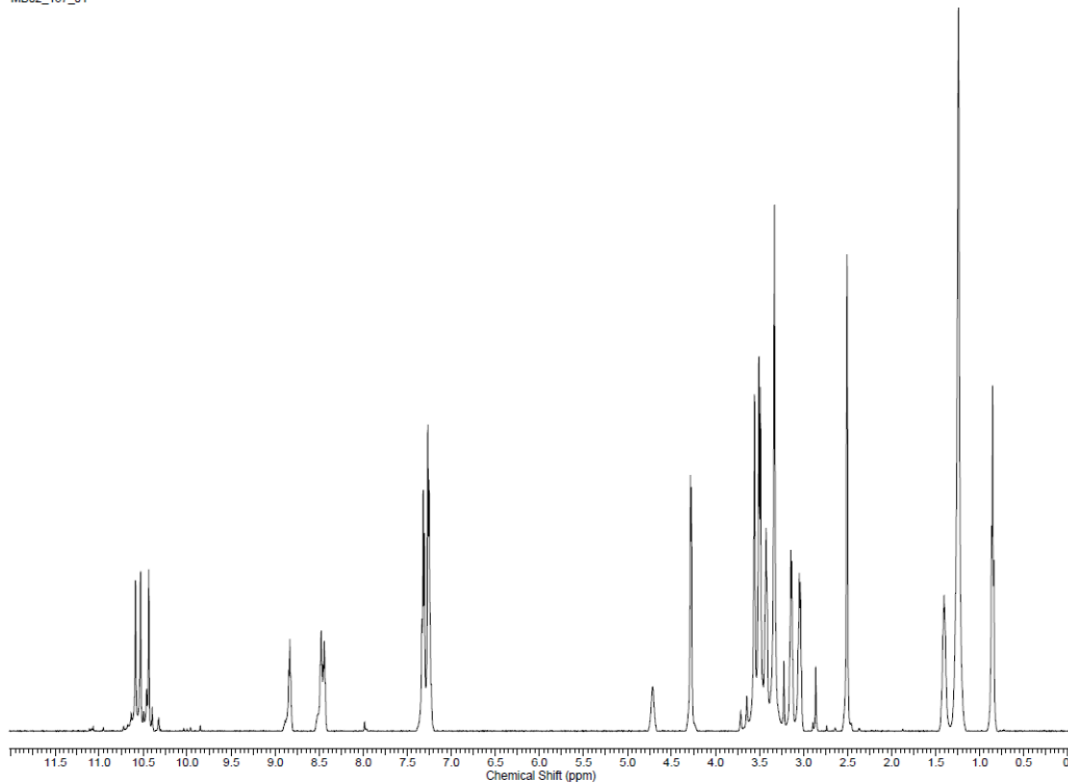


Supplementary Figure S62. ^{13}C NMR of **4cgh** in d_6 -DMSO (one pot procedure, column purified)



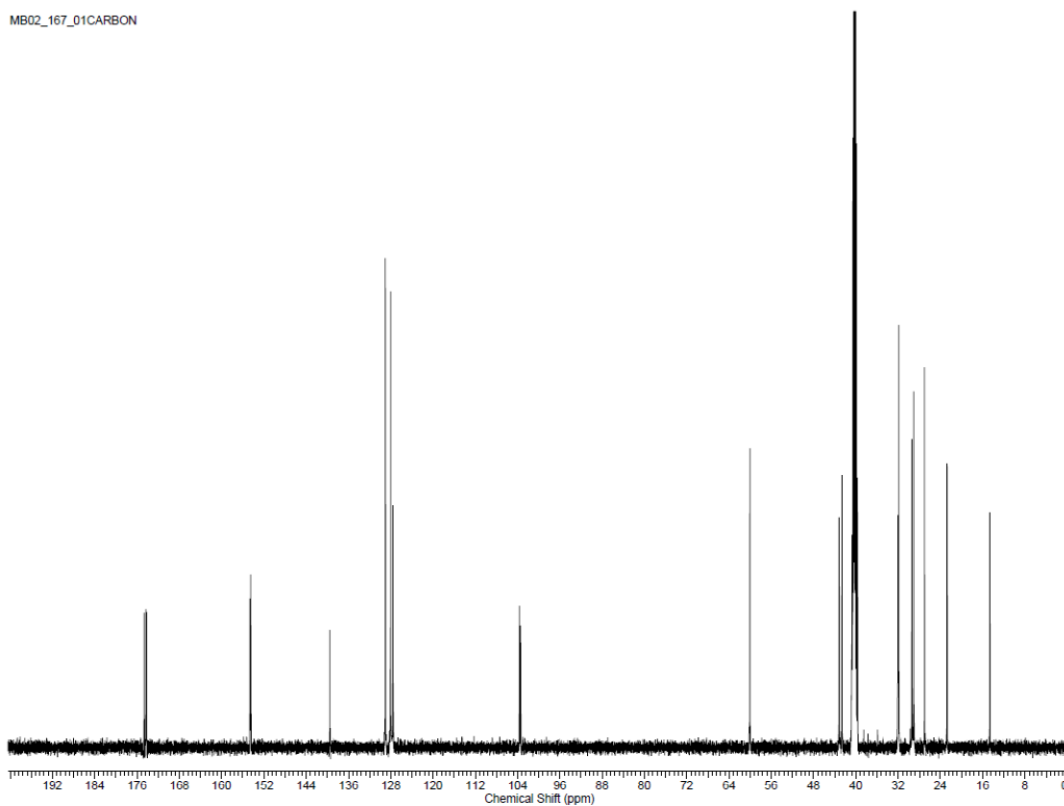
Supplementary Figure S63. ESI-MS of 4cgh (one pot procedure, column purified).

MB02_167_01



Supplementary Figure S64. ¹H NMR of 4abd in *d*₆-DMSO (one pot procedure, column purified)

MB02_167_01CARBON



Supplementary Figure S65. ¹³C NMR of 4abd in *d*₆-DMSO (one pot procedure, column purified)

References

- 1) Allouche, A. *J. Comp. Chem.* **2010**, *32*, 174.
- 2) Gaussian 03, Revision C.02, M. J. Frisch; G. W. Trucks; H. B. Schlegel; G. E. Scuseria; M. A. Robb; J. R. Cheeseman; J. A. Montgomery, Jr.; T. Vreven; K. N. Kudin; J. C. Burant; J. M. Millam; S. S. Iyengar; J. Tomasi; V. Barone; B. Mennucci; M. Cossi; G. Scalmani; N. Rega; G. A. Petersson; H. Nakatsuji; M. Hada; M. Ehara; K. Toyota; R. Fukuda; J. Hasegawa; M. Ishida; T. Nakajima; Y. Honda; O. Kitao; H. Nakai; M. Klene; X. Li; J. E. Knox; H. P. Hratchian; J. B. Cross; V. Bakken; C. Adamo; J. Jaramillo; R. Gomperts; R. E. Stratmann; O. Yazyev; A. J. Austin; R. Cammi; C. Pomelli; J. W. Ochterski; P. Y. Ayala; K. Morokuma; G. A. Voth; P. Salvador; J. J. Dannenberg; V. G. Zakrzewski; S. Dapprich; A. D. Daniels; M. C. Strain; O. Farkas; D. K. Malick; A. D. Rabuck; K. Raghavachari; J. B. Foresman; J. V. Ortiz; Q. Cui; A. G. Baboul; S. Clifford; J. Cioslowski; B. B. Stefanov; G. Liu; A. Liashenko; P. Piskorz; I. Komaromi; R. L. Martin; D. J. Fox; T. Keith; M. A. Al-Laham; C. Y. Peng; A. Nanayakkara; M. Challacombe; P. M. W. Gill; B. Johnson; W. Chen; M. W. Wong; C. Gonzalez; and J. A. Pople, Gaussian, Inc., Wallingford CT, **2004**.
- 3) Becke, A. D. *J. Chem. Phys.* **1993**, *98*, 5648.
- 4) Stephens, P.; Devlin, F.; Chabalowski, C.; Frisch, M. J. *Phys. Chem.* **1994**, *98*, 11623.
- 5) Lee, C.; Yang, W.; Parr, R. G. *Phys. Rev. B* **1988**, *37*, 785.
- 6) Petersson, G. A.; Tensfeldt, T. G.; Montgomery, J. A., *J. Chem. Phys.* **1991**, *94*, 6091.
- 7) Clark, T.; Chandrasekhar, J.; Spitznagel, G. W.; Schleyer, P. v.R. *J. Comp. Chem.* **1983**, *4*, 294.
- 8) Mulliken, R. S. *J. Chem. Phys.* **1955**, *23*, 1833.
- 9) Reed, A. E.; Curtiss, L. A.; Weinhold, F. *Chem. Rev.* **1988**, *88*, 899.
- 10) Parr, R. G.; Szentpaly, L. V.; Liu, S. *J. Am. Chem. Soc.* **1999**, *121*, 1922.
- 11) Pearson, R. G. *Inorg. Chem.* **1988**, *27*, 734.
- 12) Galabov, B.; Ilieva, S.; Hadjieva, B.; Atanasov, Y.; Schaefer, H.F. *J. Phys. Chem. A* **2008**, *112*, 6700.
- 13) Bultinck, P.; Langenaeker, W.; Lahorte, P.; De Proft, F.; Geerlings, P.; Van Alsenoy, C.; Tollenaere, J.P. *J. Phys. Chem. A* **2002**, *106*, 7895.